

5-31-2021

## Blowout - Capping - Fracturing - Relief Well, A Full Cycle Workflow

Youssuf A. Elnamany  
*Louisiana State University and Agricultural and Mechanical College*

Follow this and additional works at: [https://digitalcommons.lsu.edu/gradschool\\_theses](https://digitalcommons.lsu.edu/gradschool_theses)



Part of the [Petroleum Engineering Commons](#)

---

### Recommended Citation

Elnamany, Youssuf A., "Blowout - Capping - Fracturing - Relief Well, A Full Cycle Workflow" (2021). *LSU Master's Theses*. 5339.  
[https://digitalcommons.lsu.edu/gradschool\\_theses/5339](https://digitalcommons.lsu.edu/gradschool_theses/5339)

This Thesis is brought to you for free and open access by the Graduate School at LSU Digital Commons. It has been accepted for inclusion in LSU Master's Theses by an authorized graduate school editor of LSU Digital Commons. For more information, please contact [gradetd@lsu.edu](mailto:gradetd@lsu.edu).

# **Blowout - Capping - Fracturing - Relief Well, A Full Cycle Workflow**

A Thesis

Submitted to the Graduate Faculty of the  
Louisiana State University and  
Agricultural and Mechanical College  
in partial fulfillment of the  
requirements for the degree of  
Master of Science in Petroleum Engineering

in

Craft and Hawkins Department of Petroleum Engineering

by

Youssuf Ahmed Elnoamany  
B.S.P.E, Louisiana State University, 2018  
M.S.A, Louisiana State University, 2021  
August 2021

## Acknowledgments

I would like to thank God Almighty for giving me the strength to conduct this study. It is with genuine pleasure to express my gratitude to my advisor and mentor Dr. Ipsita Gupta for inspiring me and providing me the great opportunity of joining the Petroleum Engineering Graduate Program at LSU. Her inspirations, timely suggestions, and enthusiasm were incredibly beneficial and much appreciated. I am thankful for Dr. Paulo Waltrich and Dr. Yuanhang Chen for serving as committee members. Their technical feedback throughout my thesis research project were invaluable. Special thanks to Dr. Richard Hughes for his interest in my research.

I would like to show appreciation to the following people who always motivated me in every possible way, and pushed me the extra mile: to my parents, Ahmed Elnoamany and Nadia AbdelKader, my sisters Mariam and Nour, and brother Marwan (RIP), my grandmother Amira (RIP) and grandfather Mostafa (RIP). To my fiancé, Dalhia, thank you for always standing by my side and creating beautiful memories during this wonderful educational journey.

I am grateful for my fellow lab colleagues in the GMG group for their continued support and memorable times spent in our lab. Hope Asala, thank you for all your help and guidance; Dr. Andreas Michael, I could not have done any of this without you, your advice and input are much appreciated. I thank Petroleum Experts (*PETEX*) for their license donation. Special thanks to Dr. Tej Bhinde, Dr. Toshi Mochizuki, and Dr. Steve Todman from *PETEX* for their support and cooperation in building the models. I also wish to thank, LSU CAS for sponsorship, my manager, Mr. Matthew Mattox for his words of encouragement and leadership development. To Han'ali El-Demagh, N. Nedd, I. Elghetrify, H. Amer, G.Feo, T. Quatroy, and E. Kaldirim, thank you for the continuous laughter throughout the years. Last but not least, I want to thank me for believing in me, for the sleepless nights I spent on this hard work, for working tirelessly and never quitting.

## Table of Contents

|  |      |
|--|------|
| Acknowledgments.....   | ii   |
| List of Tables .....   | v    |
| List of Figures .....  | vi   |
| Nomenclature .....   | x    |
| Abstract .....   | xiii |
| 1. Introduction.....   | 1    |
| 1.1. Background .....  | 2    |
| 1.2. Research Hypotheses and Objectives .....                                      | 10   |
| 1.3. Thesis Outline .....  | 11   |
| 2. Literature Review.....  | 12   |
| 2.1. Overview .....  | 12   |
| 2.2. Offshore Killing Methods .....  | 14   |
| 2.3. Workflow for WCD Calculation .....  | 16   |
| 2.4. Occurrences of Broaching.....   | 18   |
| 2.5. Fracture Initiation, Propagation and Closure in Porous, Permeable Media ..... | 19   |
| 2.6. Fracture Height Assessment.....   | 22   |
| 3. Proposed Workflow for Post-WCD Capping Shut-in.....                             | 25   |
| 3.1. Modeling Process .....  | 26   |
| 3.2. Governing Equations.....  | 27   |
| 3.3. Base Case Model Description .....   | 32   |
| 3.3. Validation .....  | 42   |
| 3.4. Sensitivity Studies .....   | 44   |
| 3.5. WCD Calculation .....   | 46   |
| 3.6. Capping Shut-in.....  | 49   |
| 3.7. Relief Well Injection Strategy .....  | 51   |
| 4. Results and Discussion .....  | 53   |
| 4.1. Base Case Model Results .....   | 53   |
| 4.2. Conductor Casing Leak .....   | 65   |
| 4.3. Surface Casing Leak.....  | 69   |
| 4.4. Drilling Liner Casing Collapse .....  | 74   |
| 4.5. Perfect Cement in Casings .....   | 79   |
| 4.6. Young's Modulus Contrast .....  | 81   |
| 4.7. Reservoir Overpressure Variation .....  | 84   |
| 4.8. Total Discharge Duration .....  | 86   |
| 4.9. Intervention Time .....   | 88   |
| 4.10. Steady-State and Transient Wellbore Models .....                             | 90   |

|   |     |
|---|-----|
| 5. Conclusions, Recommendations, and Future Work.....                       | 96  |
| Appendix A. Schedule for WCD, Well Capping, and Relief Well Injection ..... | 98  |
| Appendix B. Permissions for Published Work .....                            | 101 |
| References .....  | 103 |
| Vita.....   | 109 |

## List of Tables

|  |    |
|--|----|
| Table 1. 1. Required blowout scenario by BOEM as referenced in NTL 2010 - N06a.....                      | 7  |
| Table 1. 2. Subparts of 30 CFR 250 by BSEE.....  | 8  |
| Table 2. 1. Top five US largest offshore well blowouts, ordered by volume (Buchholz et al., 2016). ..... | 12 |
| Table 3. 1. Base model reservoir and overburden layers' properties.....                                  | 33 |
| Table 4. 1. Casing design specifications and fracture name associated.....                               | 53 |
| Table 4. 2. Base Case Model Results (Fracture 5 @ 13.625" Intermediate Casing).....                      | 64 |
| Table 4. 3. Model Results (Fracture 2 @ 26" Conductor Casing).....                                       | 69 |
| Table 4. 4. Model Results (Fracture 3 @ 20" Conductor Casing).....                                       | 73 |
| Table 4. 5. Model Results (Fracture 4 @ 16" Drilling Liner). .....                                       | 78 |
| Table 4. 6. Proposed periods for assessing impact of well capping timeframes. ....                       | 86 |

## List of Figures

|   |    |
|---|----|
| Figure 1. 1. Diagram showing examples of qualitative ranking BOEM geoscientists have conducted on favorable and unfavorable pathways leading to broaching of hydrocarbons (Bjerstedt et al., 2020) (reprinted by permission of the AAPG whose permission is required for further use). .....  | 2  |
| Figure 1. 2. Comparison of wellbore integrity state a) in a blowout condition compared to b) a damaged wellbore where in a potential critical point along the wellbore (shown at casing shoe) a fracture has initiated due to high wellbore pressure (modified after Zaki et al., 2015). .....  | 4  |
| Figure 1. 3. Schematic of BP 001 Macondo Well design and lithologic section based upon analysis of data acquired during drilling. Red lines show possible flow paths of hydrocarbons that may have occurred during the blowout. An underground blowout may have formed with a possible propagating fracture as shown at the 16” linear due to a ruptured disk (reprinted by permission of PNAS whose permission is required for further use). ..... | 6  |
| Figure 1. 4. Two potential fluid paths that may occur during an uncontrolled flow of hydrocarbons scenario. a) Flow through the production casing. b) Flow through the seal assembly (modified after Bartlit et al., 2011). .....   | 10 |
| Figure 2. 1. Percentage of well kill methods for OCS in shallow depth blowouts (produced with data taken from Skalle et.al, 1999). .....  | 15 |
| Figure 2. 2. Loss of well control incidents by type from 2006 to 2013 (produced from data taken from Buchholz et al., 2016).....  | 17 |
| Figure 2. 3. Workflow proposed by Cordoba (2018) for modeling WCD scenarios under extreme blowout conditions using conventional nodal analysis approach (starting from top left to bottom right, flowchart constructed from information taken from Vasquez Cordoba, 2018)....   | 18 |
| Figure 2. 4. Pressure profile against time, expected in a typical hydraulic fracturing stimulation treatment, compared to the event of fracturing during post-blowout capping (dotted line) in a finite reservoir (modified from Zoback, 2007). .....   | 21 |
| Figure 3. 1. Well containment and response workflow (modified after Buchholz et al., 2016).....   | 26 |
| Figure 3. 2. Coupling workflow of the reservoir, geomechanics, and fracture models and solution method for each (modified after Almarri, 2020).....   | 31 |
| Figure 3. 3. Model meshing designed with incident well shown in the center (yellow line). .....   | 35 |
| Figure 3. 4. A side lateral for the purpose of simulating a relief well intersecting the main wellbore around 10,100 ft below seafloor, approximately 1500 ft above the reservoir. ....   | 36 |
| Figure 3. 5. Casing design schematic utilized for the base case model. Fracture 5 is located 2.5 feet below the 13.625” intermediate casing shoe.....   | 37 |

|  |    |
|--|----|
| Figure 3. 6. Relative permeability curves for modeling multiphase flow in the reservoir rock. Blue line is $K_{rw}$ , the relative permeability of water, while green is $K_{ro}$ , the relative permeability of oil. ....   | 38 |
| Figure 3. 7. Reservoir PVT properties: gas-oil ratio (GOR) as a function of pressure. ....   | 38 |
| Figure 3. 8. Reservoir PVT properties: oil formation volume factor (FVF) as a function of pressure. ....   | 39 |
| Figure 3. 9. Reservoir PVT properties: oil viscosity as a function of pressure. ....   | 39 |
| Figure 3. 10. Porosity relationships between shales and sandstones layers with depth below seafloor. ....  | 40 |
| Figure 3. 11. Initial pore pressure and minimum horizontal stress ( $Sh_{min}$ ) as a function of depth. The discharging reservoir is 3,000 psi over-pressured. ....   | 41 |
| Figure 3. 12. Well head capping pressure comparison between the transient numerical solution “estimate” and the steady-state analytical solution “exact” ....  | 42 |
| Figure 3. 13. Capping stack build-up pressure comparison using transient and stead-state well models. ....   | 43 |
| Figure 3. 14. WHP comparison using different transient wellbore for the multiphase flow during capping shut-in. ....   | 44 |
| Figure 3. 15. Typical deepwater wellbore schematic showing one formation susceptible to WCD (modified after SPE Report, 2015). ....  | 48 |
| Figure 3. 16. Subsea containment systems “capping stacks”. a) Cap only system. b) Cap and flow system (modified after Wood Group Kenny, 2016). ....  | 49 |
| Figure 4. 1. Wellhead oil rate and pressure with time. The three dotted black lines separate the four modeling steps described in the workflow. Blowout (WCD) is modeled for 30 days, followed by capping shut-in in incident wellbore for 10 days, then mud is injected at three different rates from the relief well for a total period of 30 days, this is lastly followed by the last period which is composed of 20 days of incident wellbore shut-in and no mud injection from the relief well. .... | 55 |
| Figure 4. 2. Fracture 5 height and length shown against wellbore block pressure where the fracture has occurred. ....  | 56 |
| Figure 4. 3. Fracture 5 pressure drops as the fracture starts propagating. Substantial drop appears as the fracture grows in height. ....  | 57 |
| Figure 4. 4. Fracture 5 pressure at wellbore with oil rate flowing into the fracture shown against time. ....  | 58 |



|   |    |
|---|----|
| Figure 4. 5. Reduction in produced oil from the reservoir into the wellbore as kill-mud is injected through the relief well. The mud density with the optimal injection rate compensates the produced oil and ceases flow 6 hours after injection through lateral hole.....       | 59 |
| Figure 4. 6. Schematic cross section of the model with wellbore shown in center. Fracture 5 growth after 4 days of abrupt capping shut-in. Fracture shading shows the fluid velocity inside the fracture. Warmer regions indicate areas of high fluid velocity.....               | 60 |
| Figure 4. 7. Top view of the model. Straight black line shows the propagating fracture approximated on a 2D plane. The perpendicular blue line is a top view of the relief well intersecting the main wellbore. ....  | 61 |
| Figure 4. 8. Fluid density shown in wellbore before kill mud is injected through the relief well at 40.16 days. Wellbore is filled with low density hydrocarbons shown by the colder colors.....  | 62 |
| Figure 4. 9. Fluid density shown in wellbore after kill mud injection through relief well at 40.26 days. Wellbore fluid density increases as high-dense kill mud fills the wellbore. Yellower regions indicate areas where less dense fluid (hydrocarbons) is still present. .... | 63 |
| Figure 4. 10. Fluid density shown in wellbore after kill mud injection through relief well at 40.42 days. Kill mud has successfully displaced the hydrocarbons and filled the wellbore. ....  | 64 |
| Figure 4. 11. Well head oil rate, capping shut-in pressure, and relief well injection rates as a function of time. The fluctuations shown in red is due to transient liquid slugs in the incident wellbore.....   | 66 |
| Figure 4. 12. Pressure at wellbore where the fracture has initiated and oil rate flowing into the fracture. Oil rate in the fracture displays an increase with time owed to the fracture broaching to the seafloor.....   | 67 |
| Figure 4. 13. Fracture pressure at wellbore with height and length shown as a function of time. ....  | 68 |
| Figure 4. 14. Graphical illustration of the propagating fracture 2 at the 26” surface casing broaching into the seafloor close to the well head. Fracture shading shows the fluid velocity inside the fracture.....   | 69 |
| Figure 4. 15. Well head oil rate, capping pressure, and relief well injection rates as a function of time for fracture 3 at 20” surface casing shoe location. Significant drop in wellhead pressure is due to fracture initiation 3,000 ft below wellhead. ....                   | 70 |
| Figure 4. 16. Fracture 3 pressure at wellbore and oil rate shown with time. Significant oil is supplied into the fracture resulting in a drop in wellbore pressure.....   | 71 |
| Figure 4. 17. Fracture 3 height and length. The rise in oil rate shown in figure 4.16 is due to the rapid fracture growth occurring upon initiation, evident here. ....   | 72 |
| Figure 4. 18. Graphical representation of fracture 3 initiating at 20” surface casing shoe location upon broaching into the seafloor.....   | 73 |

|   |    |
|---|----|
| Figure 4. 19. Well head oil rate, capping (WH) pressure, and relief well injection rates as a function of time for fracture 4 at 16” drilling liner shoe location.....  | 75 |
| Figure 4. 20. Fracture 4 pressure at wellbore and oil rate into the fracture shown with time. Significant oil is supplied into the fracture resulting in a drop in wellbore pressure. ....                    | 76 |
| Figure 4. 21. Fracture 4 height and length. The rise in oil rate shown in figure 4.20 is due to the rapid fracture growth occurring upon initiation. ....   | 77 |
| Figure 4. 22. Fracture 4 shown broaching into the seafloor 1.5 days after initiating. The fracture length exceeds the dimensions of the model resulting in fracture growing in the external grid blocks. .... | 78 |
| Figure 4. 23. Well head oil rate, mud rate injection, and well head pressure for the perfect casing integrity case study. ....  | 79 |
| Figure 4. 24. Fracture pressure at wellbore block shown with height and length. No fracture initiated; hence straight line is shown. ....   | 80 |
| Figure 4. 25. Fracture height variation against time for four different $Esh$ values. ....  | 82 |
| Figure 4. 26. Fracture length variation against time for four different $Esh$ values. ....  | 83 |
| Figure 4. 27. Reservoir over-pressure variation with fracture height as the dependent variable. ..  | 85 |
| Figure 4. 28. Fracture height with time for different well blowout periods. ....  | 87 |
| Figure 4. 29. Fracture length with time for different well blowout periods. ....  | 87 |
| Figure 4. 30. Fracture height with time for different relief well intervention periods.....   | 88 |
| Figure 4. 31. Fracture length with time for different relief well intervention periods.....   | 89 |
| Figure 4. 32. Fracture height comparison using different wellbore models for transient and steady-state conditions. Capping shut-in appeared 30 days after blowout. ....                                      | 92 |
| Figure 4. 33. Fracture length comparison using different wellbore models for transient and steady-state conditions. ....  | 93 |
| Figure 4. 34. Fracture height comparison for the multiphase flow model.....   | 94 |
| Figure 4. 35. Fracture length comparison for the multiphase flow model.....   | 95 |

## **Nomenclature**

WCD = Worst-Case Discharge

BOEM = U.S. Bureau of Ocean Energy Management

BSEE = U.S. Bureau of Safety and Environmental Enforcement

GoM = Gulf of Mexico

OCS = Oceanic Continental Shelf

APD = Application for permit to drill

OSRP = Oil spill response plan

HTHP = High Temperature and High Pressure

WCST = Well containment screening tool

SCCE = Source Control and Containment Equipment

RT = Rotary Table

BOP = Blowout Preventer

BHP = Bottom-hole Pressure, psi

WHP = Wellhead Pressure, psi

WH = Wellhead

TVD = True Vertical Depth, ft

PETEX = Petroleum Experts

2D = Two-Dimensional

3D = Three-Dimensional

ID = Internal Diameter, in

OD = Outside Diameter, in

CFR = Code of Federal Regulation

LMRP = Lower Marine Riser Package

PA = Plugging and Abandonment

WCST = Well Containment Screening tool

CFR = Code of Federal Regulations

IPR = Inflow Performance Relationship

VLP = Vertical lift profile

LOP = Leak-off Point, psi

LT = Limit Test

FIT = Formation Integrity Test

FBP = Fracture Breakdown Pressure, psi

FIP =  $p_i$  = Fracture Initiation Pressure, psi

FPP = Minimum Fracture Propagation Pressure, psi

ISIP = Instantaneous Shut-in Pressure, psi

FCP = Fracture Closure Pressure, psi

$E$  = Young's Modulus, psi

$\nu$  = Poisson's Ratio

$A$  = Biot's poroelastic constant

$\alpha_B$  = Biot's poroelastic coefficient

$S_{Hmax}$  = Maximum Horizontal Stress, psi/ft

$S_{hmin}$  = Minimum Horizontal Stress, psi/ft

$S_v$  = Overburden Stress, psi/ft

$p_p$  = Pore Pressure, psi

$p_w$  = Wellbore pressure, psi

$T$  = Rock Tensile Stress, psi

PVT = Pressure-Volume-Temperature

## **Abstract**

Broaching is defined as the uncontrolled release of hydrocarbons to ocean seafloor after a loss of subsurface well control event. Failed attempts to cap the offshore wells undergoing worst case discharge may lead to hydraulic fracture initiation and subsequent propagation, leading to renewed release of hydrocarbon to the seafloor. During the capping stack shut-in process, pressure build-up will occur along the wellbore, exposing locations of possible fracture initiation to overpressurized fluid, such as directly below the casing shoe, and critical points along the well casing. Shall there be enough build-up pressure to exceed the minimum horizontal stress in an exposed layer, a fracture will initiate and may propagate as energy is provided from the movement of fluids in the wellbore. This can lead to a severe environmental impact on marine ecology if the fracture broaches to the seafloor. A quintessential example of fracture broaching during post-blowout is the Santa Barbara Channel Alpha Well 21 blowout in 1969 which resulted in an oil slick discovered near the discharging well. To help evaluate the possibility of such an event occurring in offshore waters of the Gulf of Mexico, numerical modeling is performed on a hypothetical case study using deepwater parameters examining the propagation of a “longitudinal” (i.e., parallel to the axis along the center of the wellbore) fracture during the containment or capping shut-in period. A workflow is developed for Worst Case Discharge (WCD) calculation, assessment of fracture initiation, propagation, and broaching during the capping shut-in period, and relief well heavy-mud injection strategy. A transient wellbore model accurately captures the fracture properties as they grow in height and length. The results of this study show that the growth of a fracture initiated from the side of the wellbore is sensitive to depth of the casing shoe where the fracture had initiated, young’s modulus of overburden rocks, and the duration of the preceding discharge period. In

addition, sufficient mud density, and pump rate are needed to compensate the oil column and successfully kill the main wellbore.

## **1. Introduction**

Nearly 11 years have passed since the 2010 BP Deepwater Horizon MC 252-1 incident, claiming 11 lives, and releasing approximately 4.2 MMSTB of oil in the Gulf of Mexico (GoM) Oceanic Continental Shelf (OCS) region (Buchholz et al., 2016). This catastrophic event led government, industry, and researchers to recognize the possibility of a similar disaster occurring again. As drilling activities are progressively moving towards high temperature and high pressure (HTHP) deepwater reservoirs, wells at these depths undergoing a blowout may be vulnerable to unsuccessful capping attempts. According to the Bureau of Ocean Energy Management (BOEM), worst case discharge (WCD) is defined as the single highest daily flow rate of liquid hydrocarbon during a blowout event. In the unfortunate event of a failed subsurface containment system following a WCD period, an underground blowout may occur allowing hydrocarbons to migrate through the geological media leading to seafloor broaching. Figure 1 shows examples of the qualitative ranking of the potential to broach using different favorable and unfavorable failure pathways described by the geoscientists of BOEM. Significant advances in subsea well control response and oil remediation have resonated based on learnings from the Macondo disaster; nevertheless, limited research has addressed the possibility of a broaching event resulting from a well containment failure. (Hickman et al., 2011) analyzed wellhead pressure, investigated geological risks, and geophysical data monitoring and acquisition during shutting in the Macondo well. (Bjerstedt et al., 2020) studied the impact of overburden layers' permeability and the reservoir saturation levels for water, oil, and gas on broaching traveltime. Research areas on Source Control and Containment Equipment (SCCE) such as the impact of subsea capping stack on the blowout source and the process of regaining well control by drilling a relief well need improved understanding. Mitigating these risks is crucial, given the significant environmental impact such



an incident may cause; therefore, modeling wellbore capping failures post-blowouts is necessary to determine the key factors leading to broaching. The GoM region is of major interest owed to its active rich oil exploration and production activity, which is why the focus of this study is on typical stacked geological patterns found in the GoM OCS region. According to the Bureau of Safety and Environmental Enforcement (BSEE), 91 percent of total U.S. oil and gas production occur in the GoM OCS region with 20 percent of WCD volume and rate calculations happening in deepwater (Buchholz et al., 2016).

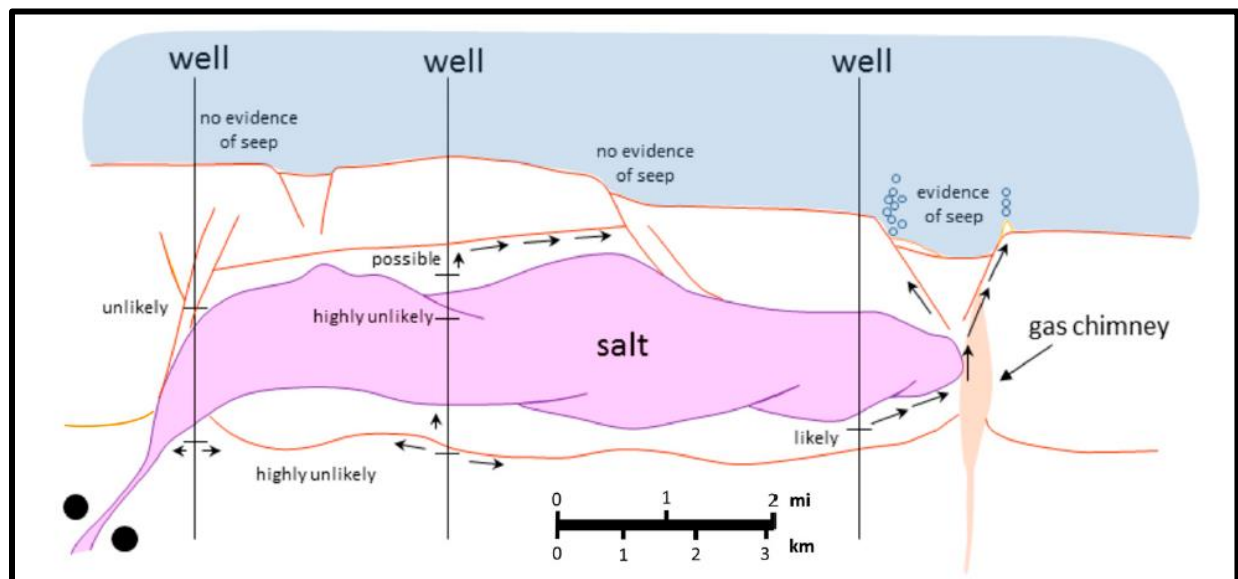


Figure 1. 1. Diagram showing examples of qualitative ranking BOEM geoscientists have conducted on favorable and unfavorable pathways leading to broaching of hydrocarbons (Bjerstedt et al., 2020) (reprinted by permission of the AAPG whose permission is required for further use).

## 1.1. Background

A WCD is an event could be associated with drilling and completions, workover, and even production operations (Willson, 2012). Kill attempts to regain control of the well include but are not limited to installing equipment on the failed blowout preventer (BOP), open pipe, or lower marine riser package (LMRP), as well as drilling a kill well laterally to intersect the uncontrolled

flowing well to dynamically bring the well under control by injecting high-density mud. During an event of loss of well control, one of the well intervention response plans of shutting in the well defined by the government and facility owners', involves positioning a capping stack on the spill source to cease hydrocarbon flow until the well is successfully plugged by drilling a relief well. Indicated in this study, under certain circumstances (extremely high WCD > 200,000 STB/day and imperfect cement jobs or casing collapse locations), wellbore pressure buildup may result in pressure exceeding fracture initiation pressure ( $p_i$ ) in a geologic layer. Fluids injected into the fracture provided by the high-energy reservoir will work to advance the fracture tip shall there be enough propagation pressure. The fracture(s) can propagate upward through the geological media and potentially broach into the seafloor or a shallow formation where they may be contained. Upon fracture initiation, the discharge fluid will exhibit a flowrate higher than the fluid loss rate into the formation during which new fracture pathways continue to expand and grow. The fracture will stop growing when the fluid pressure in the fracture minus the formation pore pressure (net pressure) becomes equal to  $S_{hmin}$  (or closure stress also known as the minimum horizontal stress) (Kholy et al., 2019). Using a robust numerical simulator, stress/strain relationships are coupled with fluid flow relationships creating a complex fracture mesh topology, evaluating fracture properties, and computing new crack pathways at each time-step. The introduced three-dimensional fracture geometry assumes linearly elastic solid behavior in response to pressure changes in the crack face. Initial simulation runs will consider a two-dimensional (2D) planar longitudinal fracture.

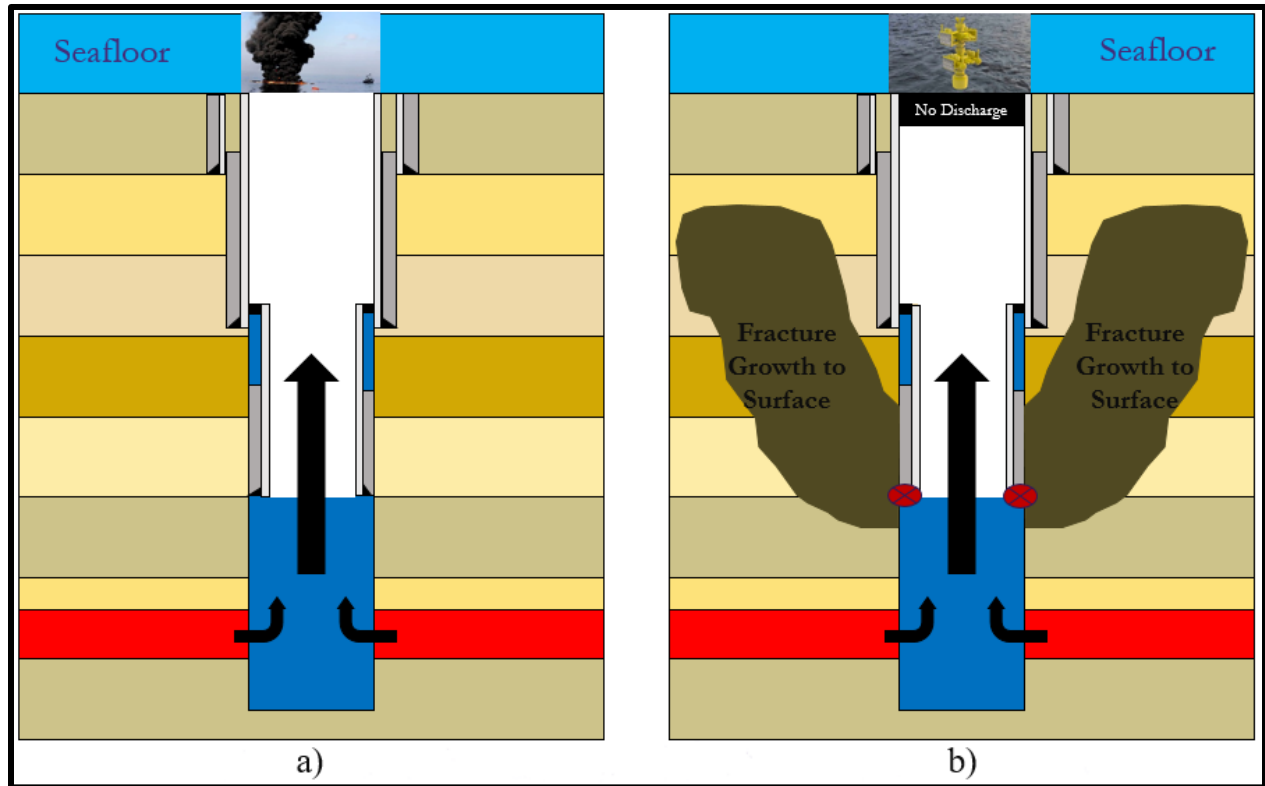


Figure 1. 2. Comparison of wellbore integrity state a) in a blowout condition compared to b) a damaged wellbore where in a potential critical point along the wellbore (shown at casing shoe) a fracture has initiated due to high wellbore pressure (modified after Zaki et al., 2015).

Several reasons can lead to the possibility of fracture initiation along a wellbore following a WCD scenario;

1. Fluid flow in an uncontrolled blowout will cause a significant rise in pressure along the wellbore walls, causing a large pressure differential to occur in any casing having a confined annulus between it and the formation. Internal wellbore pressure will be drastically lower than the adjacent hydrostatic pressure located externally to the casing resulting in a casing collapse. Consequently, the failed casing point may allow hydrocarbon leakage and after successful capping shut-in, pressure build-up may surpass  $p_i$ , leading to fracture initiation (Zaki et al., 2015).

2. In the case of a poor cement job, a void (microannulus) will exist between the formation and the external side of the casing. Subsequently, providing a potential leaky pathway for the overpressurized hydrocarbons to flow after exiting the well and initiate a fracture in the formation.
3. Assuming no casing collapse and perfect cement integrity, a fracture may also originate in the open-hole section close the last/deepest positioned casing.

Moreover, a fracture will initiate and tend to propagate for a certain period of time. Propagation of fractures can provide a pathway for hydrocarbon fluids to broach into the seafloor causing a major ecological disaster. Classic examples of unsuccessful capping attempts resulting in seafloor broaching is the 1969 Union Oil's Channel Alpha Well 21 blowout and oil spill in Santa Barbara, California. In the Macondo well, concerns regarding the collapsed rupture disks in the 16-in" drilling liner surfaced as an oil slick approximately 2 miles of the well was detected by numerous spill response vessels only 2 days after capping shut-in (Bjerstedt et al., 2020). However, further analyses postulated that the oil slick was due to a natural fault in the basin. Figure 1.3 shows the location of the rupture disks in the well design and lithology section based upon analysis of data acquired during drilling.

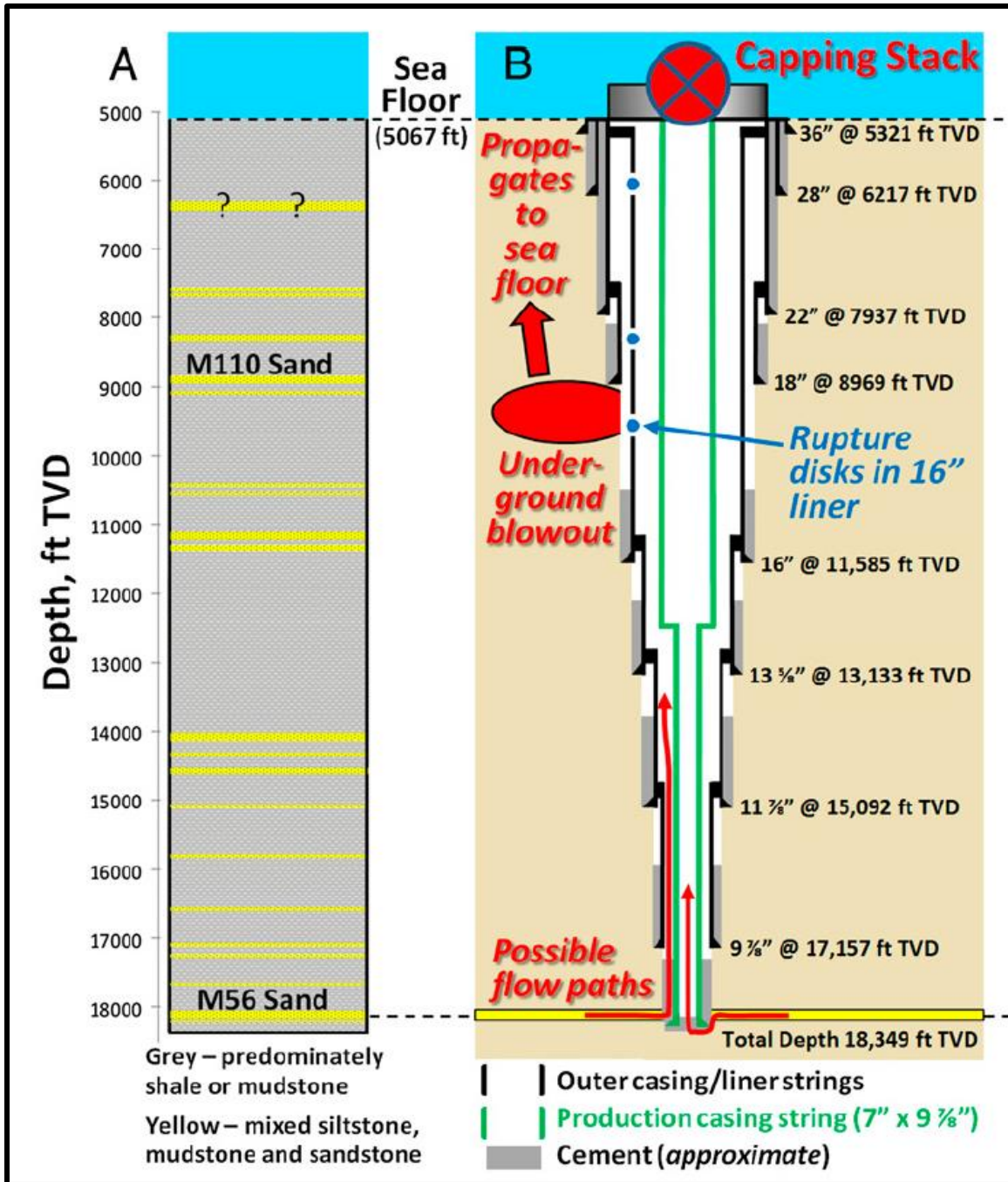


Figure 1. 3. Schematic of BP 001 Macondo Well design and lithologic section based upon analysis of data acquired during drilling. Red lines show possible flow paths of hydrocarbons that may have occurred during the blowout. An underground blowout may have formed with a possible propagating fracture as shown at the 16" linear due to a ruptured disk (reprinted by permission of PNAS whose permission is required for further use).

Following the Macondo disaster, significant advances in WCD estimation and evaluation of wellbore integrity have been published while limited reviews were performed on the possibility of broaching due to capping shut-in. BOEM requires that for every permit to drill an offshore well, the facilities operator must provide a blowout scenario in the initial plan. One of the main drawbacks of the required blowout scenario is that it suffers from evaluating the impact of shutting in the well and the duration upon which a relief well should be drilled before failure of containment takes place. The blowout plan is limited to only provide estimations of WCD calculations, availability, type, and capabilities of subsea capping stack as well as the nearest capable rig of drilling a relief well. Table 1.1 provides the blowout scenario required by BOEM as referenced by NTL 2010 – N06a.

Table 1. 1. Required blowout scenario by BOEM as referenced in NTL 2010 - N06a.

| <b>1) Blowout Scenario</b> |  |
|----------------------------|--|
| <b>a)</b>                  | Estimated flow rate (STB/day)  |
| <b>b)</b>                  | Maximum duration of blowout (days)   |
| <b>c)</b>                  | Total volume of spill (STB)  |
| <b>d)</b>                  | Discussion of potential bridging   |
| <b>e)</b>                  | Discussion of likelihood for surface intervention to stop blowout  |
| <b>2) Relief Well</b>      |  |
| <b>a)</b>                  | Identification of rig type capable of drilling a relief well in a timely manner  |
| <b>b)</b>                  | Rig package constraints  |
| <b>c)</b>                  | Estimated time to drill a relief well, including: <ul style="list-style-type: none"> <li>I. Time to acquire a rig (days)</li> <li>II. Time to move rig onsite (days)</li> <li>III. Drilling time (days)</li> </ul> |
| <b>d)</b>                  | Statement whether the possibility of using a nearby platform was considered, if feasible   |

(table cont'd.)

| <b>3) Others</b> |  |
|------------------|--|
| <b>a)</b>        | Measures to enhance ability to prevent a blowout   |
| <b>b)</b>        | Measure to reduce the likelihood of a blowout  |
| <b>c)</b>        | Measure to enhance ability to conduct effective and early intervention in the event of blowout |
| <b>d)</b>        | Arrangements for drilling relief wells   |
| <b>e)</b>        | Any other measures   |

Furthermore, BSEE provides operators with current and periodically updated Code of Federal Regulations (CFR) with information regarding oil and gas drilling, lease planning, well design, well control, well completion, workover rig regulations, production operations, and plugging and abandonment. Provided under the name “Oil and Gas and Sulphur Operations in the Outer Continental Shelf” and referred to as (30 CFR 250), these plans and requirements, include minimum BOP system capabilities, and well control regulations. Table 2.1 provides complete list with subparts, numbering, and titles as of January 27<sup>th</sup>, 2021.

Table 1. 2. Subparts of 30 CFR 250 by BSEE.

| <b>Subpart</b> | <b>CFR Numbering</b> | <b>Subpart Title</b>  |
|----------------|----------------------|---|
| <b>A</b>       | §250.101             | General   |
| <b>B</b>       | §250.200             | Plans and Information   |
| <b>C</b>       | §250.300             | Pollution Prevention and Control                                      |
| <b>D</b>       | §250.400             | Oil and Gas Drilling Operations                                       |
| <b>E</b>       | §250.500             | Oil and Gas Well-Completion Operations                                |
| <b>F</b>       | §250.600             | Oil and Gas Well-Workover Operations                                  |
| <b>G</b>       | §250.700             | Well Operations and Equipment   |
| <b>H</b>       | §250.800             | Oil and Gas Production Safety Systems                                 |
| <b>I</b>       | §250.900             | Platforms and Structures  |
| <b>J</b>       | §250.1000            | Pipelines and Pipeline Rights-of-Way                                  |
| <b>K</b>       | §250.1150            | Oil and Gas Production Requirements                                   |
| <b>L</b>       | §250.1200            | Oil and Gas Production Measurement, Surface Commingling, and Security |
| <b>M</b>       | §250.1300            | Unitization   |

(table cont'd.)

| Subpart  | CFR Numbering | Subpart Title                                      |
|----------|---------------|--|
| <b>N</b> | §250.1400     | Outer Continental Shelf Civil Penalties            |
| <b>O</b> | §250.1500     | Well Control and Production Safety Training        |
| <b>P</b> | §250.1600     | Sulphur Operations                                 |
| <b>Q</b> | §250.1700     | Decommissioning Activities                         |
| <b>R</b> | §250.1800     | <i>**Reserved</i>                                  |
| <b>S</b> | §250.1900     | Safety and Environmental Management Systems (SEMS) |

As operators continue to explore for recoverable hydrocarbon resources, offshore oil and gas drilling is advancing into deepwater prospects. More challenges emerge to drillers as narrower drilling margins are expected, increasing the possibility of a kick events leading to blowouts. Although the probability of a blowout occurring with spill volume over 1 MMSTB or more is only 0.6 percent (Buchholz et al., 2016), the likelihood is likely to increase as we move into deepwater and ultra-deepwater HTHP wells. It is essential to model such wellbore failure occurrences to enhance our understanding of wellbore integrity, well control and mitigation efforts, and assess the possibility of broaching post-blowout capping.



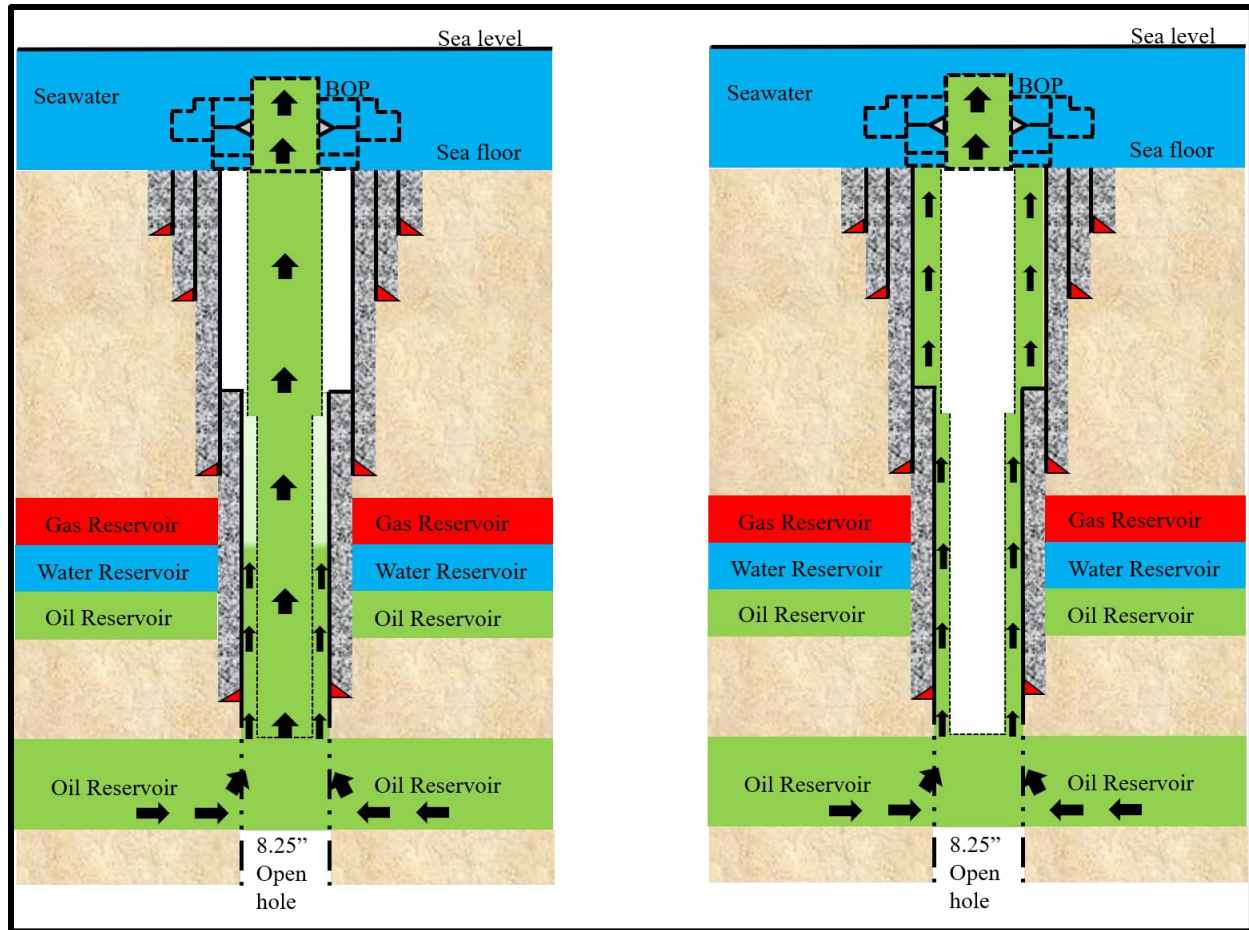


Figure 1. 4. Two potential fluid paths that may occur during an uncontrolled flow of hydrocarbons scenario. a) Flow through the production casing. b) Flow through the seal assembly (modified after Bartlit et al., 2011).

## 1.2. Research Hypotheses and Objectives

The objective of this work is to investigate fracture initiation and fracture growth through porous media caused by excess wellbore pressure buildup resulting from containment system “capping stack” shut-in. A novel workflow is designed for WCD estimation, evaluation of fracture initiation and growth post shut-in, and relief well mud injection strategy for a successful kill. A set of loss of well control situations will be assessed to investigate the possibility of fracture initiation, upward propagation in the geologic media, and potential broaching into seafloor.

The secondary goals are to evaluate and quantify the factors influencing fracture growth and potential for broaching during post-blowout capping shut-in. These factors would include different scenarios of casing shoe depth, cement job integrity, variation in reservoir pressure, and geomechanical rock properties such as young's modulus. Other factors would incorporate longer periods of WCD discharge period, and relief well intervention time.

### **1.3. Thesis Outline**

This thesis is divided into five chapters. Chapter 1 presents a brief introduction of the problem, research hypotheses and objectives, and motivation of this research. Chapter 2 consists of the literature review related to current WCD workflow, killing methods including capping shut-in types and relief well drilling in deepwater, occurrences of broaching events, and fracture criteria and height containment following well capping. Chapter 3 describes the proposed workflow, governing equations used in the simulator, base case model description, sensitivity analyses to be conducted to evaluate broaching, as well as the detailed methodology used for modeling the WCD period, shut-in period, and relief well injection strategy. Chapter 4 presents the results and discussion for the different scenarios and case studies described in Chapter 3. Lastly, Chapter 5 describes the conclusions and recommendations for future work. Appendix A introduces the workflow used for the base case model. Appendix B displays the permissions for published work used in this research.

## 2. Literature Review

### 2.1. Overview

To study and understand the problem at hand, two main terms commonly used throughout this paper are defined; WCD and Broaching. First and foremost, BOEM defines WCD as the single highest daily flow rate of liquid hydrocarbon during an uncontrolled wellbore flow event (SPE Report, 2015). The continuous uncontained release of fluids (oil, gas and water) from the well source into the environment, either through a BOP, open-pipe, or LMRP is known as a well blowout. An oil spill is a consequence of a blowout event. Table 2.1 shows the top 5 largest spilled volumes over the duration of the blowout in offshore blowouts occurring in the US.

Table 2. 1. Top five US largest offshore well blowouts, ordered by volume (Buchholz et al., 2016).

| Well                               | Date      | Duration (days) | Region  | Total Discharge Volume (STB) |
|------------------------------------|-----------|-----------------|---------|------------------------------|
| <b>Deepwater Horizon MC252</b>     | 4/20/2010 | 84              | GoM     | 4,200,000                    |
| <b>Alpha Well 21 Platform A</b>    | 1/28/1969 | 11              | Pacific | 80,000 – 100,000             |
| <b>Main Pass Block 42</b>          | 2/10/2970 | 30              | GoM     | 65,000                       |
| <b>ST-26B</b>                      | 12/1/1970 | N/A             | GoM     | 53,000                       |
| <b>Greenhill Timbalier Bay 251</b> | 9/29/1992 | 14              | GoM     | 11,500                       |

Published reviews of past blowout occurrences and their killing methods are mostly on shallow water drilled wells, which are not representative of current and future deepwater wells, the main focus of this thesis. The Union Oil Santa Barbara Well 21 in 1969 and the Gulf of Mexico British Petroleum (BP) Deepwater Horizon MC252 Well 001 in 2010 blowouts are quintessential examples of deepwater oil spills with significant oil volume over the duration of the spill. In the wake of the Macondo accident, significant number of research focusing on WCD rate and volume calculation has emerged (Liu et al., 2015; Cordoba, 2018).

In response to a blowout incident, planned regulations for SCCE procedures intended to stop or divert the uncontrolled hydrocarbons from wellhead to a containment vessel, include subsea capping stack installation as a containment system. Moreover, conditions of the wellbore may result in casing collapse to occur along weak casing points in the preceding discharge period prior to capping shut-in. Failure at the referenced casing point(s) may allow hydrocarbon leakage and with enough build-up pressure to exceed the exposed formation fracture initiation pressure during the shut-in process, a fracture will initiate leading to an underground blowout. Provided that an adequate energy from the reservoir to the wellbore exists, fracture propagation driven by the hydrocarbons flowing from the damaged wellbore to the fracture tip will allow for further fracture encroachment (Zaki et al., 2015). Bowman (2012) discussed the effects of WCD on casing design while Wu (2013) considered improvements on casing designs to withstand extreme WCD scenarios. Waltrich et al., (2019) investigated two-phase flow in large diameter pipes under worst case discharge scenario. An underground blowout may ultimately result in broaching. Secondly, according to Bjerstedt et al., (2020), broaching is defined as the uncontrolled discharge of hydrocarbons at the seafloor after subsurface well containment failure. Zaki et al., (2015) examined the potential for leak pathways from casing to seafloor along geological media after the well is capped. Michael and Gupta (2020) analyzed geomechanics of fluid driven fracture initiation and the impact of depleted reservoirs on propagation. Furthermore, to successfully kill the well after it has been capped, a kill well, also known as a relief well, is drilled at a safe distance adjacent to the discharging wellbore. The relief well is designed to intersect the main wellbore at a certain point so that high-density mud can be injected into the incident wellbore to ensure sufficient hydrostatic mud column compensates the oil column and successfully stop the reservoir from delivering hydrocarbons into the wellbore (IOGP, 2020). After this process is completed and

adequate downhole pressure is achieved, cement plugs are placed in the borehole through the relief well to prevent migration of fluids up the wellbore and between distinct geological layers. This is followed by a plugging and abandonment (PA) operation. Lage et al., 2016 assesses relief well planning post-WCD and capping.

## **2.2. Offshore Killing Methods**

It is important to mention that surface, shallow and deepwater well killing or intervention methods are different in terms of SCCE operations. Several methods are deployed to bring the well under control; a static kill method known as the weighted mud involves pumping mud through coiled tubing via a gate valve from the capping stack into the existing well's metal casing pipes. The injected mud would then force the hydrocarbons back down the annulus into the reservoir. This process is then followed by cement injection to seal the well (API RP 16ST). Other methods involve shutting-in the well by just installing and positioning a subsea capping stack over the BOP, open-pipe, or LMRP. Depending on conditions of the BOP or the riser pipe, a containment dome may be lowered on the vicinity of the leak to contain and separate the escaping fluid into the environment and divert it into a floating vessel (Andreussi, H.P., and De Ghetto, G., 2013). Figure 2.1 shows killing methods used for blowout occurrences in shallow marine wells. According to Willson, 2012, natural causes, such as reservoir depressurization (depletion), water breakthrough from exposed water-bearing formations, wellbore instability and collapse, cavings transport, and even bridging at choke points by sands and formation solids transported with the hydrocarbons are more likely to be encountered in shallow water than in deepwater. Self-killing methods such as bridging and reservoir depletion are less likely to occur in deepwater wells due to the inherent higher pressures and more prolific oil reservoirs encountered (Willson, 2012). Therefore, this

research focuses on evaluating kill attempts using methods such capping shut-in and relief well drilling more likely to occur in deepwater HTHP wells.

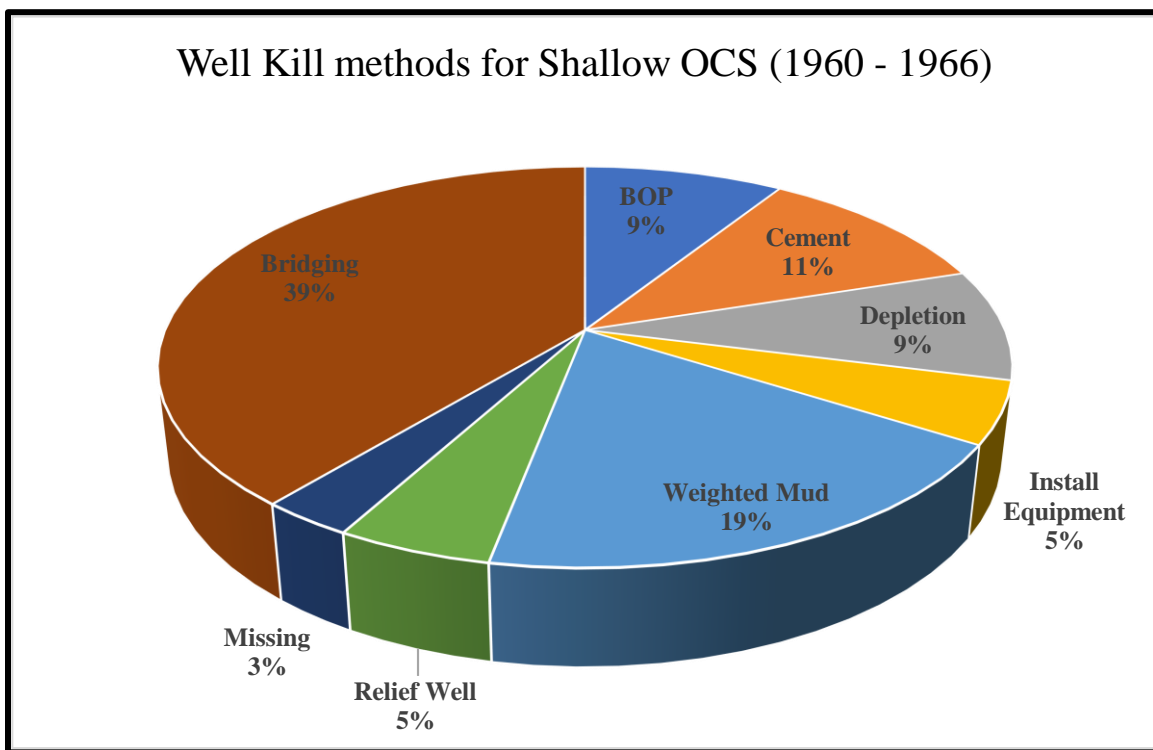


Figure 2. 1. Percentage of well kill methods for OCS in shallow depth blowouts (produced with data taken from Skalle et.al, 1999).

For activities in both shallow water (< 500 ft) and deepwater ( $\geq 500$  ft), BSEE requires an oil spill and response plan (OSRP) from operators of the oil and gas wells. The OSRP determines the procedures and spill response resources necessary to respond in an adequate timeframe to the facilities' WCD (Buchholz et al., 2016). This plan would include the type of subsea capping equipment accessible in case of a spill event and the deployment time after initial blowout given potentially minor delays such as slightly unfavorable weather conditions, government approval, and near-wellhead subsurface debris removal (Buchholz et al., 2016). It is important to note that, BSEE and BOEM, conduct analysis of likelihood of broaching in the event of a failed capping system only after a capping system has failed the well containment screening tool (WCST), which

is processed after a blowout has occurred, such as in the case of the Macondo well (Bjerstedt et al., 2020). The process of broaching analysis at potential failure point in the wellbore, led by BOEM geoscientists can be very time-consuming (up to more than 3 months) per Bjerstedt et al. (2020). If the analysis concluded that broaching is likely to occur, BSEE would require a cap and flow system and rig capable of drilling a relief well on standby; otherwise, a cap only system would be used. BSEE and BOEM indicate that operators must specify and estimate the duration of days required to move and deploy at least one suitable rig to the WCD location to complete drilling a relief well operation and successfully stop flow of oil to the environment. Refer to Table 1.1 for required blowout scenario by BOEM as referenced in NTL 2010 - N06a.

### **2.3. Workflow for WCD Calculation**

As part of the OSRP for shallow or deepwater OCS, BSEE requires that each operator conduct its own WCD calculation for every well to be drilled. A WCD scenario calculation should include highest daily flow rate of liquid hydrocarbon during an uncontrolled wellbore flow event, daily discharge rates, and total volume discharged into the environment over the duration of the spill. Equation 1 illustrates how the total volume of spill is calculated using daily flow rates obtained from nodal analysis or numerical simulations.

$$Total\ volume\ of\ spill\ (STB) = Average\ flowrate\ \left(\frac{stb}{day}\right) * Duration\ of\ spill\ (days) \quad (1)$$

In a recent analysis, BSEE identified 288 loss of well control situations occurring between 1956 and 2010, concluding that only 8 scenarios involve a WCD of oil into the environment (Herbst, 2014). Figure 2.2 presents the percentage of each loss of well control incident occurring between 2006 and 2013.

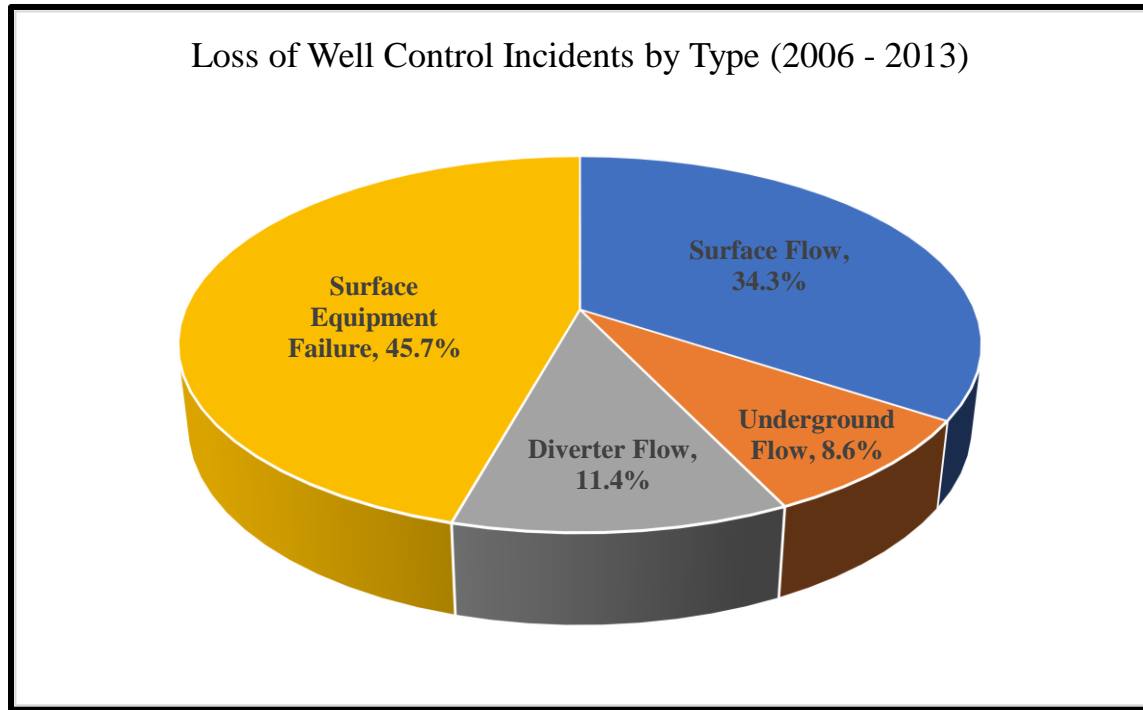


Figure 2. 2. Loss of well control incidents by type from 2006 to 2013 (produced from data taken from Buchholz et al., 2016).

The workflow adapted in this study is based on Cordoba (2018) which outlines detailed steps for modeling WCD under extreme conditions using nodal analysis and reservoir simulation following SPE 2015 report guidelines. Figure 2.3 shows the workflow used to model WCD using conventional nodal analysis. The novelty of this approach is that it can easily be replicated using other software packages like MS Excel (Cordoba, 2018). The workflow was validated by the specialized reservoir simulator *REVEAL* by Petroleum Experts (PETEX), which is the reservoir simulator utilized in this study.



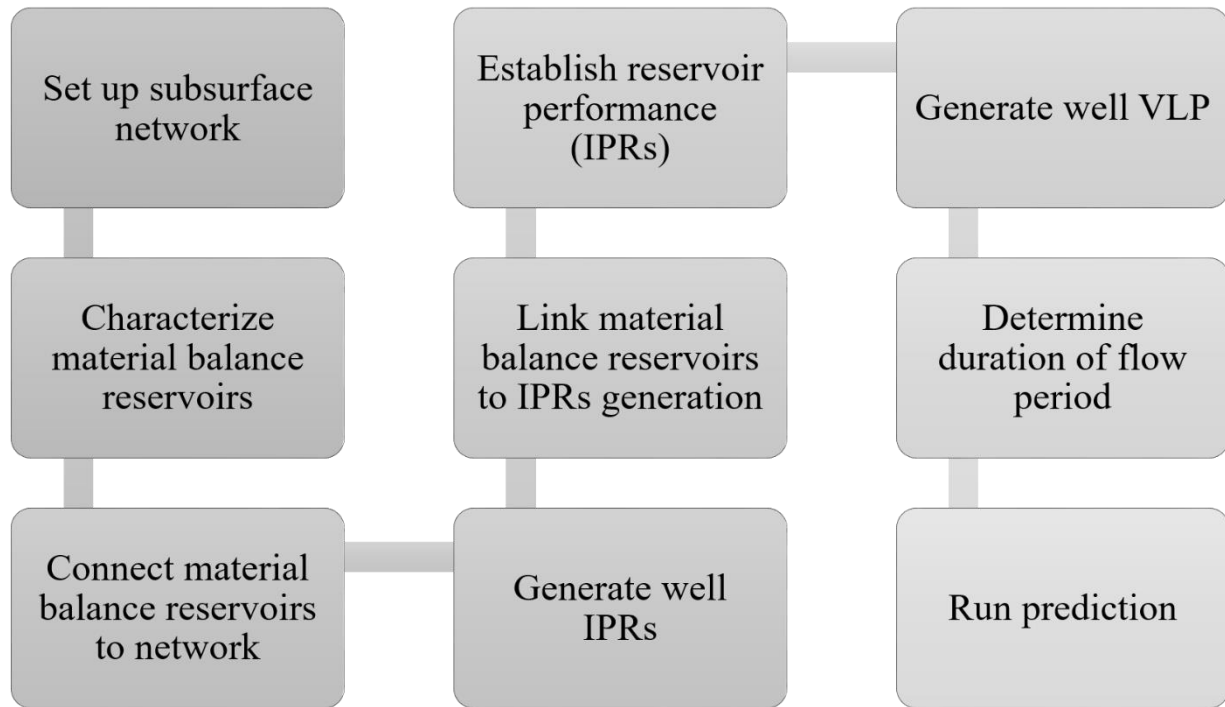


Figure 2. 3. Workflow proposed by Cordoba (2018) for modeling WCD scenarios under extreme blowout conditions using conventional nodal analysis approach (starting from top left to bottom right, flowchart constructed from information taken from Vasquez Cordoba, 2018).

## 2.4. Occurrences of Broaching

The 2010 BP Macondo disaster has made the industry become aware of the risk of containment failure and consequently broaching of hydrocarbons. Broaching studies have received wide attention in the past decade as operators have switched to the possibility of broaching occurring during the capping shut-in period (Hickman et al., 2012; Bjerstedt et al., 2020). In such a situation, a hydraulic fracture would initiate along critical points in the casing and have the propensity to propagate upward until it is either arrested by a shallower containment layer(s) or broach to the seafloor (Zaki et al., 2015; Elnoamany et al., 2020). In the latter case, additional disaster would emerge as more hydrocarbons can flow through the fracture. Broaching of an underground blowout can release significant amounts of hydrocarbons into the seafloor, which would be very time-consuming and costly to observe, and extremely hard to stop contain. As far

as the author's knowledge, no research has attempted to exploit methods and ways to mitigate and stop hydrocarbons encroaching to the seafloor via fracture broaching. Broaching of fluids is likely to occur several hundred feet and up to miles from the capped wellhead (McNutt, 2012). The 1969 Santa Barbara blowout (Easton RO, 1972), the 2008 Tordis, North Sea incident (Eidvin and Overland, 2009), and the 1974 and 1979 Campion Field, Brunei blowouts (Tingay et al, 2005) are prime examples of broaching events (Hickman et al., 2012). According to McNutt, 2012 while a fracture can broach several miles away from the wellhead, a broach can occur much closer to the wellhead such as in the case of the Macondo well, leading to severe wellhead stability and possibility of soft-sediment erosion in the annulus region. Recently, remote operating vehicles used to explore the ocean seafloor for seep and slick oil locations have observed multiple seep locations near the Macondo wellhead. Several geologists have concluded that broaching far from the wellhead has occurred in the Macondo incident, however BOEM's water-bottom seismic anomaly mapping program concluded that this is a result of natural seepage in the basin.

Moreover, oil and gas wells are not the only wells susceptible to broaching, wells related to surface broaching as well as extensive cratering are associated with steam flood operations in heavy oil reservoirs (Energy Resources Conservation Board, 2010) and geothermal energy wells (Bolton et al, 2009), which have been reported in literature and have been suggested to be involved in the Lusi mud eruption in East Java (Davis et al, 2010; Sawolo et al, 2010).

## **2.5. Fracture Initiation, Propagation and Closure in Porous, Permeable Media**

Tensile, "Mode I" fractures "open" by doing work against the least compressive stress  $S_{hmin}$  (minimum horizontal stress) in the subsurface (Michael, 2016). The work required for rock tensile failure can be provided by fluid pressure. Fluid-driven fracturing and height containment in layered media was researched by numerical modeling (Simonson et al., 1978; Zhang et al., 2007;

Liu et al., 2015; Yue, 2017), laboratory-scale experiments (Teufel and Clark, 1984; Wu et al., 2008; Ispas et al., 2012), and field-scale mineback studies (Warpinski, 1982; Fisher and Warpinski, 2012). (Van Eekelen, 1982; Bhardwaj et al., 2016) used a three-dimensional hydraulic fracture propagation model, which quantified the impact of operational parameters such as the *in-situ* stress profile, critical rock intensity, and well architecture in unconventional reservoirs on fracture height growth. (Usman, 1988; Fisher and Warpinski, 2012; Yue, 2017) addressed fracture height growth estimation related to the mechanical and interface properties of the layers present. (Elnoamany et al., 2020) investigated through numerical modeling fracture propagation following capping shut-in examining geomechanical properties such as in-situ stress and Young's modulus contrast between sand and shale layers. The complexity of the fracture geometry is primarily controlled by the well trajectory, *in-situ* stress state, fluid injection rate and properties, layers' geomechanics, and pre-existing natural fracture system. In general, most of the work from literature focused on a controlled fluid-driven fracture propagation.

During post-blowout capping shut-in procedures, wellbore pressure increases. At the weakest point along the casing wall, when the wellbore pressure  $p_w$  becomes equal to the breakdown pressure  $p_{bp}$  of the rock exceeding  $p_i$ , a crack(s) is created where a fracture(s) may start to grow. In other words, the formation will break when the hydrocarbons exert enough pressure to exceed the formations fracture gradient (FG). Figure 2.4 illustrates this scenario in a hydraulic fracture scenario compared to an uncontrolled fluid-driven fracture. In a conventional fracture treatment, hydraulic fracturing fluid is injected at a steady rate. At the point of injection, pressure will increase linearly as a function of time until it begins to leak into the rock formation shown by a deviation from linearity. Determined by leak-off testing, the leak-off pressure (LOP) is the pressure at which this leakage begins (Fu, 2014). Despite fluids leaking-off, pressure will

continue to increase until the rock eventually breaks down at fracture breakdown pressure  $p_{bp}$  with fracture(s) forming. The fracture is extended, propagating further into the formation by injecting fluids at  $FPP \approx LOP$ . On the other hand, in a broaching scenario where an uncontrolled fracture initiation and propagation occur, unsteady and perhaps increasing or decreasing hydrocarbon injection will take place depending on the energy supplied by the reservoir and the near-by system (faults). The pressure profile against time at the fracture tip will behave differently and follow a curved path until fracture closure pressure (FCP) is met or a confining layer is encountered. When the reservoir pressure stabilizes, movement of fluids in the wellbore ceases and subsequently injection into the fracture, the fracture's net pressure starts to reduce, and closure begins. The fracture closure stress is approximately equal to the minimum principal stress,  $S_{hmin}$ , for vertical wells (Michael, 2016).

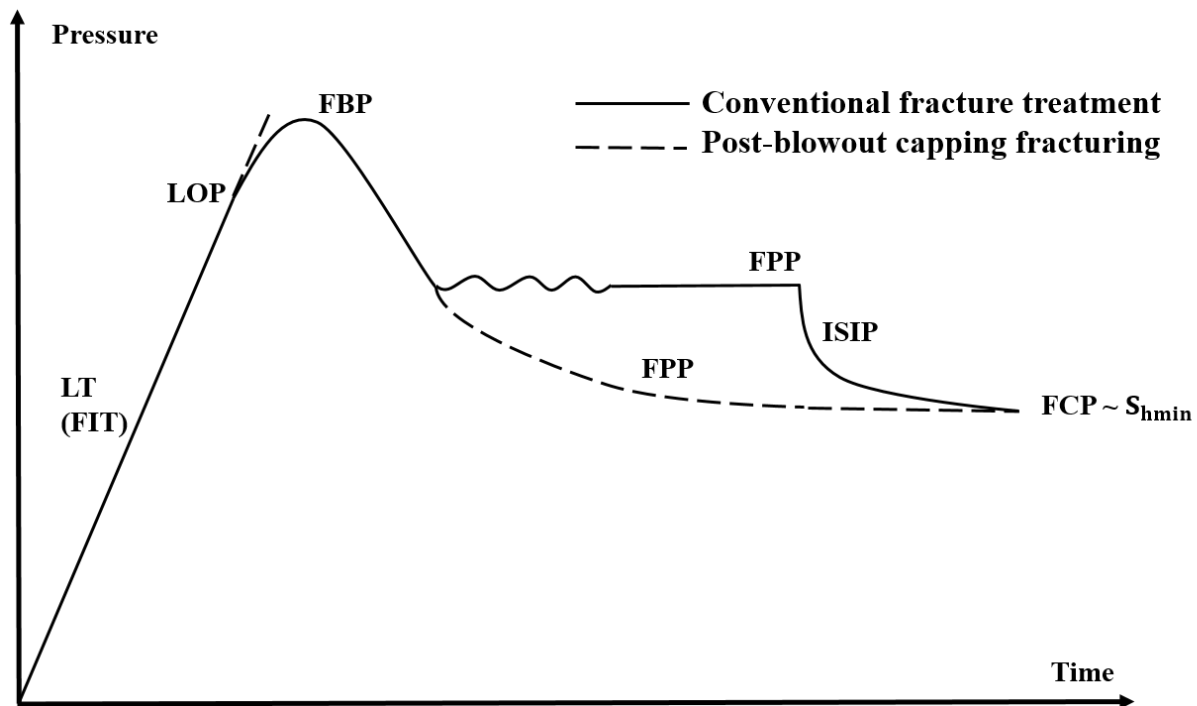


Figure 2. 4. Pressure profile against time, expected in a typical hydraulic fracturing stimulation treatment, compared to the event of fracturing during post-blowout capping (dotted line) in a finite reservoir (modified from Zoback, 2007).

Several studies throughout the years proposed different equations for measuring breakdown pressures (Hubbert and Willis, 1957; Hoek and Brown, 1980). Haimson and Fairhurst (1967) developed analytical models for the stresses near a pressurized wellbore, considering infiltration of injected fluid into the porous-permeable rock medium. The suggested equation for fracture initiation for longitudinal fracture initiation at  $\theta = 0^\circ$  is shown in equation 8 in the governing equations (section 3.2).

In 1951, Horner analytically solved the pressure build-up for single step “hard” shut-in (equation 13 in section 3.2). Matthews and Russell (1967) developed an expression for multi-step “soft” shut-in strategy, of  $N$  steps,  $q_i = q \left(1 - \frac{i}{N}\right)$ , where  $i = 1, 2, 3, \dots N$ , is replaced in Horner’s equation. Upon initiation, flow equation will be used to enable fluid flow calculations inside the fracture, as well as the leak-off rates. Calculation of leak-off rates will be dependent on the pressure distribution along the fracture walls (*REVEAL* user guide, 2020). Rock mechanics equation (stress/strain) are coupled with flow equations to solve for the fracture width and bottom hole pressure. The stress intensity at the fracture tip is calculated and if it exceeds the critical stress intensity of the rock, then the fracture will continue to propagate. Iterations on fracture shape are performed on the flow and rock mechanics equation until the tip’s stress intensity is equal to the rock’s critical stress intensity. Once this criterion is met, fracture propagation stops. The stress intensity at the tip is dependent on the net pressure inside the fracture. Critical stress intensity of the overburden rocks populated in the models are obtained from several geomechanical rock properties datasets for the GoM region.

## **2.6. Fracture Height Assessment**

Cormack et al. (1983) predicted the vertical (height) variation of fractures in multi-layer formations with varying interface and mechanical properties. Chuprakov et al. (2017) examined

continued hydraulic fracturing propagation growth in stratified geologic media following a shut-in for well treatment. Zaki et al. (2015) investigated fracture broaching and containment resulting from a hypothetical WCD case in GoM, simulating a casing failure event resulting in fluid-driven fracture growth in different lithostratigraphic sequences of layers, while also addressing well design and casing shoe displacement on fracture containment. A more recent analysis of fracture initiation and broaching was performed by mimicking fracture initiation following Union Oil's blowout and subsequent oil spill in 1969 in Santa Barbara, California (Michael and Gupta, 2019).

All aforementioned literature indicated that fracture geometry is rather complex. Fracture geometry dimensions (height, length, and width) are predominantly controlled by heterogeneities in the *in-situ* stress state, geomechanical properties (Young's Modulus, Poisson's Ratio), and bedding plane interface attributes. Most of the literature on fracture propagation behavior is limited to hydraulic fracturing fluid properties subjected to controlled low fluid injection rate with very limited discussion on fracture growth differences in uncontrolled fluid-driven fracture growth post-blowout capping period. Many questions remain unanswered on fundamental fracture growth behavior following extreme WCD conditions (deepwater HTHP GoM reservoir fluid properties, high flow rates > 300 MSTB/day, and complex wellbore trajectory).

To unravel the objectives of this thesis, a three-dimensional (3D) mathematical model describing the fracturing process will be used. 3D models allow fracture height to vary with injection rate while including the vertical components of fluid flow (Gidley et al., 1989).

In this work, fluid flow equations are coupled with rock mechanics (stress/strain) to generate a fixed fracture topology using a numerical finite-element model, which analyzes the fracture properties and computes the propagation pathway at each time-step. Once the fracture is generated, a finite-element (FE) grid is introduced, with triangular sub-elements and quadrilateral

boundary elements. The FE fracture grid is coupled to the 3D finite-difference (FD) main grid composed of hexahedral elements. A 2D plane with fracture widths defined over this plane is approximated by the FE grid introduced. Fluid injected (hydrocarbons) into the fractures are assumed to flow between two parallel plates (porous walls), which is recommended for modelling propagation. The difference between the pressure of the fluid inside the fracture and the pore fluid pressure of the rock, along with the time elapsed since the fracture walls have been first exposed to the fluid (hydrocarbons), determines the rate of leak-off through the crack face (Gidley et al., 1989).

### **3. Proposed Workflow for Post-WCD Capping Shut-in**

After loss of well control in an offshore well, hydrocarbons will flow from the BOP, open-pipe or LMRP for the discharge period until it has been shut-in by positioning a capping stack over the wellhead followed by a successful plugging through a relief well. Pressure build-up along critical points of the wellbore may exceed fracture initiation and subsequently fracture propagation pressure which will cause a fracture to grow in the geological media, propagating through the layers and potentially broach into the seafloor. A relief well can be drilled laterally to the blowing well intersecting the main wellbore as a well control mechanism to successfully kill the well and perform PA. Figure 3.1 displays the well containment and response workflow for bringing a well under control. It is evident from the current workflow that there is no rule on when a relief well should be drilled. The objectives for establishing this workflow are to:

- I. evaluate conditions under which fracture initiation may take place,
- II. fracture propagation may occur,
- III. broaching scenarios may be evaluated,
- IV. determine timing for drilling a relief well

The novelty of this work over previous work is that the full cycle of wellbore blowout, fracture initiation and propagation, possibility of broaching, and relief well drills is captured.



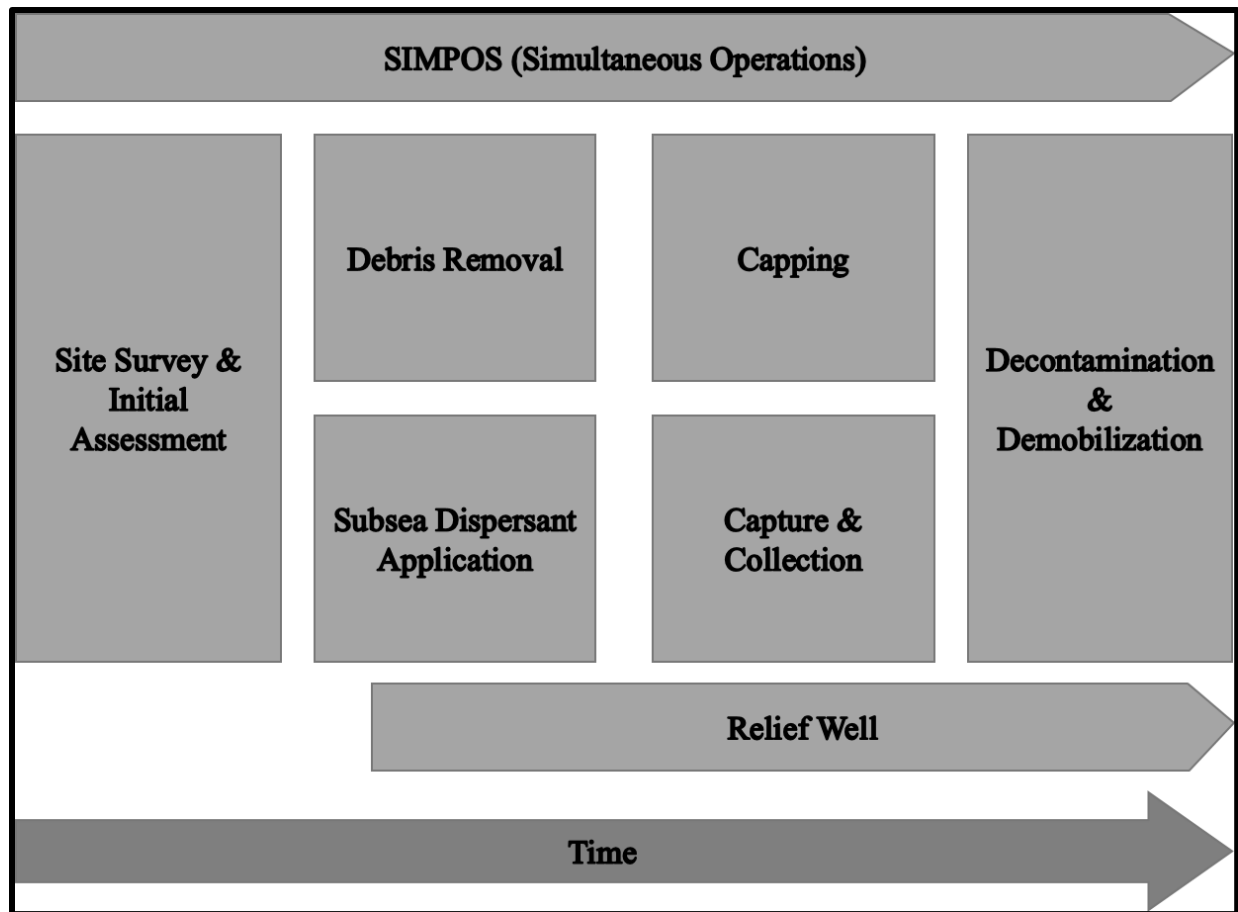


Figure 3. 1. Well containment and response workflow (modified after Buchholz et al., 2016).

The next subsection describes the modeling process designed to assess possible broaching scenarios. Steps (1-3, 5-6) used in the process are advised from PETEX.

### 3.1. Modeling Process

1. (Optional) Initialize the model with drilling mud in the completion.
2. Simulate WCD following a blowout with WHP corresponding discharging well pressure owed to hydrostatic column of seawater, or atmosphere if above sea level.
3. Forecast WCD rates and volumes for discharge period.

4. Mimic capping shut-in with wellhead (WH) boundary condition as fixed rate = 0 STB/day if single-step shut-in, or declining fixed rate occurring over incremental steps until WH rate = 0 STB/day, observe fracture initiation and growth if any.
5. Initialize high-density kill mud injection through the relief well and allow fluid movement in incident wellbore (flow through WH).
6. Shut-in main well and relief well to stabilize the reservoir and wellbore pressures.

In reality, step 6 would contain cement plug injection through relief well followed by shut-in in both main wellbore and relief well. Cement plugging is not modeled as part of this process. The modeling process described above will be implemented in the base case model and several case studies described in Section 3.3 will be developed to assess the impact of varying the period of some steps (Step 3: well capping period and step 4: relief well intervention period) on fracture initiation and branching. Section 3.2 defines the base case model upon which the valuation is conducted in this study.

### 3.2. Governing Equations

The governing equations used to achieve the objectives of this study are divided into three categories: the reservoir performance, the transient wellbore model, and the criteria for fracture initiation, and propagation following pressure build-up in wellbore.

#### Reservoir Performance

Darcy's law is used to describe the transport equation for fluid flow in porous medium. Equation 2 used by the solver, describes in oilfield units the Darcy velocity for each phase. The negative sign implies that the phase flow occurs from high to low pressure.

$$q_p = -6.3266 \frac{kk_r p}{\mu_p} \nabla \left( P_w + P_{c_p} - \frac{\rho_p h}{144} \right) \quad (2)$$

where  $q_p$  is darcy velocity (ft/d),  $k$  is rock permeability (D),  $kr_p$  is phase relative permeability,  $\mu_p$  is the phase viscosity (cp),  $\rho_p$  is the phase density (lb/ft<sup>3</sup>),  $h$  is the depth (ft),  $P_w$  is the water phase pressure (psi),  $Pc_p$  is the phase capillary pressure (psi).

### **Transient Wellbore Model**

A transient wellbore model is essential to achieve the objectives of this study. The transient wellbore model enables time-dependent pressures and flow rates to be calculated. The steady-state assumption cannot be used for investigating the wellbore abrupt shut-in process (Al-Safran and Brill, 2017), as well as the fast (transient) liquid slugging shall they occur with heavy-weight kill mud injection. The transient wellbore model provides an accurate calculation of the wellbore pressure build-up occurring during the capping period. Due to proprietary reasons, PETEX does not publish their precise equations and solution techniques. REVEAL honors the full mass balance laws and fluid properties (PVT) (Bird et al., 2002), while chemical reactions for mass generation effects are considered negligible (Houston PETEX, personal communication, March 15, 2021). Flow properties are calculated along the length of the well and across the length. All forms of heat transfer (conduction, convection, radiation) are accounted for in the vertical and radial directions (Houston PETEX, personal communication, March 15, 2021). Our model, neglects compressibility, inertia, or accumulation since their effects on this type of modeling are negligible. The steady-state fluid flow options are incorporated in the transient wellbore model. Pressure loss calculations along the wellbore are modeled using the empirical multi-phase flow correlation, Petroleum Experts 2, PE2 (Houston PETEX, personal communication, March 15, 2021).

### **Fracture Initiation**

In 1967, Haimson and Fairhurst derived equation 3 for a longitudinal fracture initiation from a vertical wellbore under normal faulting stress state ( $S_v > S_{Hmax} > S_{hmin}$ ) propagating in a

direction perpendicular to  $S_{hmin}$ . Initiation occurs when  $p_w > p_i$  where  $p_w$  is the wellbore pressure,  $p_i$  is fracture initiation pressure,  $p_p$  is the formation pore pressure and  $T$  is the tensile stress of the rock,

$$p_i = \frac{S_{Hmax} - 3 S_{hmin} + A p_p - T}{A - 2} \quad (3)$$

where  $A$  is the Biot's poroelastic constant expressed as

$$A = \left( \frac{1 - 2\nu}{1 - \nu} \right) \alpha_B \quad (4)$$

and  $\alpha_B$  is the Biot's poro-elastic coefficient calculated as

$$\alpha_B = \left( 1 - \frac{c_g}{c_b} \right) \quad (5)$$

where  $c_g$  is the matrix grain compressibility,  $c_b$  is the bulk matrix compressibility. The Biot's poroelastic constant  $A$  depends on  $\nu$ , the formations' Poisson's ratio, and  $\alpha_B$ , Biot's poroelastic coefficient.

Equation 6 describes the single-step "abrupt" shut-in build-up equation developed by Horner in 1951.

$$p_{ws} = p_{initial} - 162.6 \frac{q \mu_o B_o}{kh} \log \left( \frac{t_p + \Delta t}{\Delta t} \right) \quad (6)$$

where  $\mu_o$  is the viscosity of oil,  $B_o$  is the oil formation factor,  $t_p$  is time since production started,  $\Delta t$  post-capping time,  $q$  flow rate prior to shut-in,  $k$  average permeability of reservoir, and  $h$  the net pay zone thickness.

To obtain the critical WCD rate upon which a fracture will initiate following an abrupt shut-in process given by Equation 7 after Michael and Gupta (2019),  $p_{ws}$  from Equation 13 will be replaced with the expression for  $p_i$  from Equation 3.

$$q_{crit} = \frac{p_{initial} - 3S_{hmin} + S_{Hmax} + p_p - T}{162.6 \frac{q\mu_o B_o}{kh} \log\left(\frac{t_p + \Delta t}{\Delta t}\right)} \quad (7)$$

### Fracture Propagation

The initiated fracture is introduced as a finite-element grid. The internal pressure and width at different nodes within the fracture are related by equation 8 (*REVEAL* user guide, 2020; Almarri, 2020).

$$(P - \sigma)(x, z) = \frac{G}{4\pi(1 - \nu)} \int \left[ \frac{\partial}{\partial x} \left( \frac{1}{R} \right) \frac{\partial w_f}{\partial x'} + \frac{\partial}{\partial z} \left( \frac{1}{R} \right) \frac{\partial w_f}{\partial z'} \right] dx' dz' \quad (8)$$

$$R = \sqrt{(x - x')^2 + (z - z')^2} \quad (9)$$

where  $R$  is radius of the fracture,  $w_f$  is the fracture width,  $G$  is the shear modulus and related to Young's Modulus  $E$  and Poisson's ratio  $\nu$  by:

$$G = \frac{E}{2(1 - \nu)} \quad (10)$$

The fracture will propagate when the critical width,  $w_c$ , defined at a fixed distance,  $a$ , from the fracture tip is attained provided that the rock's critical stress intensity  $K_{Ic}$  is equal to the tip's stress intensity. Equation 11 describes the relationship (*REVEAL* user guide, 2020; Almarri, 2020).

$$w_c = \frac{4K_{Ic}(1 - \nu)}{G} \sqrt{\frac{a}{2\pi}} \quad (11)$$

where  $a$  is defined as a small distance from the fracture tip. The propagation criteria is met when  $w_f > w_c$ .

Flow inside the fracture is idealized as a laminar flow of an incompressible Non-Newtonian fluid. Flow equations inside the fracture assume to flow between two parallel porous plates relating the fracture leak-off rate, the flow rate, and pressure inside the fracture. Equation 12 relates the leak-off rate inside the fracture with the internal flow and pressure of the fracture (*REVEAL* user guide, 2020; Almarri, 2020).

$$-\int \frac{w_f^2}{12\mu} \nabla^2 \left( P - \frac{\rho h}{144} \right) dV + \int M(P - p_p) dA + \frac{\int w_f dA - V_0}{\Delta t_f} - Q_f \quad (12)$$

where  $\mu$  is the fluid viscosity,  $\rho$  is the fluid density,  $p_p$  is the pore pressure at far field,  $\Delta t_f$  is the time increment,  $M$  is the mobility connection factor, and  $Q_f$  is the flow rate inside the fracture. Coupling between each process described above and their solution method are shown in figure 3.2.

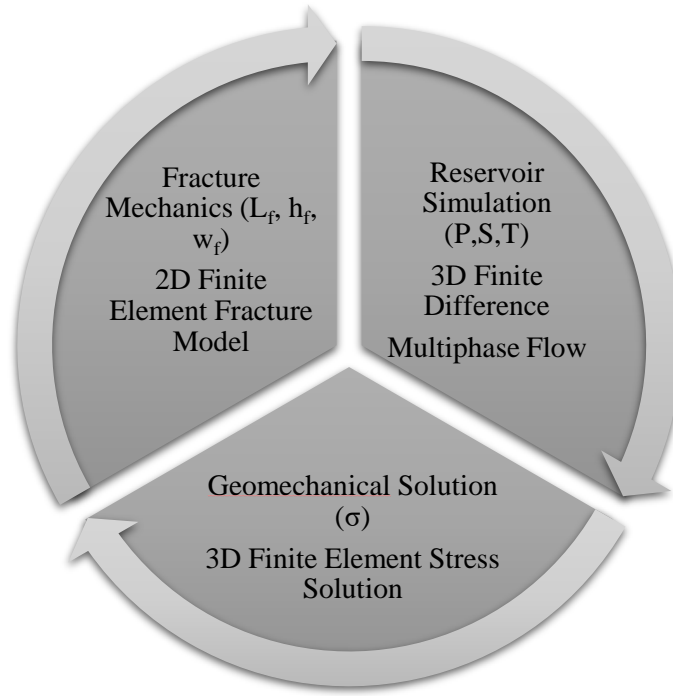


Figure 3. 2. Coupling workflow of the reservoir, geomechanics, and fracture models and solution method for each (modified after Almarri, 2020).

### 3.3. Base Case Model Description

A static, multi-layer model will be developed using typical deepwater (8,000 ft water depth) GoM parameters. Overburden layers composed of stacked shale and reservoir layers are assumed as fully water saturated. Figure 3.3 displays the 3D model consisting of 36 x 36 x 120 (a total of 155,520) grid cell spanning an area of 1 squared mile with 100 ft of each block in the vertical direction. A  $9\frac{5}{8}$  in (ID = 8.5 in) casing will be set at true vertical depth (TVD) of 19,400 ft (11,400 ft below seafloor) from the rotary table (RT) with no post drilling restrictions. The average reservoir depth is around 11,800 ft. Typical GoM casing design schematic, porous media petrophysical, and geomechanical are replicated in the model. A tartan grid is used to generate a log scale meshing appropriate for capturing the physics near the wellbore. The outer boundary condition of the model is set as a constant pressure boundary with infinite acting aquifer support. Rock compressibility, Poisson's ratio, young's modulus values of sandstones and shales are assumed to be constant throughout the systems' layers. In this model, a void in cement-rock interface is modeled as a microannulus in the 13.625" intermediate casing (shown in Figure 3.6). The microannulus introduced between the cement and the drilled region is approximately 0.003 in. An initially closed bi-wing fracture with 1-ft dimensions (half-height and length) will be introduced and modeled using the parallel plate method. Fluid flow inside an isolated, single fracture is often modeled as having a smooth, parallel plates (Philipp et al., 2013). Fluid flow inside the fracture including oil rates broached to the seafloor are included in the results, however, despite their importance, are not thoroughly discussed as flow inside an uncontrolled fracture is not well-understood by literature and not an objective in this study (Faybishenko et al., 2000; Berkowitz, 2002). Following fracture initiation, the fracture height and length which are the main dependent variables, will be monitored with time. Table 3.1 summarizes the parameters for this model. The

blowout duration is set as 30 days followed by 10 days of capping abrupt shut-in, afterwards, 30 days of kill mud injection through the relief well, lastly, 20 days of main wellbore and relief wells shut-in. Figure 3.4 displays the side lateral for the purpose of simulating a relief well intersecting the main wellbore around 10,100 ft below seafloor, approximately 1500 ft above the reservoir. Results have shown that the pressure at the shoe has exceeded the fracture gradient resulting in an initiated fracture at the casing shoe. Upon initiation, hydrocarbon fluids are supplied into the initiated fracture, resulting in a decrease in wellbore pressure and more movement of hydrocarbons occurring from the reservoir into the wellbore as the fracture propagates. If the net pressure inside the fracture generates stress intensity at the fracture tip greater than the critical stress intensity of the rock, fracture propagation criterion is met and the fracture will keep growing. A quite strong reservoir is designed for this study, aiming to model HTHP deepwater GoM wells approximately 3,000 psi overpressured, for this reason, the reservoir supplies significant amount of hydrocarbons into the wellbore following the fracture initiation period. Figure 3.6 through 3.11 shows the relative permeability curves for the sandstone reservoir, oil pressure-volume-temperature (PVT) properties such as gas-oil ratio (GOR), oil formation volume factor (FVF), and oil viscosity as a function of pressure, porosity relationships for sandstone and shale layers, and minimum horizontal stress compared to pore pressure as a function of depth below seafloor.

Table 3. 1. Base model reservoir and overburden layers' properties.

| Property (units)                      | Value     |
|---------------------------------------|-----------|
| Absolute depth of OWC (bellow RT), ft | 11,600    |
| Seafloor pressure, psia               | 3,720     |
| Depth of reservoir, ft                | 11,600    |
| Formation type                        | Sandstone |
| Pay zone, ft                          | 400       |
| Permeability, mD                      | 375       |
| Porosity, unitless                    | 0.20      |

(table cont'd.)



| Property (units)                               | Value             |
|--|-------------------|
| Water saturation, unitless                     | 0.25              |
| Average formation temperature, °F              | 178               |
| Average formation pressure, psia               | 12,120            |
| Young's Modulus (sands), psi                   | $2 \times 10^6$   |
| Young's Modulus (shales), psi                  | $3.2 \times 10^6$ |
| Poisson's ratio (sands), unitless              | 0.25              |
| Poisson's ratio (shales), unitless             | 0.35              |
| Biot's poroelastic coefficient                 | 0.8               |
| Thermo elastic coefficient, $1/^\circ\text{F}$ | $1 \times 10^5$   |
| Overburden stress, psi/ft                      | 0.82              |
| Maximum horizontal stress, psi/ft              | 0.779             |
| Minimum horizontal stress, psi/ft              | 0.7134            |

The workflow discussed in section 3.1 will be applied to the following model. Steps 1 – 5 list the procedures applied to simulate WCD, WH capping abrupt shut-in, and kill mud injection through a relief well. Examination of any fracture growth and potential broaching to seafloor will be studied during the capping period (step 3). The time and boundary condition dedicated for each procedure is highlighted in red.

1. Run for **1** hour with a low WHP to initiate the blowout (WHP = **3,720 psia**)
2. Forecast for **30** days to model the well in a blowout situation (WHP = **3,720 psia**)
3. Simulate for **10** days to model single-step “abrupt” capping shut-in, and observe any fracture growth (Main wellbore with **1 STB/day** as fixed rate).
4. Inject high-rate high-density mud injection (**105 lb/ft<sup>3</sup>** kill mud density) for **30** days through the relief/kill well (initial **20** days with **70,000 STB/day**, followed by **5** days with **40,000 STB/day**, then lastly **5** days with **20,000 STB/day**).
5. Run for **20** days (main wellbore is shut-in with no mud injection).

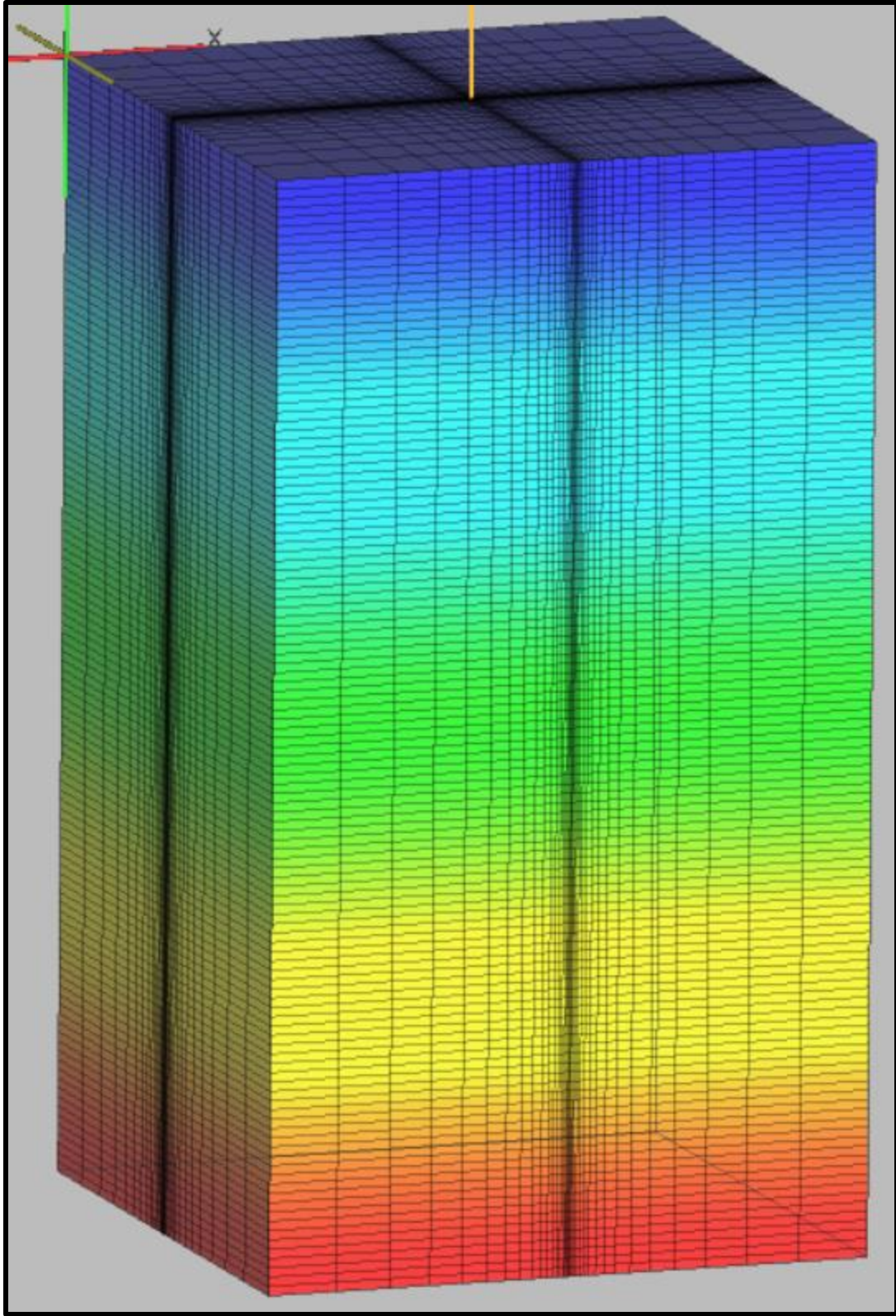


Figure 3. 3. Model meshing designed with incident well shown in the center (yellow line).

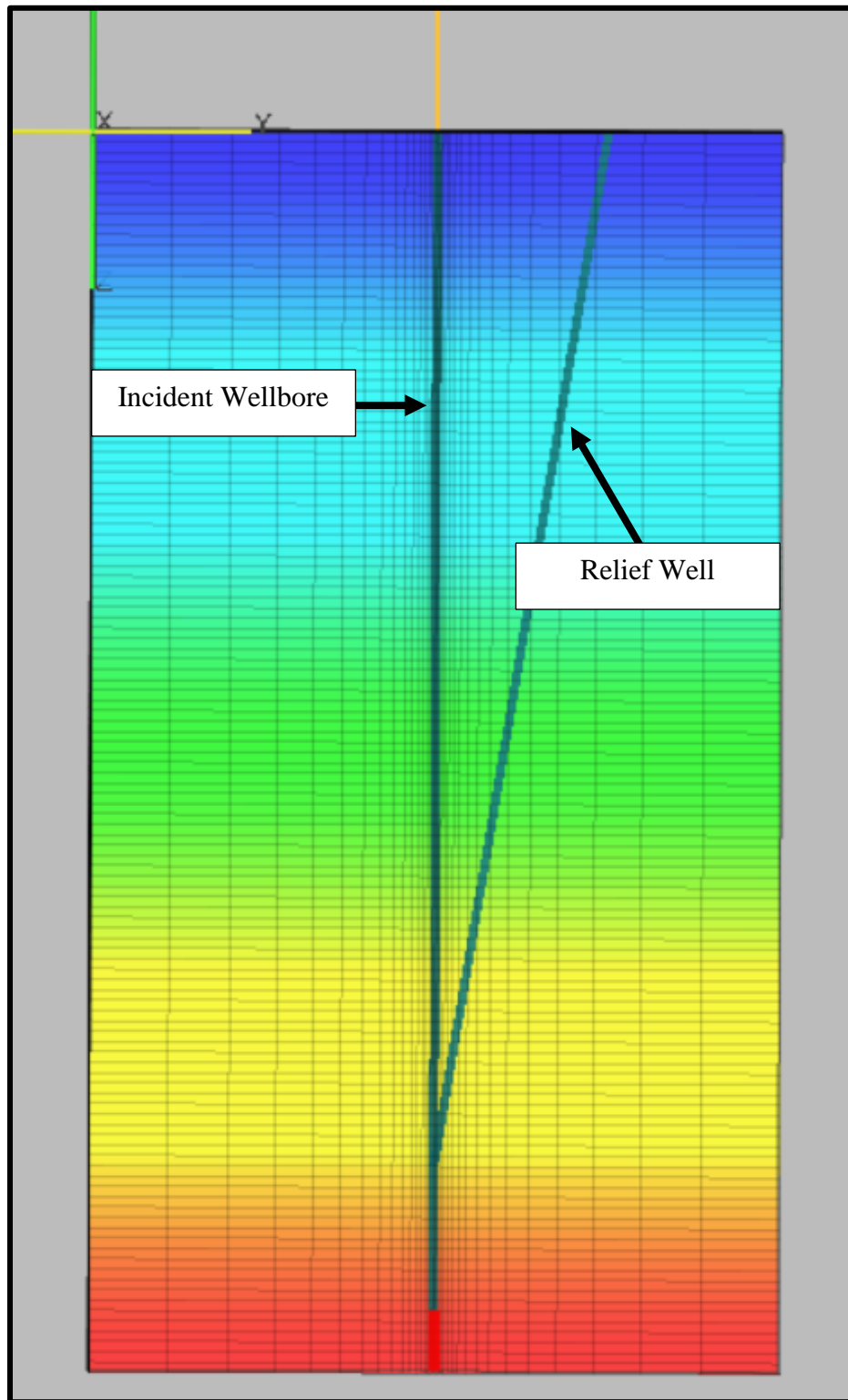


Figure 3. 4. A side lateral for the purpose of simulating a relief well intersecting the main wellbore around 10,100 ft below seafloor, approximately 1500 ft above the reservoir.

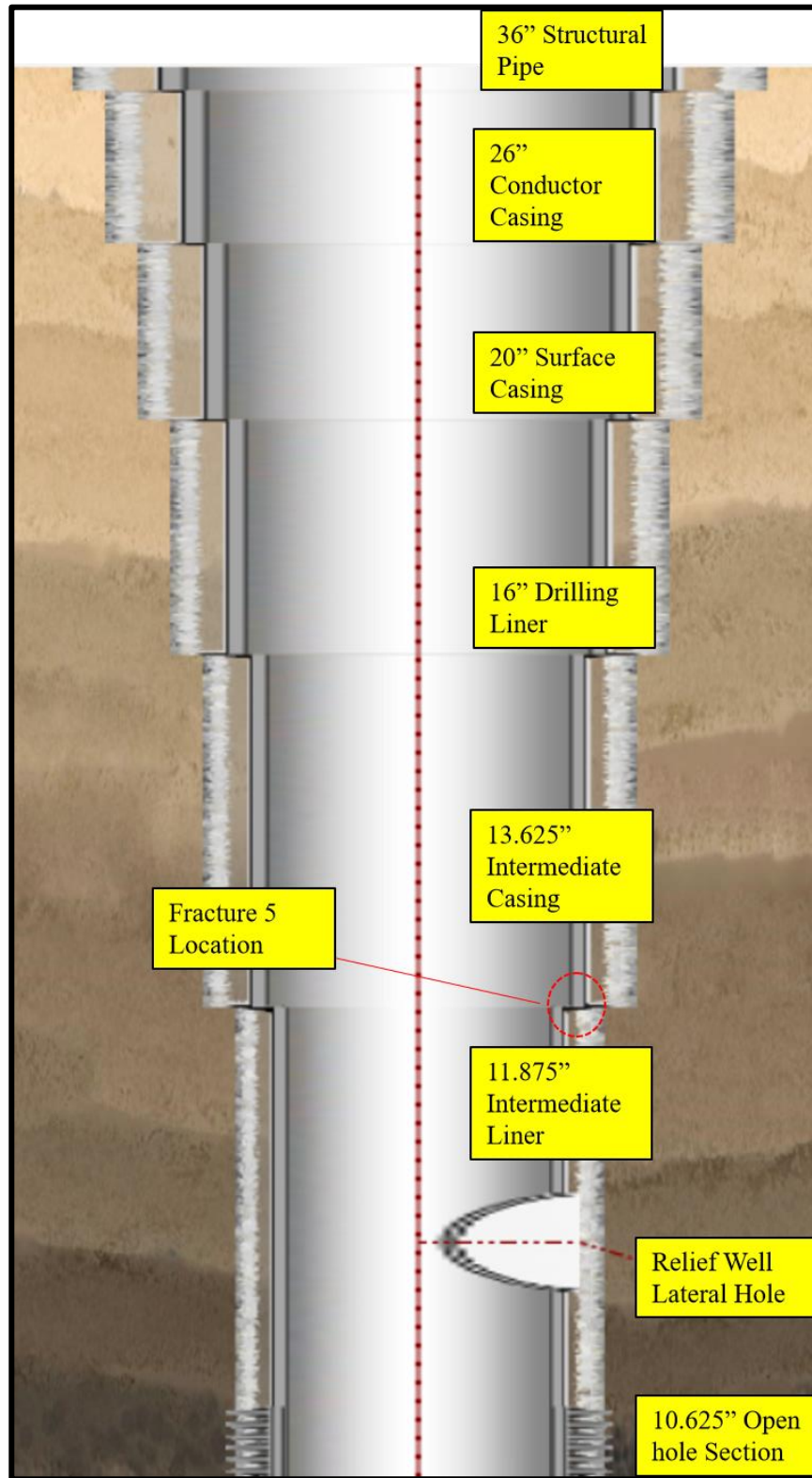


Figure 3. 5. Casing design schematic utilized for the base case model. Fracture 5 is located 2.5 feet below the 13.625" intermediate casing shoe.

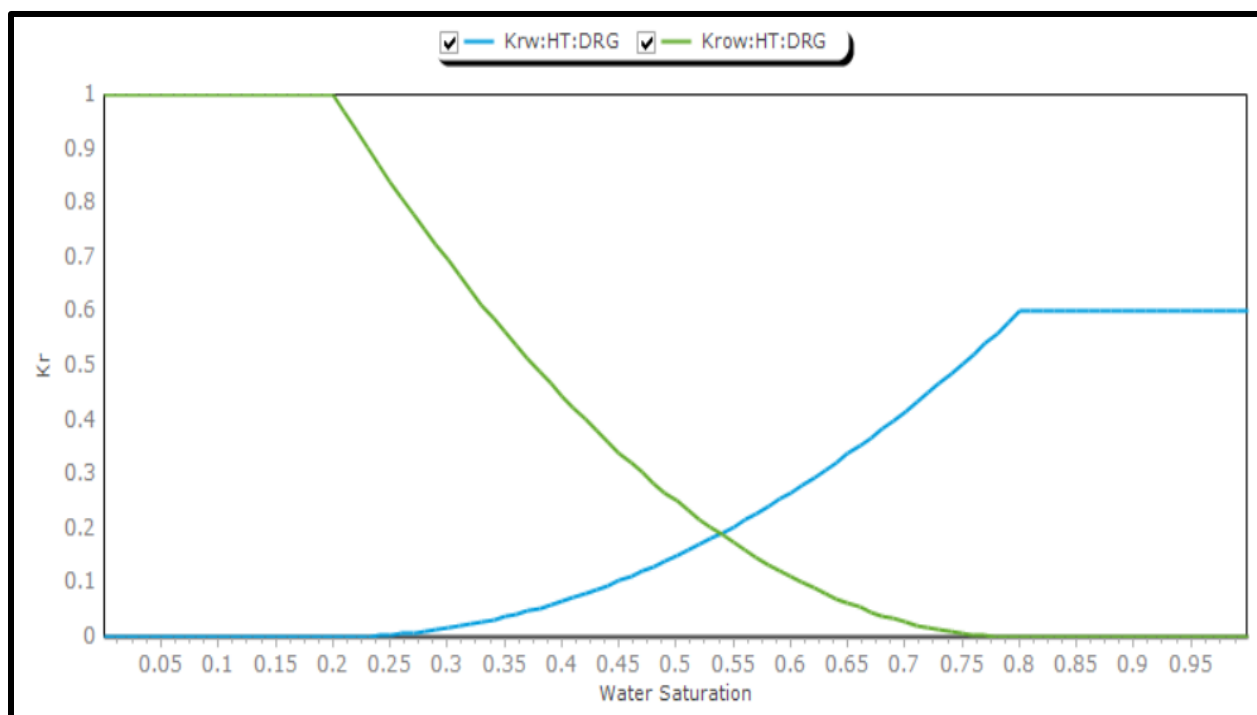


Figure 3. 6. Relative permeability curves for modeling multiphase flow in the reservoir rock. Blue line is  $K_{rw}$ , the relative permeability of water, while green is  $K_{ro}$ , the relative permeability of oil.

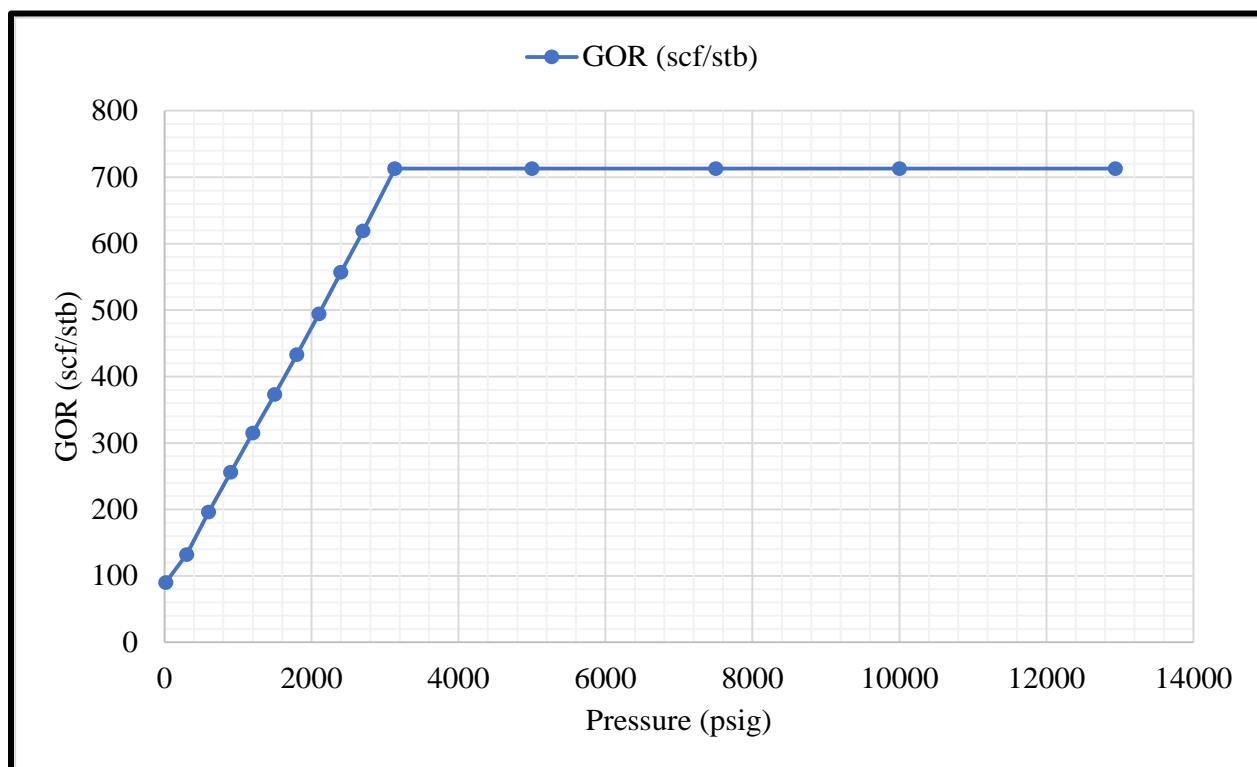


Figure 3. 7. Reservoir PVT properties: gas-oil ratio (GOR) as a function of pressure.

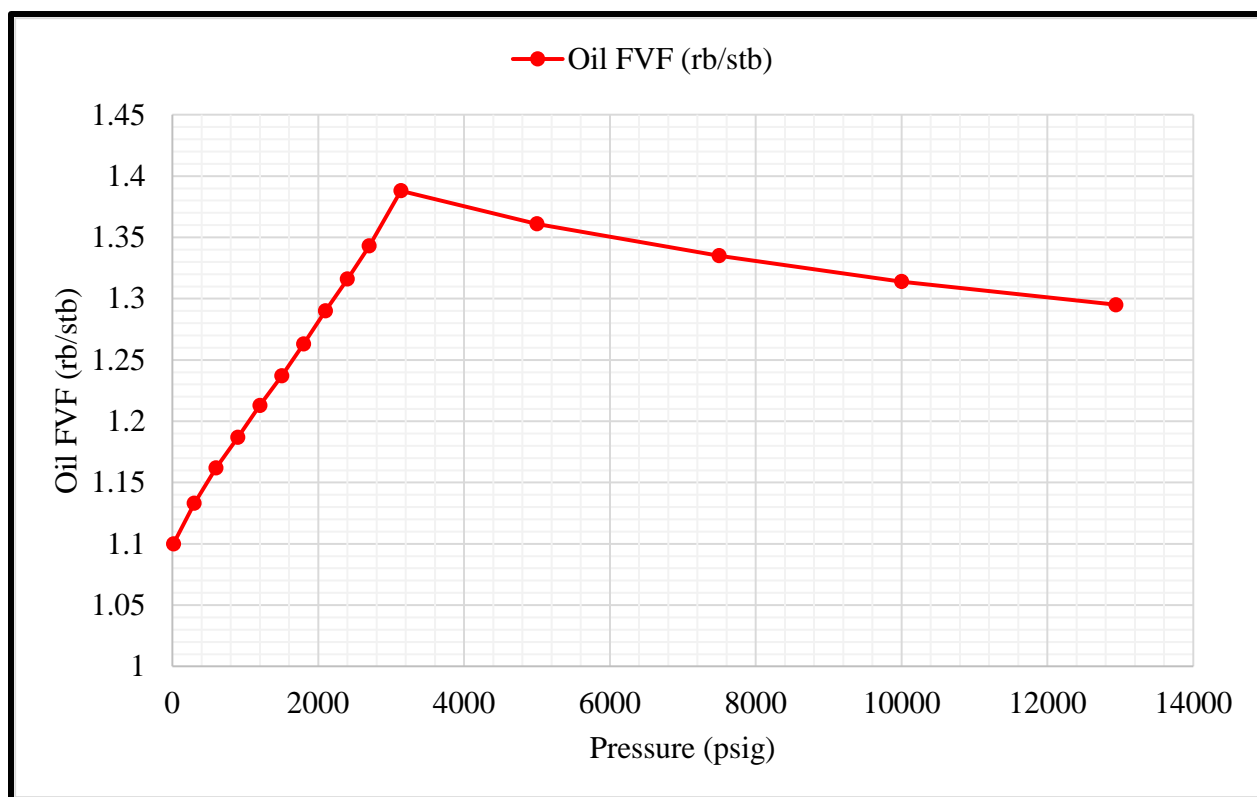


Figure 3. 8. Reservoir PVT properties: oil formation volume factor (FVF) as a function of pressure.

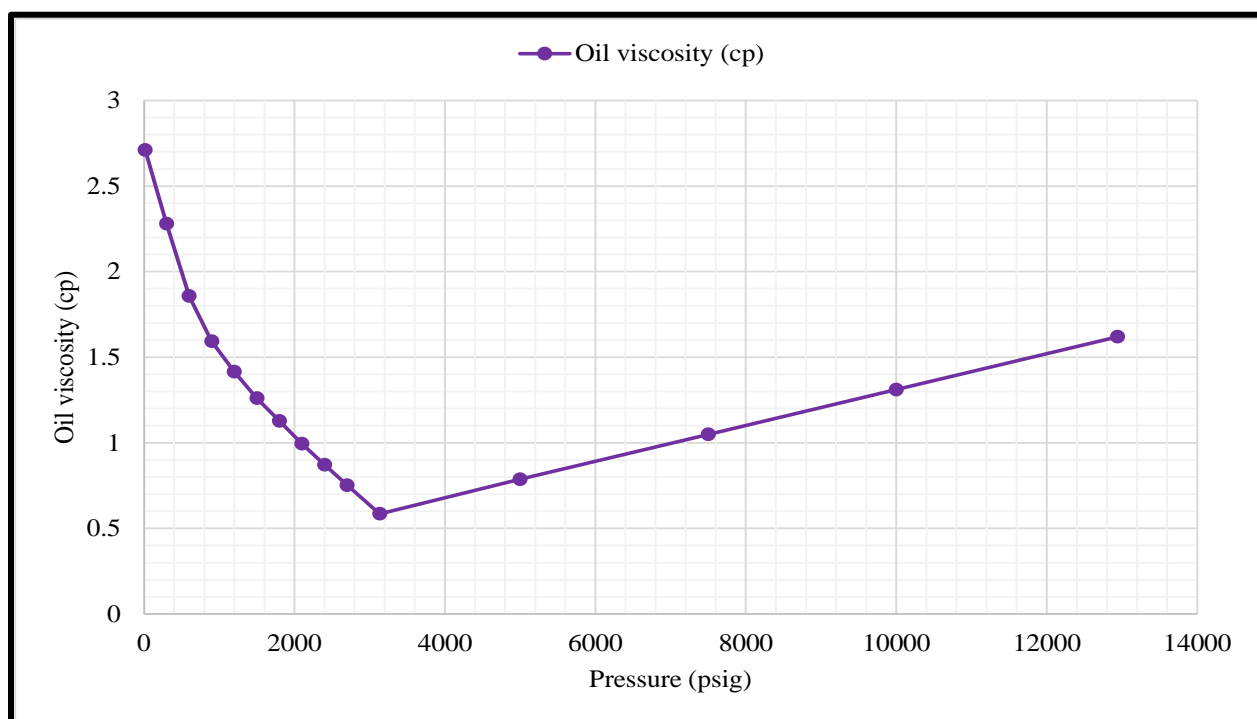


Figure 3. 9. Reservoir PVT properties: oil viscosity as a function of pressure.



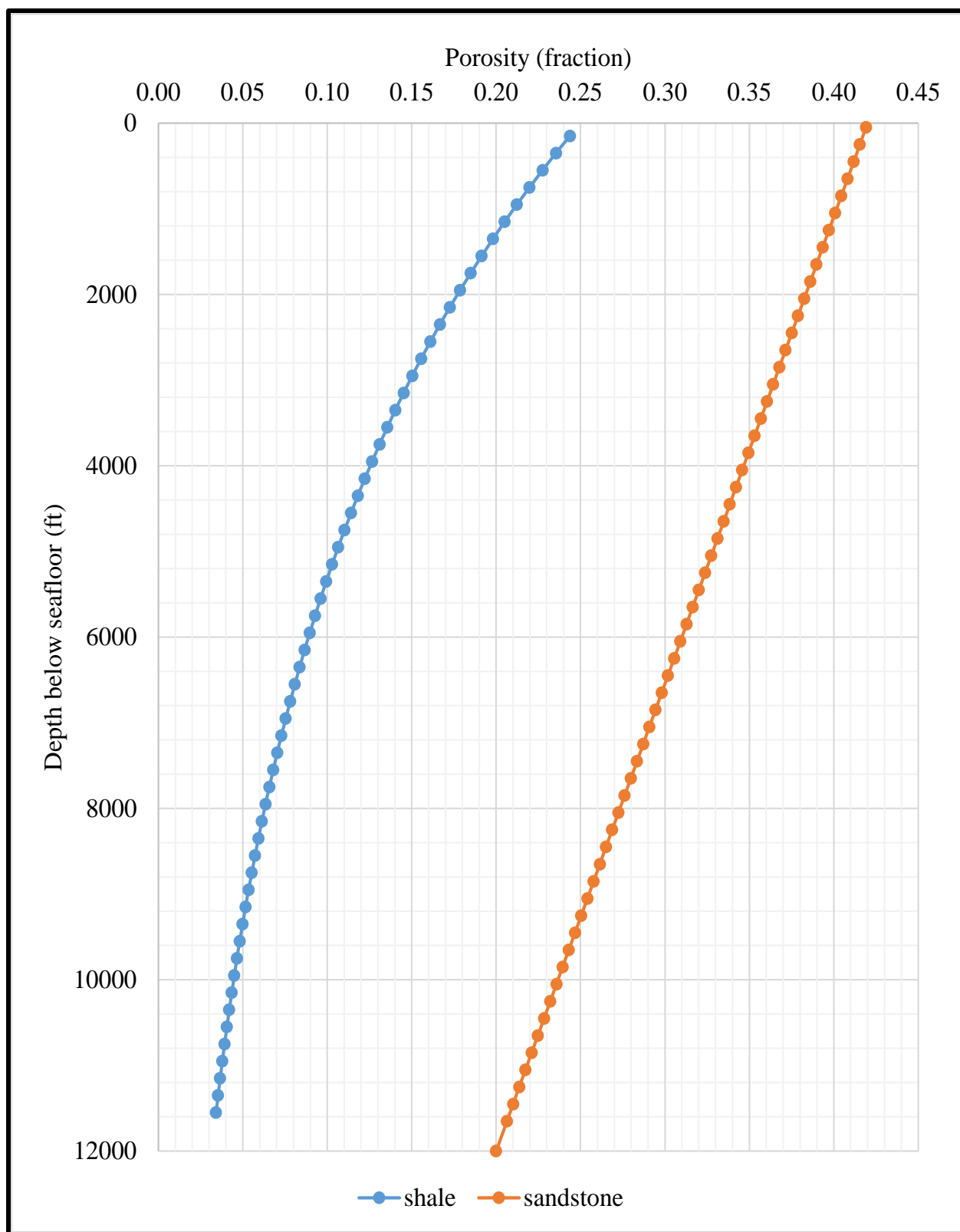


Figure 3. 10. Porosity relationships between shales and sandstones layers with depth below seafloor.

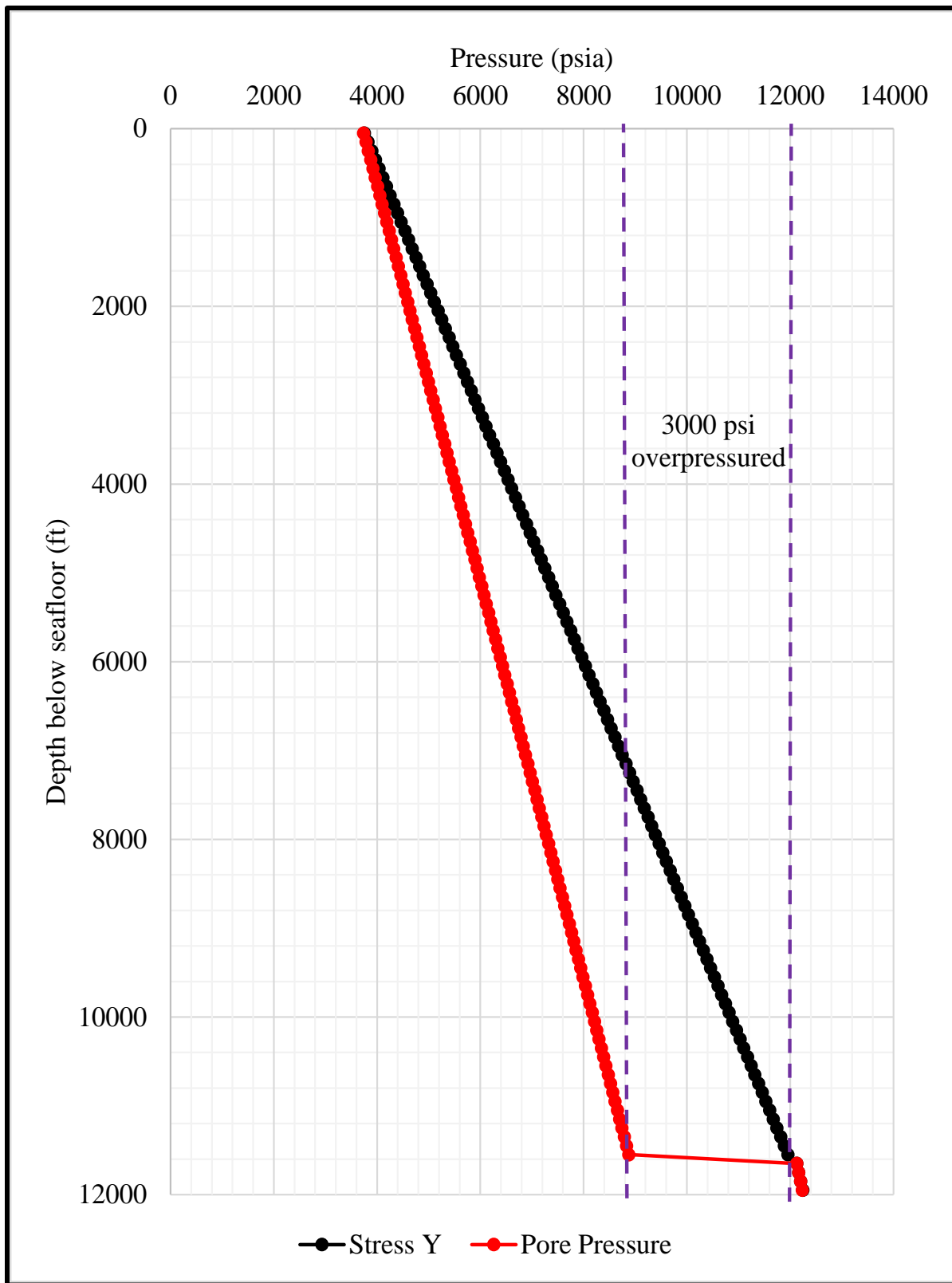


Figure 3. 11. Initial pore pressure and minimum horizontal stress ( $S_{hmin}$ ) as a function of depth. The discharging reservoir is 3,000 psi over-pressured.



### 3.3. Validation

To validate the mathematical algorithms and equations used in the numerical simulation, a comparison with an exact analytical solution is performed. Horner's build-up equation for abrupt single-step shut-in (equation 6) and equation 3 for fracture initiation are utilized for this purpose. Initiation pressure for the numerical solution occurred at a wellhead pressure of 8,046 psia, while initiation pressure with the analytical solution calculated at a wellhead pressure is of 8,033 psia. A 0.16 percent match is present between the numerical and analytical solution indicating the reliability of the designed model. To further validate the wellbore build-up pressure using the transient well bore model, comparison between different well models is included in figure 3.13. Discussion on the transient and steady-state models are included in section 4.10.

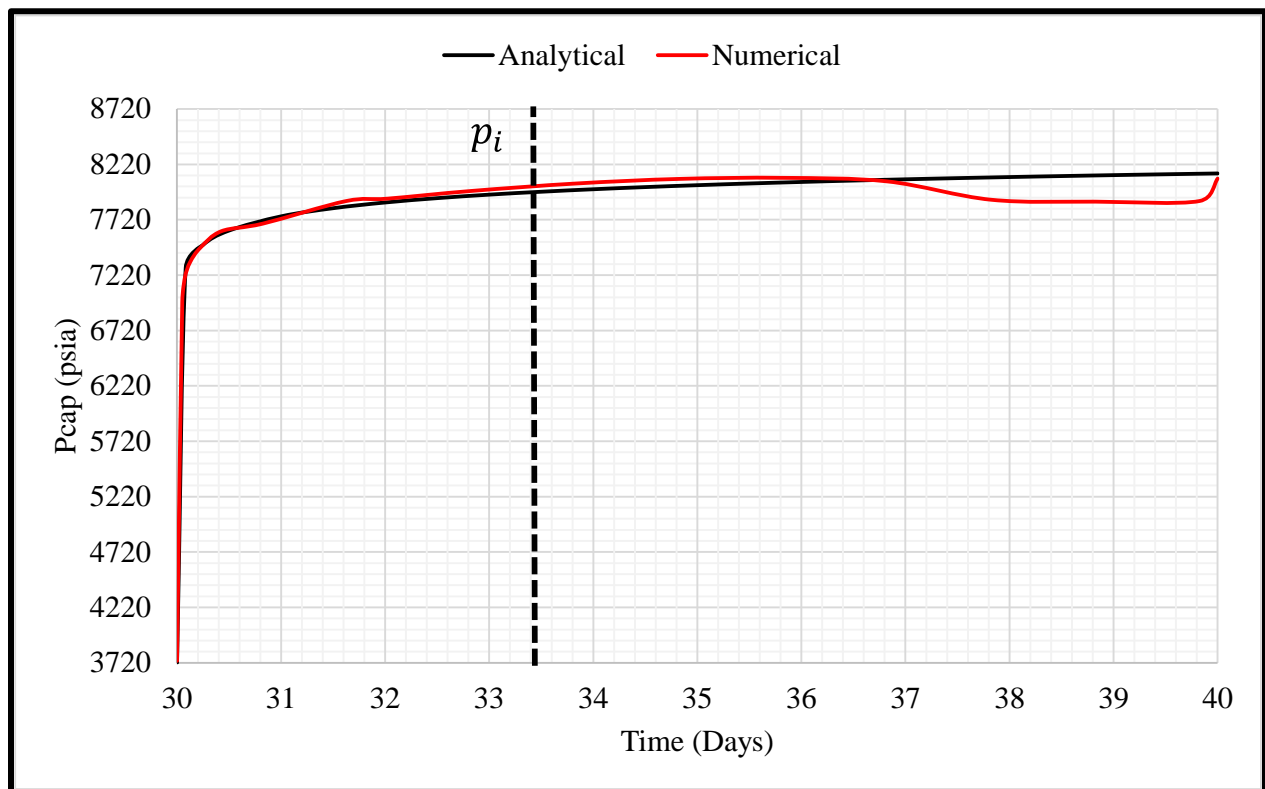


Figure 3. 12. Well head capping pressure comparison between the transient numerical solution “estimate” and the steady-state analytical solution “exact”.

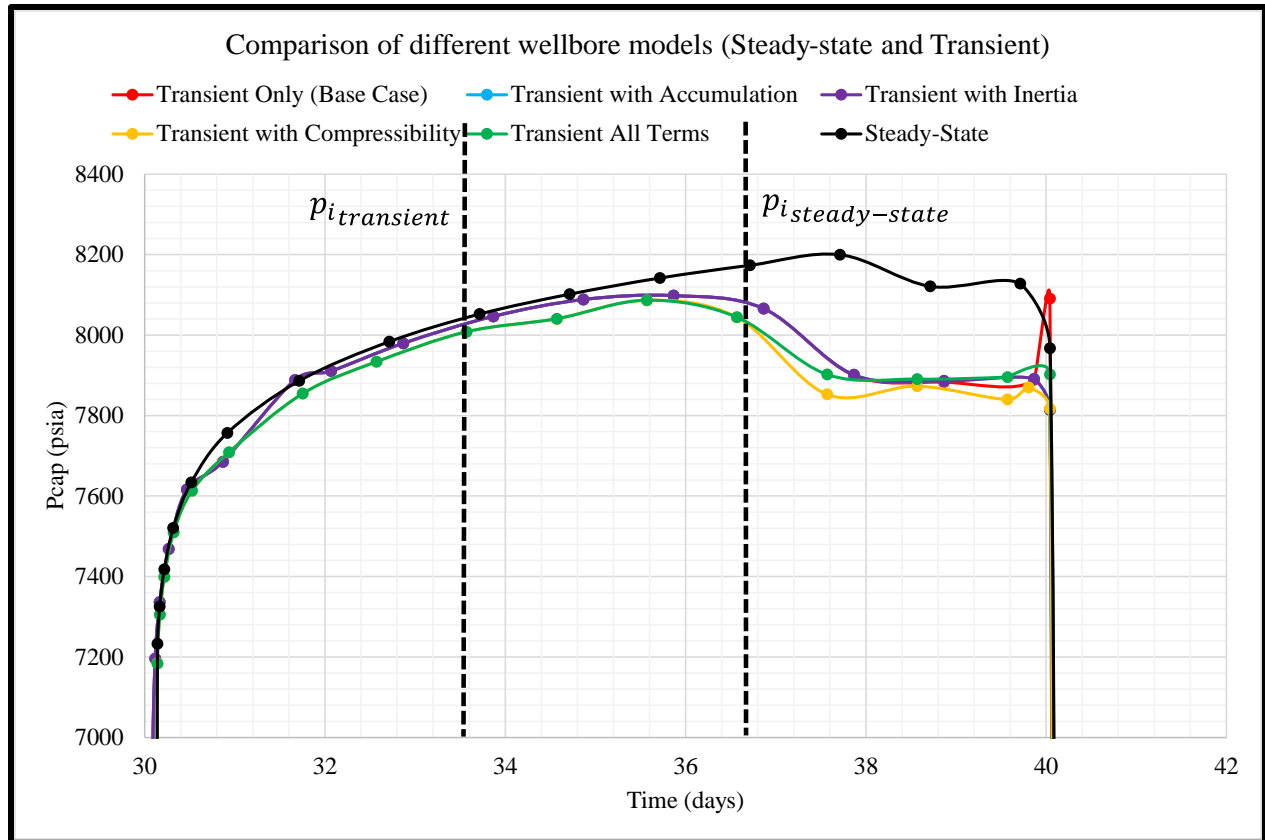


Figure 3. 13. Capping stack build-up pressure comparison using transient and stead-state well models.

In this study, seafloor pressure, where discharge of oil takes place is above the reservoir's fluid bubble point pressure. In attempt to capture the impact of multiphase flow, a sensitivity study is conducted to compare the impact of different transient wellbore model on capping stack build-up pressure, and fracture properties (height and length). Overburden and reservoir properties were replicated in shallow water conditions (500 ft). Fracture height and length results for the multiphase flow run are included in section 4.10. Figure 3.14 describe the result of such comparison.

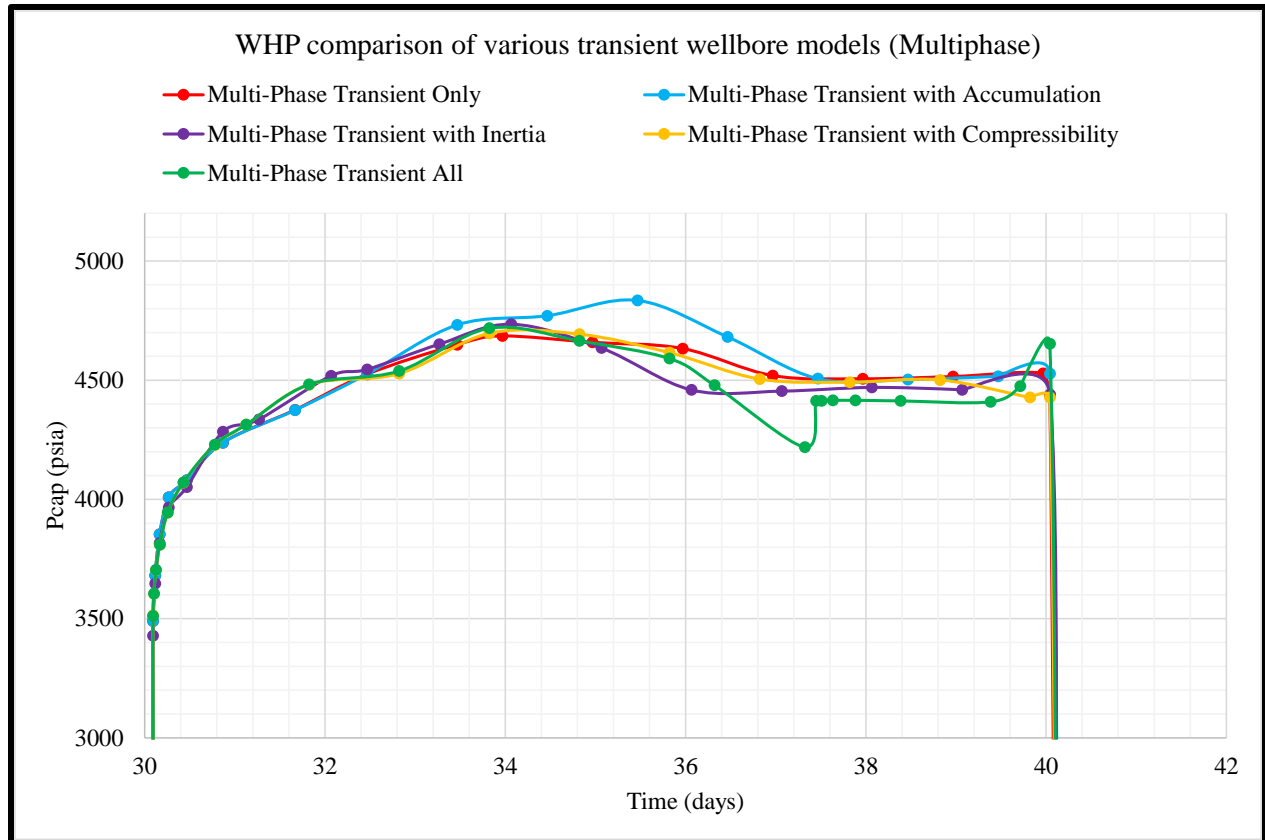


Figure 3. 14. WHP comparison using different transient wellbore for the multiphase flow during capping shut-in.

### 3.4. Sensitivity Studies

In this study, sensitivity studies are performed on a variety of scenarios to determine impact of voids in cement-rock interface at different casing shoe depths leading to the formation of a microannulus, points of casing collapse where fluids can leak and initiate a fracture, Young's modulus contrast between the sandstone and shale layer where the fracture initiates, reservoir overpressure variation, blowout spill duration, and relief well intervention period on fracture initiation, propagation and potential broaching. Steps 1 through 6 outline the sensitivity analyses accomplished and the results section dedicated to each.

1. Void in the cement-rock interface at the 13.625" intermediate casing (Section 4.1)

2. Microannulus between the 26” conductor casing and drill region (Section 4.2)
3. Microannulus between the 20” surface casing and drill region (Section 4.3)
4. Casing collapse at the 16” drilling liner (Section 4.4)
5. Perfect cement integrity (Section 4.5)
6. Young’s Modulus contrast between sandstone and shale layers (Section 4.6)
7. Variation in reservoir over pressurization (Section 4.7)
8. Total blowout duration (Section 4.8)
9. Relief well intervention period (Section 4.9)
10. Steady-state and transient well bore model (Section 4.9)

Despite the recent advances in WCD calculations and to the best of the author’s knowledge, previous research has failed to address the possible issues that may arise in certain well blowout scenarios. The uniqueness of this study goes beyond computing the highest blowout rate (WCD), total discharge volume, profile for flow rate decline, and duration of flow period (until well capping). The study further evaluates widely known techniques and practices, such as subsea capping stack shut-in and dynamic relief well drilling engineers would execute for bringing a well under control after a blowout has occurred. Traditional nodal analysis and wellbore models for calculating WCD rates have been used extensively; however, the procedure of regaining control of the well using either capping shut-in or a kill well is a transient phenomenon and hence, conventional steady state models cannot be utilized to address the requirements stated in the objectives (Bendiksen et al., 1991). A fully transient wellbore model is developed and deployed for the purpose of this problem. The transient wellbore modelling is fully coupled to the reservoir providing the ability to model crossflow, well shut-in and start-up, well kick off, bullheading and injection, and transient flowline response (*REVEAL* user guide, 2020), a specialized reservoir

simulator *REVEAL* from PETEX is used to perform the complex physics-based procedure. The following subsections describe the modeling process of each step stated in the workflow (section 3.1).

### **3.5. WCD Calculation**

In this study, we adapted the WCD workflow described by Vasquez Cordoba (2018), which prescribes an integrated reservoir-wellbore nodal analysis assessment for WCD modeling. The workflow is further validated with reservoir simulation. A deepwater drilling scenario is presented. Figure 3.13 illustrates a lithology with one formation susceptible to WCD. Multiple stacked patterns of alternating non-producing water-bearing sandstones and shales and oil-bearing sandstone reservoirs commonly encountered while drilling the GoM OCS are incorporated in the base case model. In accordance with SPE 2015 report on estimating WCD rates, the wellbore has no post-drilling restrictions (such as tubing string) with reservoirs discharging into the open-hole section of the wellbore. Bridging is assumed to not be expected during the duration of the blowout. A typical deepwater well drilling plan is incorporated in the model reflecting GoM casing designs. The discharge point is at seafloor assuming failure or disconnection of the riser pipe from the BOP system, with the boundary condition as constant pressure due to the hydrostatic seawater column acting above the wellhead. An open-hole (uncased) section extending several hundred feet above the reservoirs is presumably considered as an unexpected influx is encountered while drilling. The reservoirs are assumed to be under steady-state constant pressure boundary conditions with infinite acting aquifers. Local GoM geothermal and stress gradients, geomechanical, porosity and permeability properties are populated throughout the model. PVT data utilized in the model were obtained from deepwater GoM core laboratory experiments donated by GeoMark Research, Ltd. The reservoirs are discharging into the main wellbore over some specified duration until the well

has been capped. Cross flow of fluids is allowed between different layers. The first schedule (60 minutes in this study) initializes the model to stabilize and fill the pipes with blowout hydrocarbons and appropriate flow rates (*REVEAL* user guide, 2020). The next schedule is then used to forecast the WCD production for the duration of the spill. The following section discusses the capping stack shut-in process and boundary condition adapted to perform the objectives of this study.

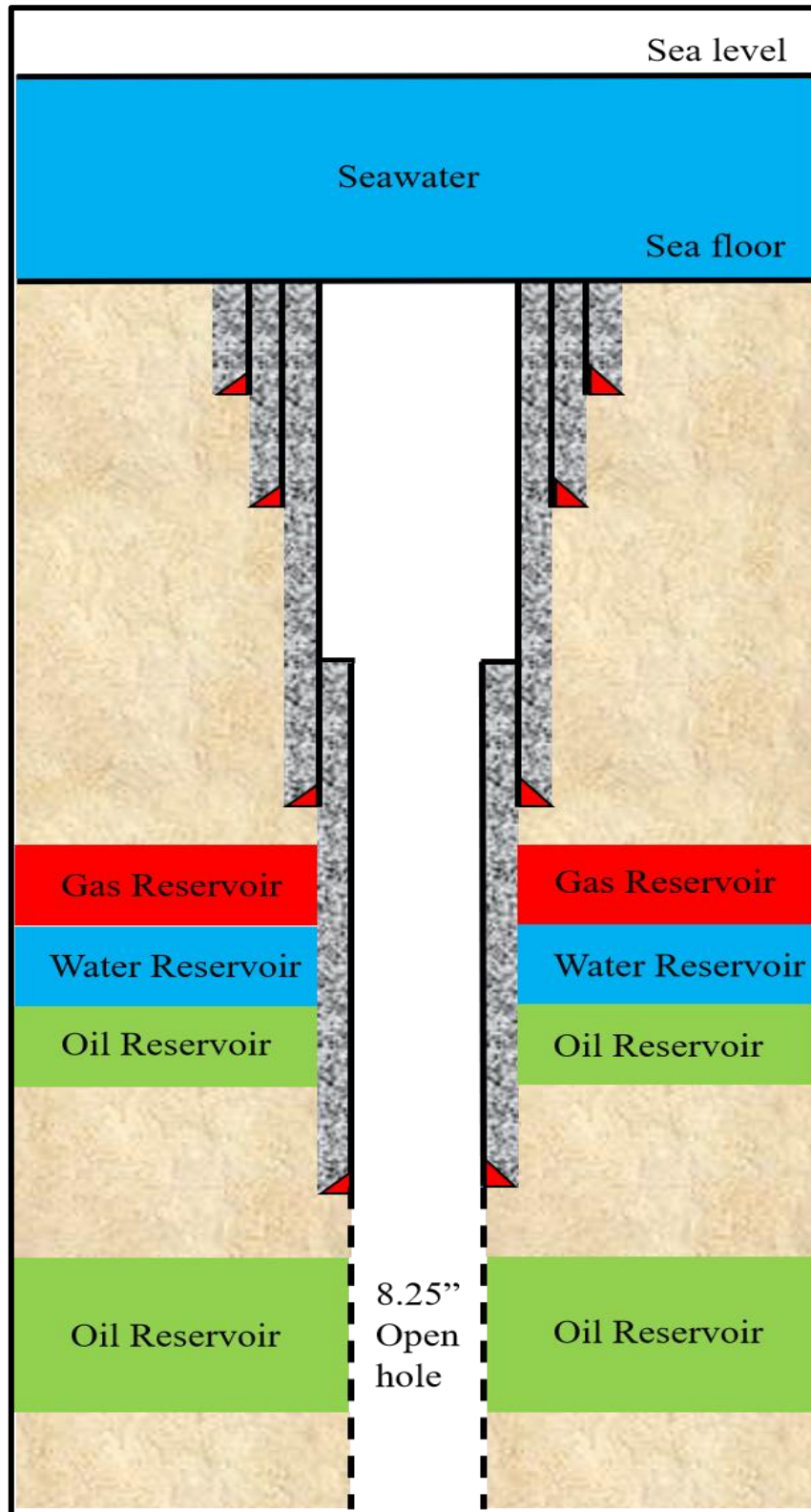


Figure 3. 15. Typical deepwater wellbore schematic showing one formation susceptible to WCD (modified after SPE Report, 2015).

### 3.6. Capping Shut-in

Two widely used systems of mechanically integrated devices are typically used for subsea containment system; cap and flow system (multi-step “soft” shut-in) and cap only system (single-step “abrupt” shut-in). This study focuses on the use of single-step “abrupt” shut-in cap only system. The capping stack is positioned on top of the wellhead or failed blowout preventer to cease the uncontrolled flow of fluids into the environment (Bratslavsky and SolstenXP, 2018). The ‘cap only’ capping stack acts in a single-step mechanism completely shutting off the flow of hydrocarbons. On the other hand, the “cap and flow” system acts in a multi-step closure mechanism and momentarily redirects the hydrocarbons to enable closure of the wellbore, followed by closure of the diverter outlets (Bratslavsky and SolstenXP, 2018). Figure 3.14 compares the ‘cap only’ to the ‘cap and flow’ subsea capping system. The cap and flow mechanism redirects the flow of hydrocarbons through flexible pipes to offshore vessels.

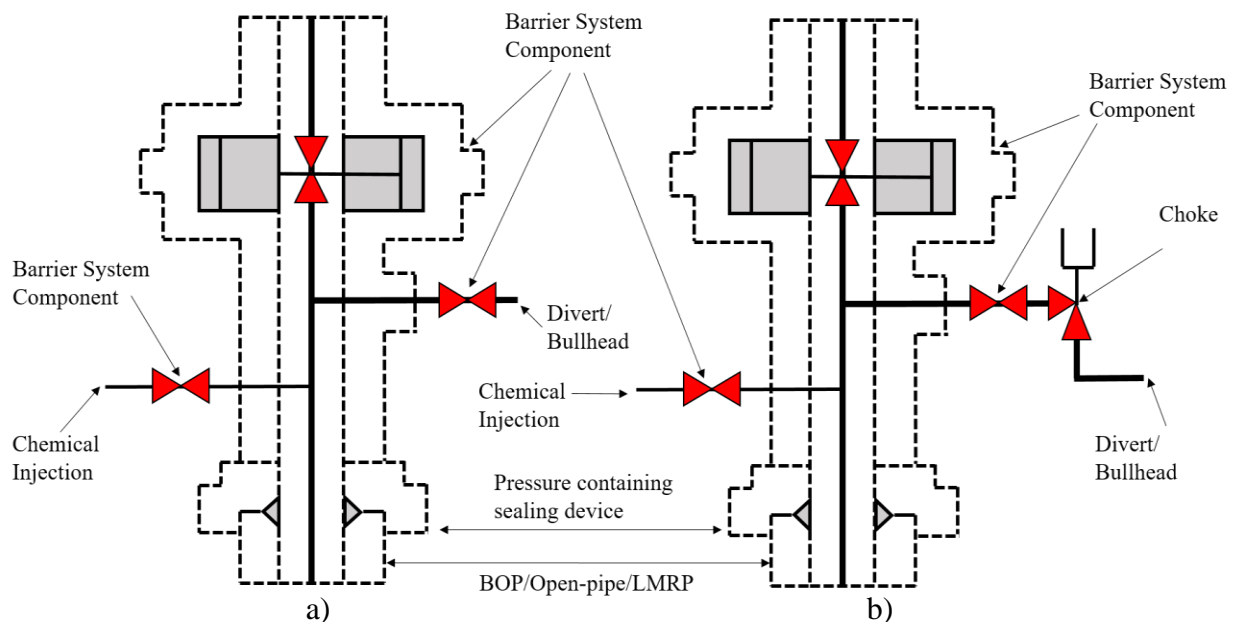


Figure 3. 16. Subsea containment systems “capping stacks”. a) Cap only system. b) Cap and flow system (modified after Wood Group Kenny, 2016).



To model this intervention technique, the boundary condition at the top of seafloor is set at fixed rate of 0 STB/day following the preceding blowout period (WHP = seafloor hydrostatic pressure). Depending on the current energy state of the reservoir, during this period, wellbore pressure significantly rises. Subsequently, it can take a few days depending on the diffusivity of the reservoir for the reservoir pressures to stabilize. In this time, movement of fluids in the wellbore still occurs (liquid slugs produced/changing liquid levels) until the reservoir pressure stabilizes (PETEX Newsletter, 2016). Under certain wellbore conditions, such as in the presence of a micro-annulus due to poor cement jobs and casing collapse due to large pressure differential between internal annulus region and external side of casing, leakage of fluids may occur. This leakage creates a flow path of hydrocarbons that under intensive annulus pressure build-up due to trapped annulus fluids, may allow a fracture to initiate. Shall there be enough energy supplied to the initiated fracture by the movement of fluids from the reservoir into the wellbore and then the damaged wall region, extension of the fracture may occur. After several days, hydrocarbons may broach into the seafloor if the propagated fracture have reached the top layer below the seafloor. In general, once a fracture initiates and starts propagating, it releases pressure from the capping stack and the WHP decreases. However, the behavior depends on the strengths of the reservoir (energy source) and the fracture inlet/wellbore damage (energy outlet). In some cases, the width of the fracture may be small while the length and height are increasing, which makes the tubing control the volume of discharge and consequently WHP. On the other hand, if the fracture size is large, it will deliver more fluids and hence control the volume in the tubing, and consequently the WHP. Therefore, it is a balance of the strength of the energy source (reservoir) and the outlet (wellbore damage) that controls the behavior of the volume of fluids in the tubing and the WHP at capping.

### 3.7. Relief Well Injection Strategy

Once the period of blowout and capping shut-in is simulated, high density kill mud (105 lb/ft<sup>3</sup>) is injected through a relief well drilled laterally to the main wellbore. The intent of drilling a relief well is to intersect the main wellbore at some pre-determined depth below the seafloor (Bruist, 1972). The main purpose of drilling a relief well is to permanently kill the discharging well by pumping heavy weight kill mud, followed by injecting cement to plug in the wellbore to prevent any further fluid movement. Essentially, the operation of drilling a relief well involves casings and cement design just as any other drilling operation. The downside of drilling a relief well resides in the precision directional drilling techniques, and the associated additional time required to find a rig capable of accomplishing this.

Moreover, a relief well consists of a multi-step mud injection process. Heavy weight kill mud is injected with different declining injection rates over a certain period of days or weeks until cemented. This is typically done until the mud has displaced the hydrocarbon filled wellbore and the reservoir has ceased producing fluids into the open-hole section. Sufficiently high-density mud should be used to build a heavy column of liquid enough to replace and stop the reservoirs from further producing oil into the incident wellbore. Injecting very high-density mud is not optimum as it would introduce unphysical surface pressures (PETEX Newsletter, 2016). To simulate this complex process, the boundary condition at the wellhead of the main lateral is set as the pressure exerted by the hydrostatic column of seawater, assuming the facilities operator has completely reopened the diverter valves to allow circulation of heavy mud along with any other associated fluid. This process is done for all declining injection rates until the cement plug is injected into the wellbore. In this study, three injection rates from the secondary relief well will be used during the total injection period. Depending on the density of the kill mud, injection rates will at least

compensate the produced hydrocarbon rate to effectively stop production from the reservoir (PETEX Newsletter, 2016). High density kill mud of 300,000 ppm equivalent to 105 lb/ft<sup>3</sup> is used throughout this study.

Drilling a relief well is a complex time-consuming process that requires high resolution at-the-bit magnetometer equipment to determine the precise location of intersecting the well. The magnetometer allows for accurate measurement of the distance and direction to the existing main wellbore (Robinson and Vogiatzis, 1972). A lateral hole is introduced by drilling into the casing or open-hole section at a point above the reservoir to allow injection of kill mud. An optimum size of the hole is designed for this purpose, a small hole can generate a large friction pressure loss while injecting the mud compared to a very large hole, which would take longer to be drilled (PETEX Newsletter, 2016).

## 4. Results and Discussion

This chapter represents the results of the numerical study and analyzes what they signify in relation to the pre-stated hypotheses. Eight case studies are performed to investigate the impact of microannulus resulting from voids in cement-rock interface at different casing shoe depth, young's modulus contrast between the shale and sandstone layer's, variation in reservoir pressure, extended total discharge period until capping, and intervention time of relief well drilling. Table 4.1 lists casing design properties used across various models.

Table 4. 1. Casing design specifications and fracture name associated.

| Casing Type                 | Depth (ft) | ID (inches) | Fracture Name |
|-----------------------------|------------|-------------|---------------|
| 36" Structural Pipe         | 200        | 30.875      | -             |
| 26" Conductor Casing        | 1,500      | 22          | Fracture 2    |
| 20" Surface Casing          | 3,000      | 18.375      | Fracture 3    |
| 16" Drilling Liner          | 5,000      | 14.75       | Fracture 4    |
| 13.625" Intermediate Casing | 8,000      | 12.25       | Fracture 5    |
| 11.875" Intermediate Liner  | 11,400     | 10.625      | -             |
| 10.625" Open-hole section   | 600        | 10.625      | Fracture 6    |
| Relief Well                 | 10,100     | 6           |               |

### 4.1. Base Case Model Results

After a period of 3.825 days following wellbore abrupt capping shut-in, fracture initiation was observed along the 0.0003" void introduced in the cement-rock interface where the fracture is set as initially closed. The initiated fracture propagates for 5 days until it is contained in the geologic media. In this model, the depth of the fracture is around 8000 ft located at the 13.625" intermediate casing shoe reaching a maximum upward height and length of approximately 4,336 ft and 4,450 ft, respectively. Once the reservoir pressure starts to stabilize, movement of fluids in the wellbore stops, no more fluid is injected into the fracture, and the fracture reaches it maximum growth. The fracture's net pressure starts to reduce, the width of the fracture decreases, and closure

begins. Located at its maximum upward height of 3,550 below seafloor, the fracture will not broach during the well capping period investigated in this study. A sensitivity study to investigate the impact of well capping period on fracture growth is conducted in section 4.9. Following the capping shut-in duration, the well is successfully killed as drilling mud is injected from the relief well with enough density ( $105 \text{ lb/ft}^3$ ) to compensate and cease the movement of oil from the reservoir into the wellbore. This is shown by a decrease in oil rate to 0 STB/day as mud is injected (Figure 4.5). Sufficient kill mud density and injection rate are required for a successful kill operation. An insufficient mud density will result in liquid slugs occurring as mud, oil, gas, and water are simultaneously flowing in the wellbore. Figure 4.1 describe full process of the workflow applied to the base case model. The first period initiates the blowout (oil rate profile in red), followed by period where the WH is shut-in while allowing movement to occur in the wellbore (WH pressure build-up shown in green), followed by a period of high-density kill mud injection through the relief well (purple line shows mud injection strategy), then finally complete shut-in of both relief well and main well. Figure 4.8 through 4.11 shows the displacement of kill mud density in the wellbore at successive time-steps. Quantitative results are shown in table 4.1.

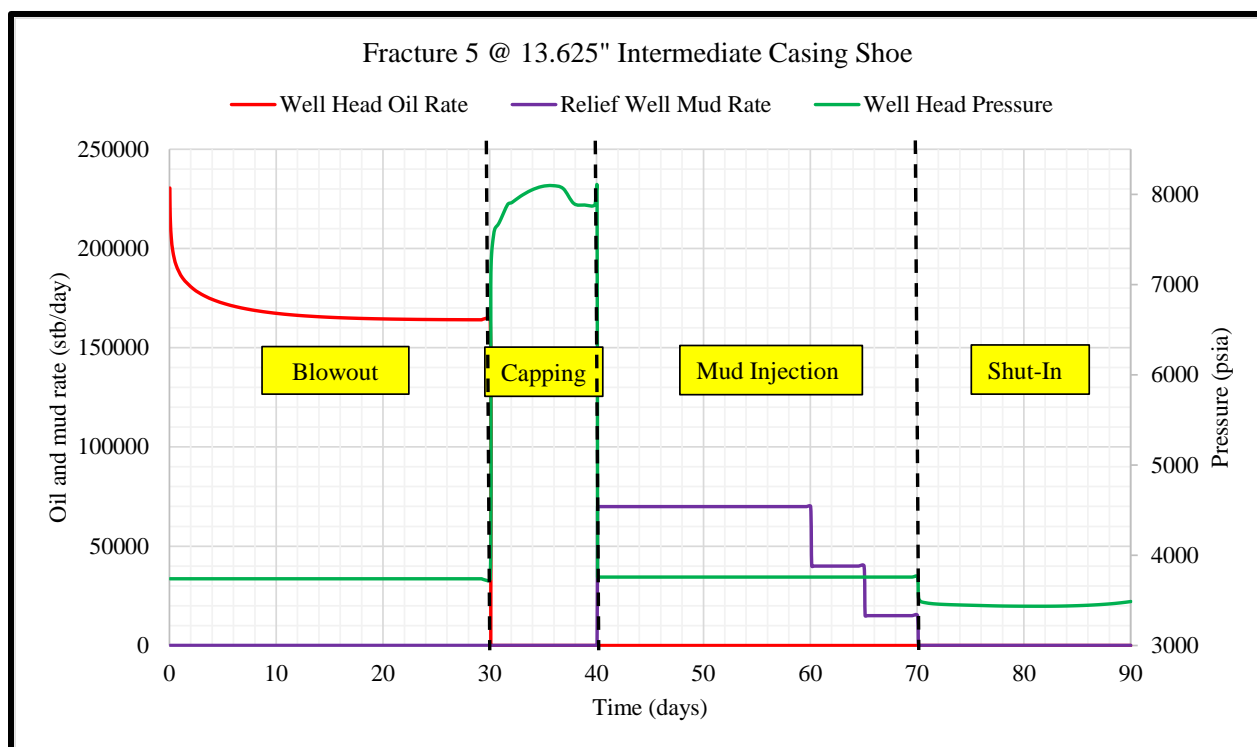


Figure 4. 1. Wellhead oil rate and pressure with time. The three dotted black lines separate the four modeling steps described in the workflow. Blowout (WCD) is modeled for 30 days, followed by capping shut-in in incident wellbore for 10 days, then mud is injected at three different rates from the relief well for a total period of 30 days, this is lastly followed by the last period which is composed of 20 days of incident wellbore shut-in and no mud injection from the relief well.

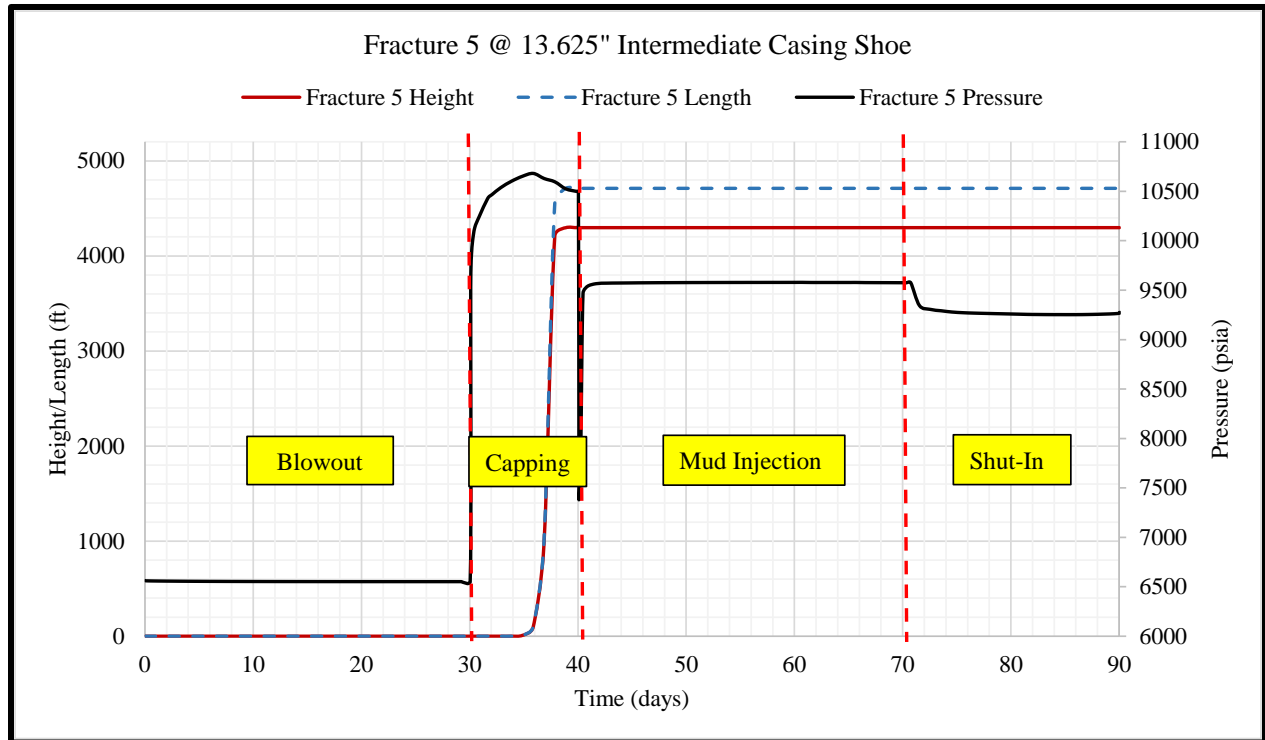


Figure 4. 2. Fracture 5 height and length shown against wellbore block pressure where the fracture has occurred.

Figure 4.2 and 4.3 shows the fracture height and length compared to the wellbore block (black line) where the fracture initiates. The wellbore pressure significantly drops as the fracture starts to propagate vertically (shown at 36 days in figure 4.3). This suggests that the fracture initially grows laterally before vertical propagation takes place. Lateral fracture growth does not impact wellbore pressure in this case. Vertical growth occurs 20 hours after the fracture has initiated. As the fracture starts propagating through the geologically stacked sandstones and shales, oil from reservoir and the damaged wellbore starts moving into the fracture increasing the fracture's net pressure and stress at tip. Since the fracture does not broach into the seafloor, the oil would remain in the fracture after reservoir stabilization is reached. Cumulative oil flowing into the fracture is reported in table 4.1. Figure 4.6 and 4.7 displays a cross-section and top view of the model showing the fracture location 4 days after initiation.

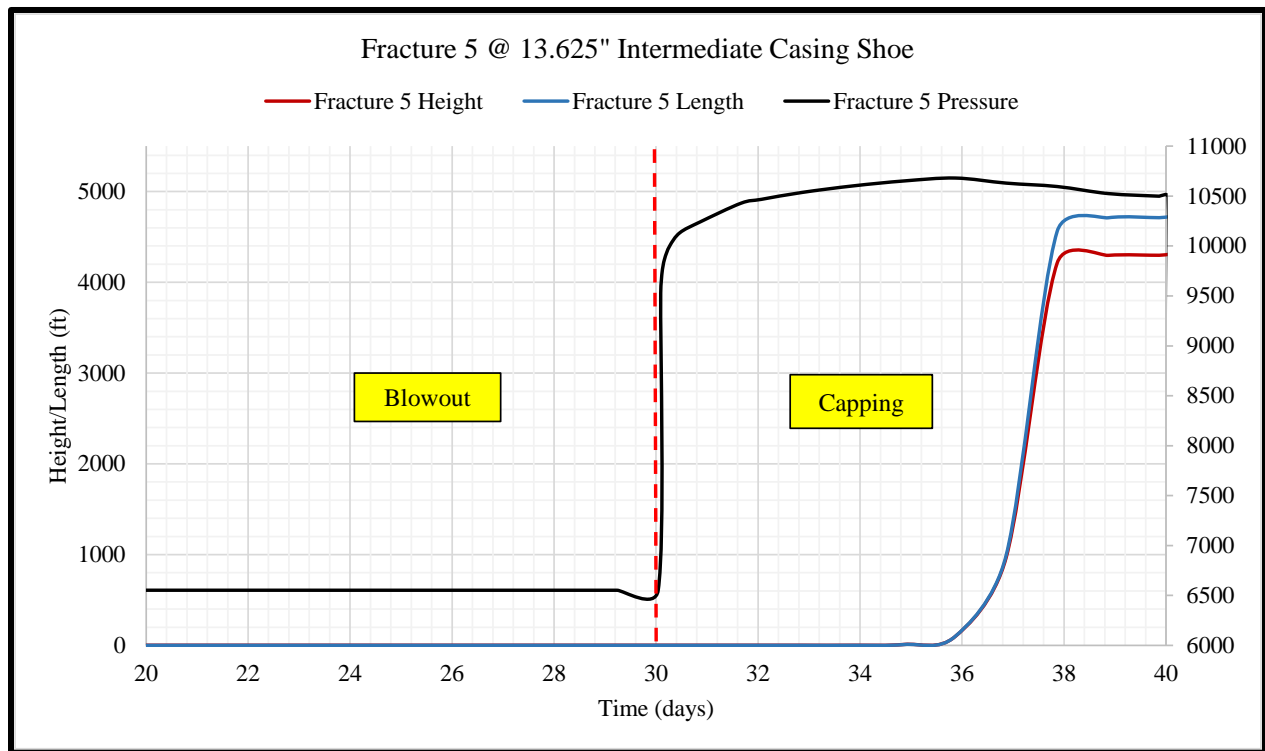


Figure 4. 3. Fracture 5 pressure drops as the fracture starts propagating. Substantial drop appears as the fracture grows in height.



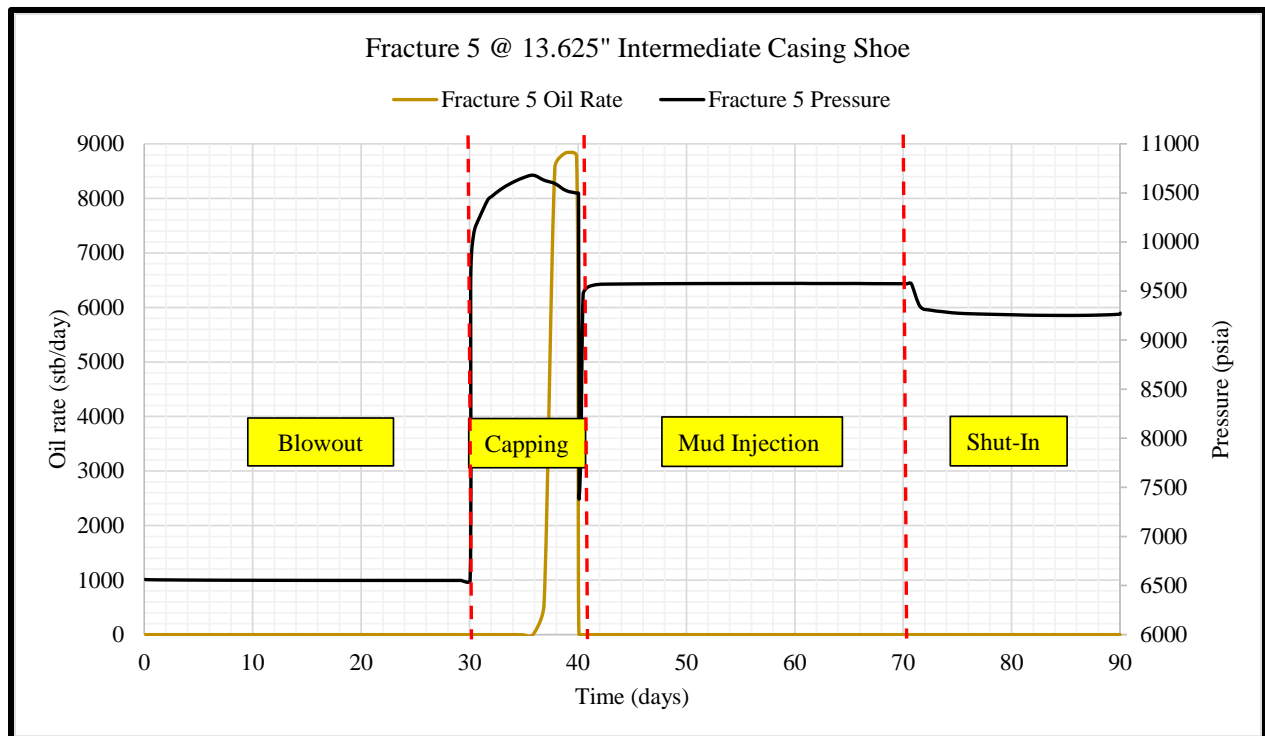


Figure 4. 4. Fracture 5 pressure at wellbore with oil rate flowing into the fracture shown against time.

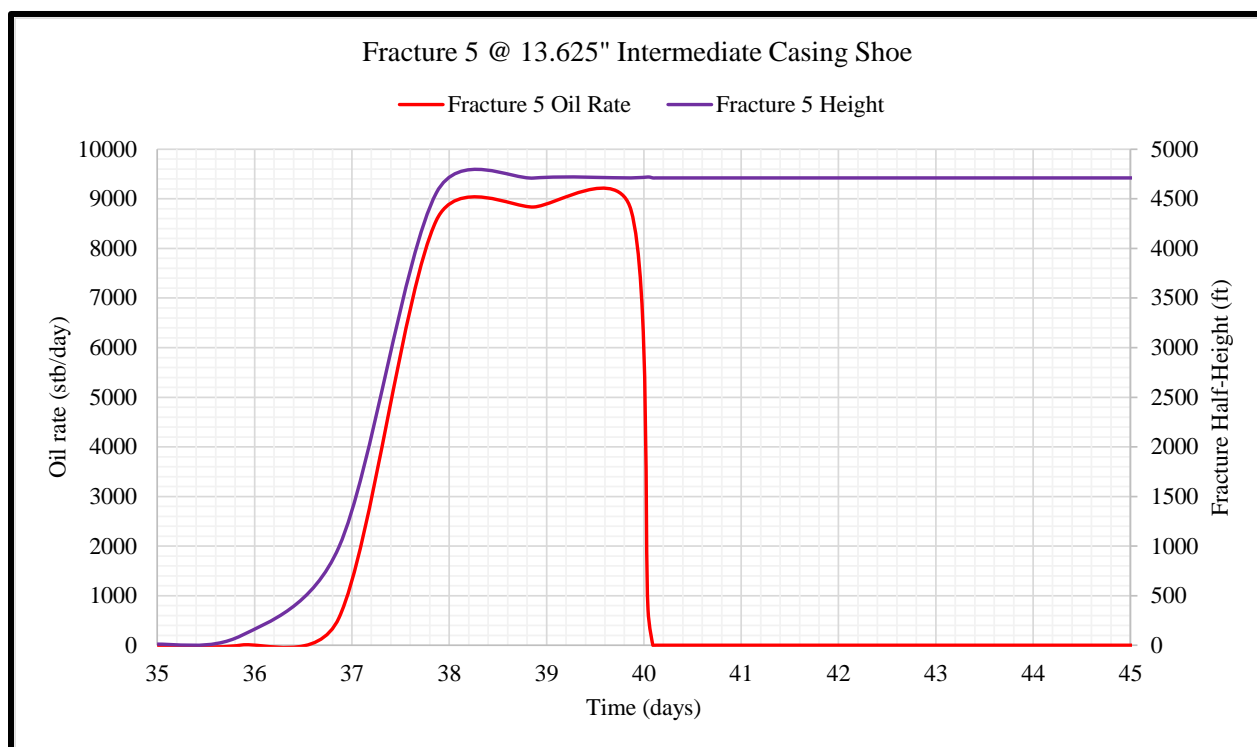


Figure 4. 5. Reduction in produced oil from the reservoir into the wellbore as kill-mud is injected through the relief well. The mud density with the optimal injection rate compensates the produced oil and ceases flow 6 hours after injection through lateral hole.

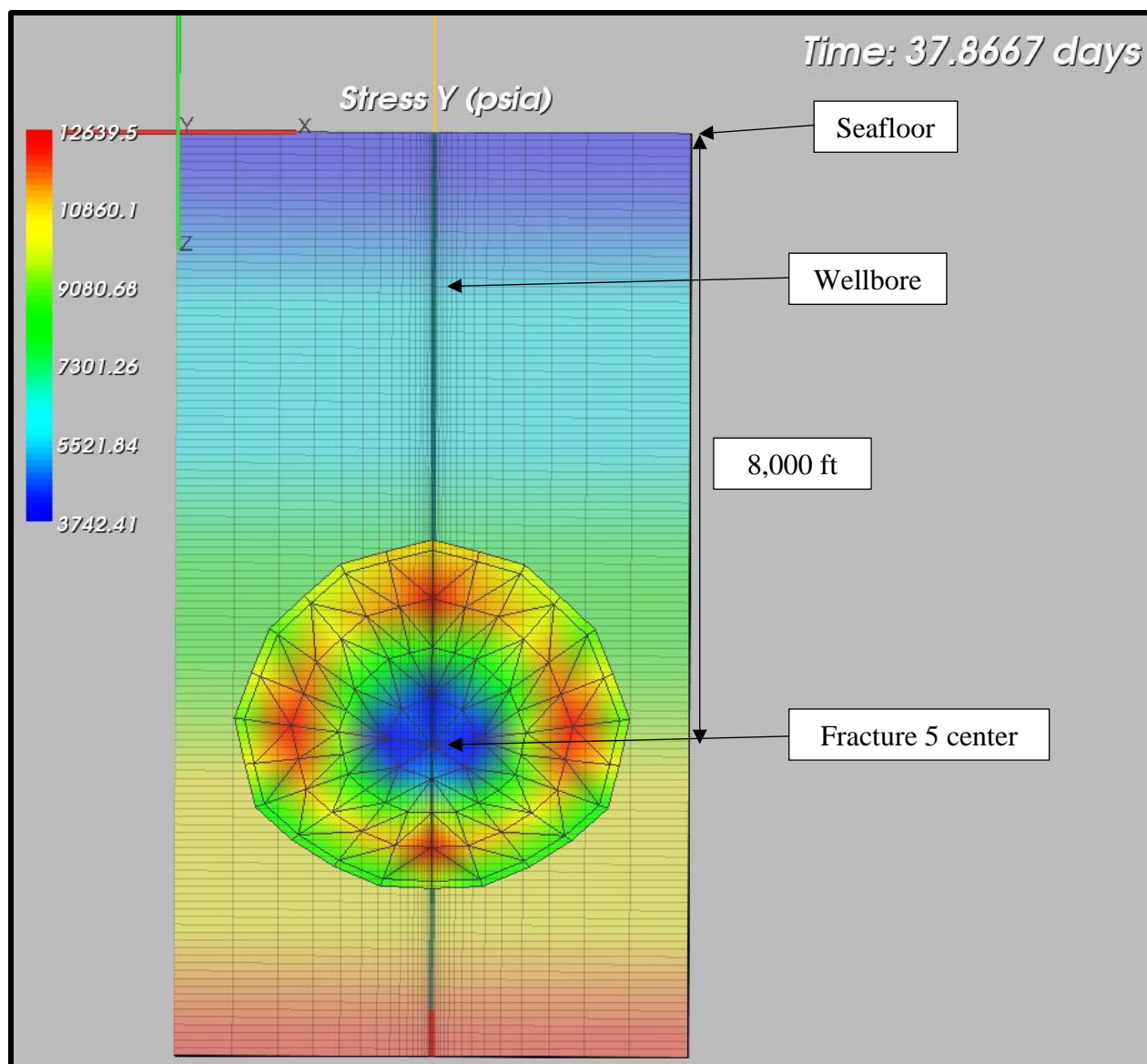


Figure 4. 6. Schematic cross section of the model with wellbore shown in center. Fracture 5 growth after 4 days of abrupt capping shut-in. Fracture shading shows the fluid velocity inside the fracture. Warmer regions indicate areas of high fluid velocity.

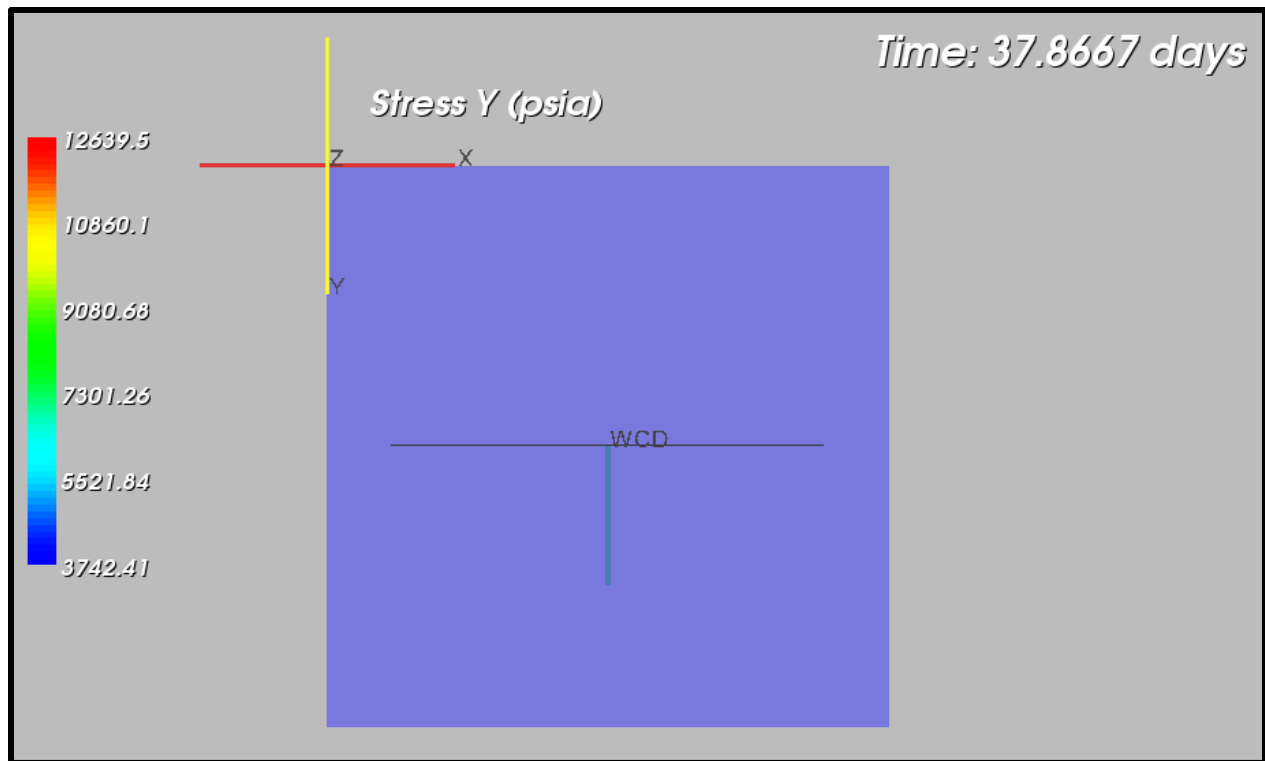


Figure 4. 7. Top view of the model. Straight black line shows the propagating fracture approximated on a 2D plane. The perpendicular blue line is a top view of the relief well intersecting the main wellbore.

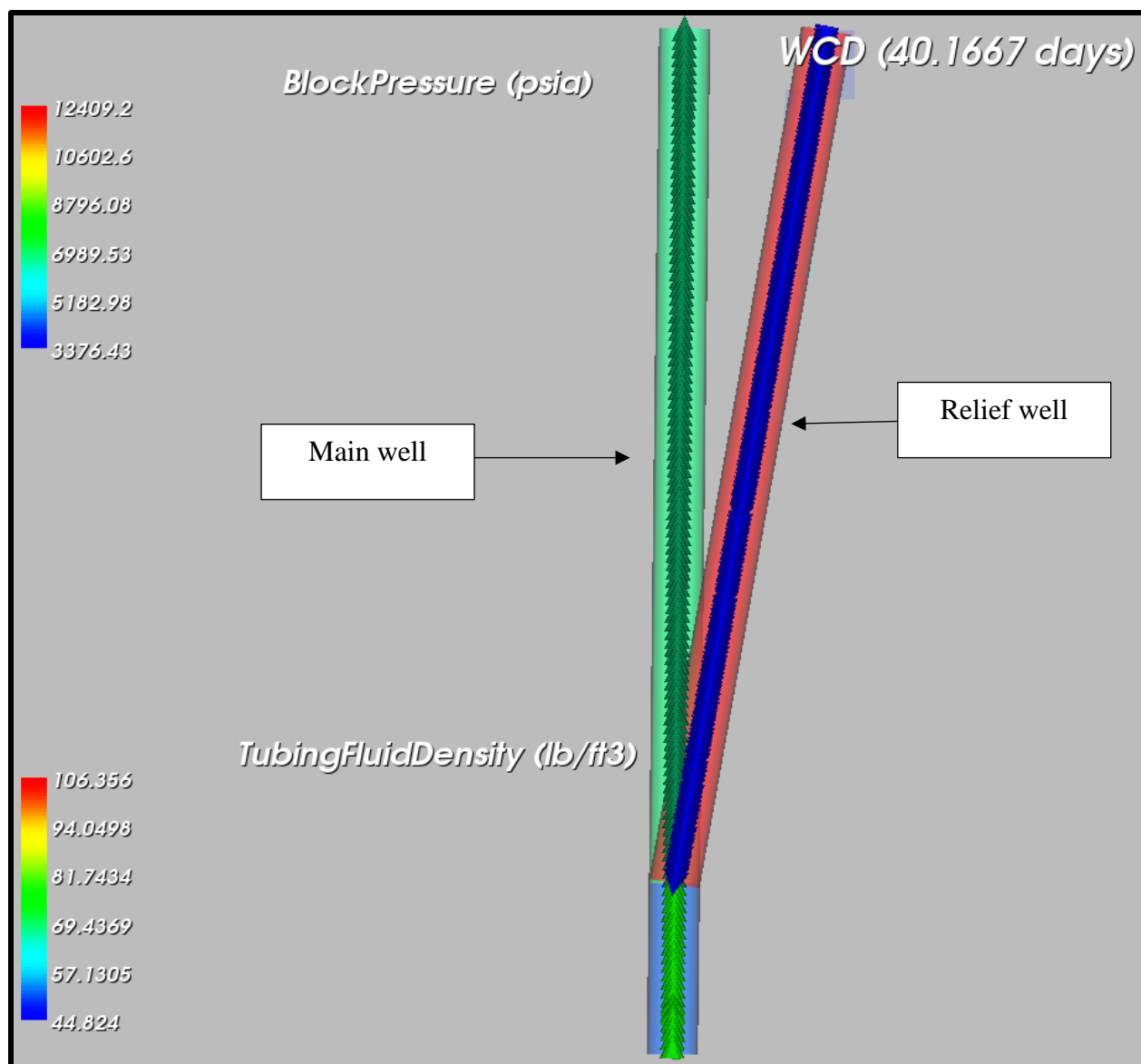


Figure 4. 8. Fluid density shown in wellbore before kill mud is injected through the relief well at 40.16 days. Wellbore is filled with low density hydrocarbons shown by the colder colors.

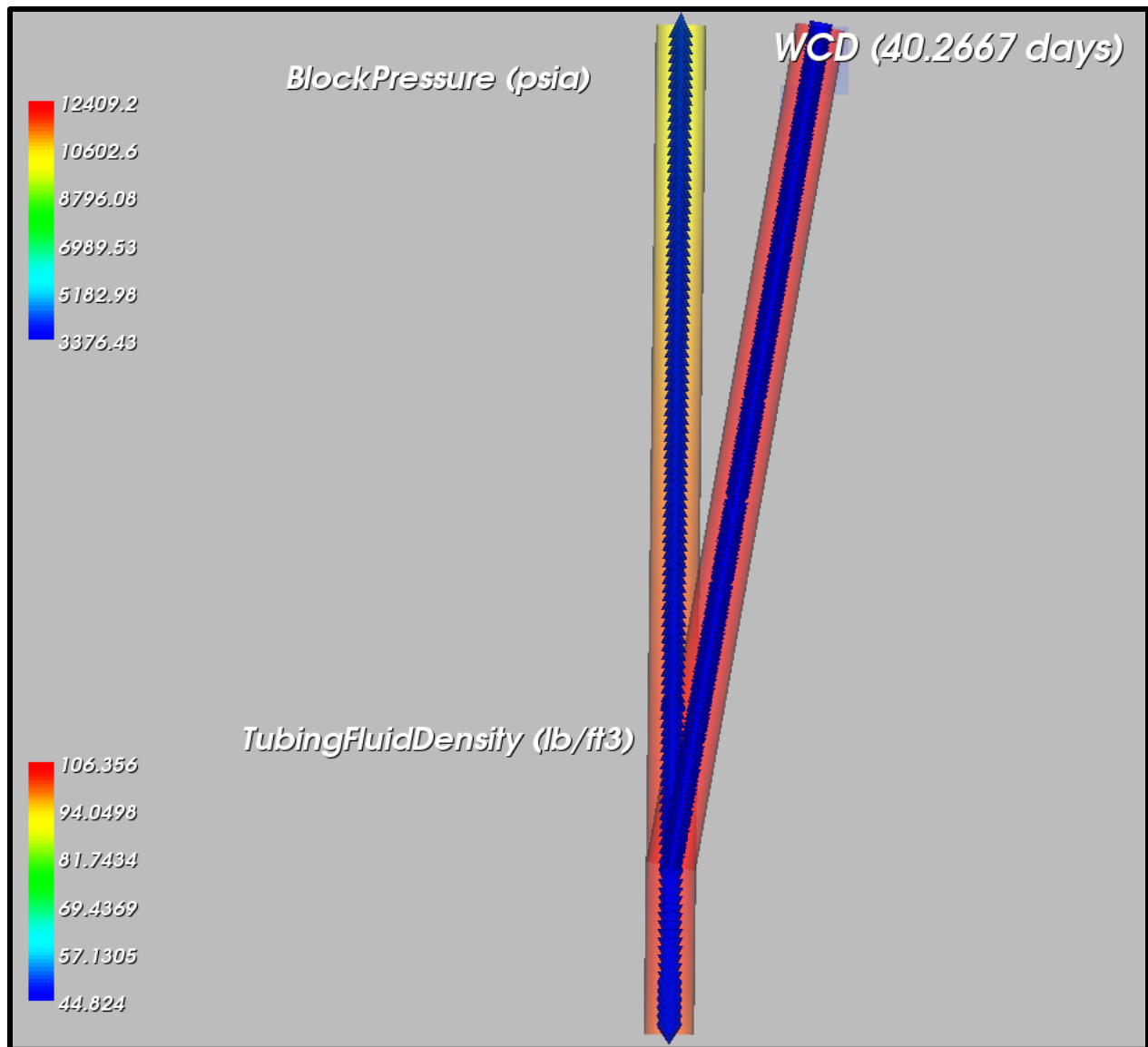


Figure 4. 9. Fluid density shown in wellbore after kill mud injection through relief well at 40.26 days. Wellbore fluid density increases as high-dense kill mud fills the wellbore. Yellower regions indicate areas where less dense fluid (hydrocarbons) is still present.

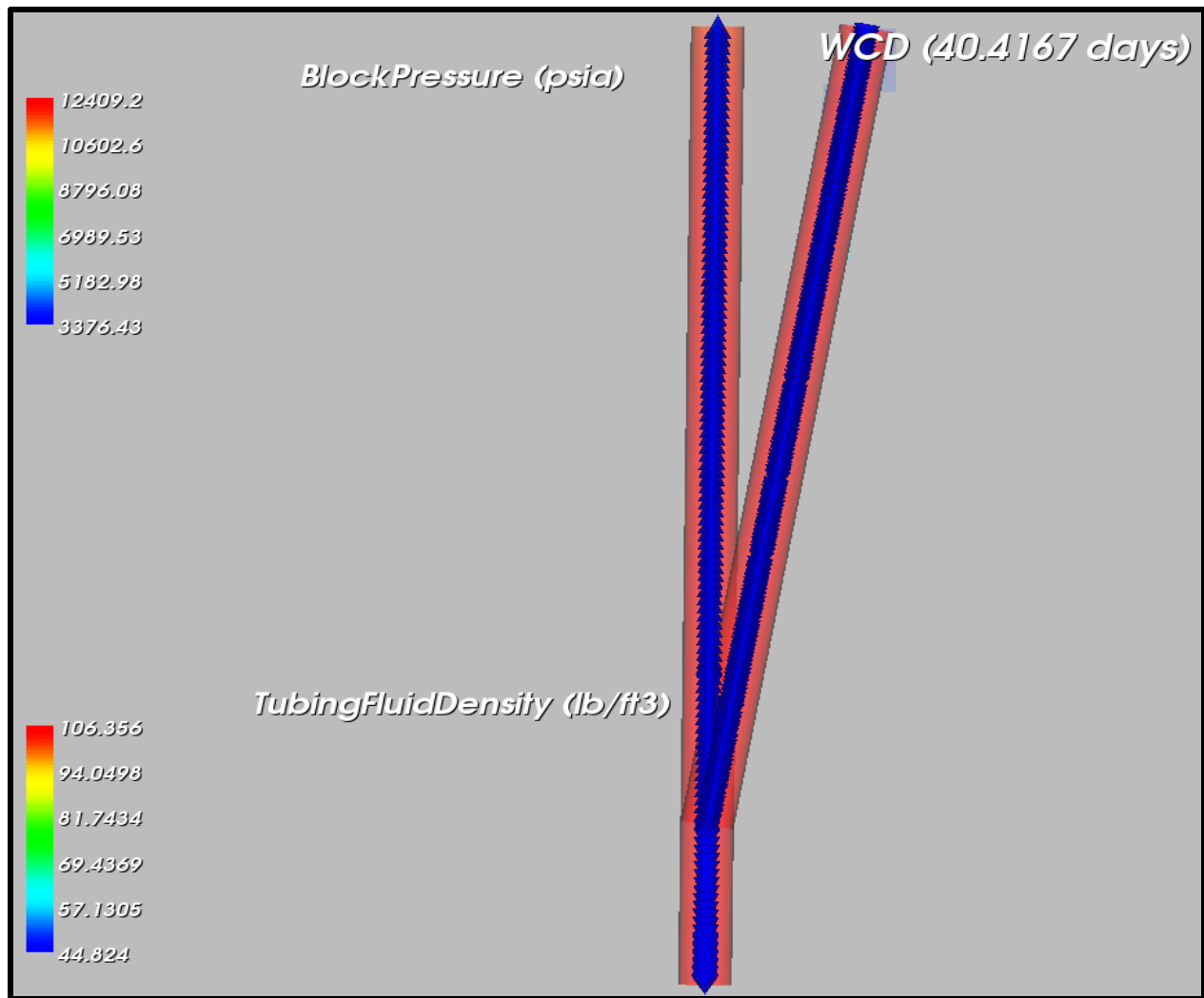


Figure 4. 10. Fluid density shown in wellbore after kill mud injection through relief well at 40.42 days. Kill mud has successfully displaced the hydrocarbons and filled the wellbore.

Table 4. 2. Base Case Model Results (Fracture 5 @ 13.625" Intermediate Casing).

| Property   | Value   |
|--|---------|
| WCD, STB/day                                     | 230,450 |
| Total Discharge Volume, MMSTB                    | 6.12    |
| Period of fracture initiation post capping, days | 3.86    |
| Fracture depth, ft below seafloor                | 7,997.5 |
| Maximum fracture length, ft                      | 4,712   |
| Maximum fracture height, ft                      | 4,299   |
| Cumulative oil rate flowing into fracture, STB   | 27,453  |
| Broach into seafloor?                            | No      |

## 4.2. Conductor Casing Leak

The following model assess the integrity of the 26" conductor casing (second casing) and the possibility of a fracture initiating at the casing shoe location located 1,500 ft below seafloor. The model simulates a continuously connected microannulus along the wellbore from the 11.875" intermediate liner to the 26" surface casing resulting from a void in the cement-casing interface from an imperfect cement job. The width of the microannulus is 0.0003" modeled as a confined annulus between the cement and the drilled region. The fracture initiates only 0.13 days after capping and broaches to the seafloor approximately 1 day after. This rapid growth is supported by the low permeability, low porosity, layers' pore pressure, and in-situ stress states near the seafloor. At this depth, the fracture toughness exceeds the rock critical stress intensity of all overburden rocks resulting in fracture propagation and eventually broaching to the seafloor. Figure 4.12 displays the rate oil flowing into the fracture. Thousands of barrels are spilled in the ocean at a rate of 2,750 STB/day. Figure 4.11 shows the wellhead oil rate, capping build-up pressure, and relief well kill mud injection rates.



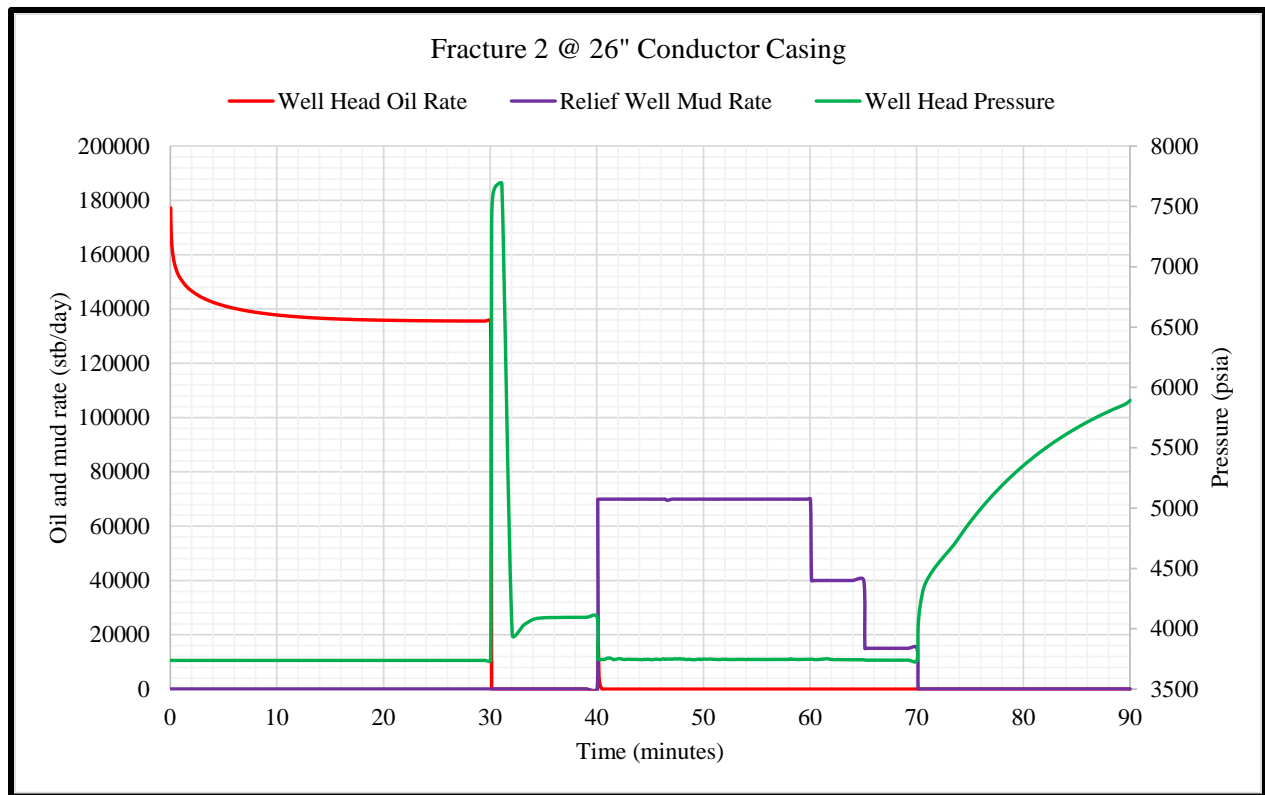


Figure 4. 11. Well head oil rate, capping shut-in pressure, and relief well injection rates as a function of time. The fluctuations shown in red is due to transient liquid slugs in the incident wellbore.

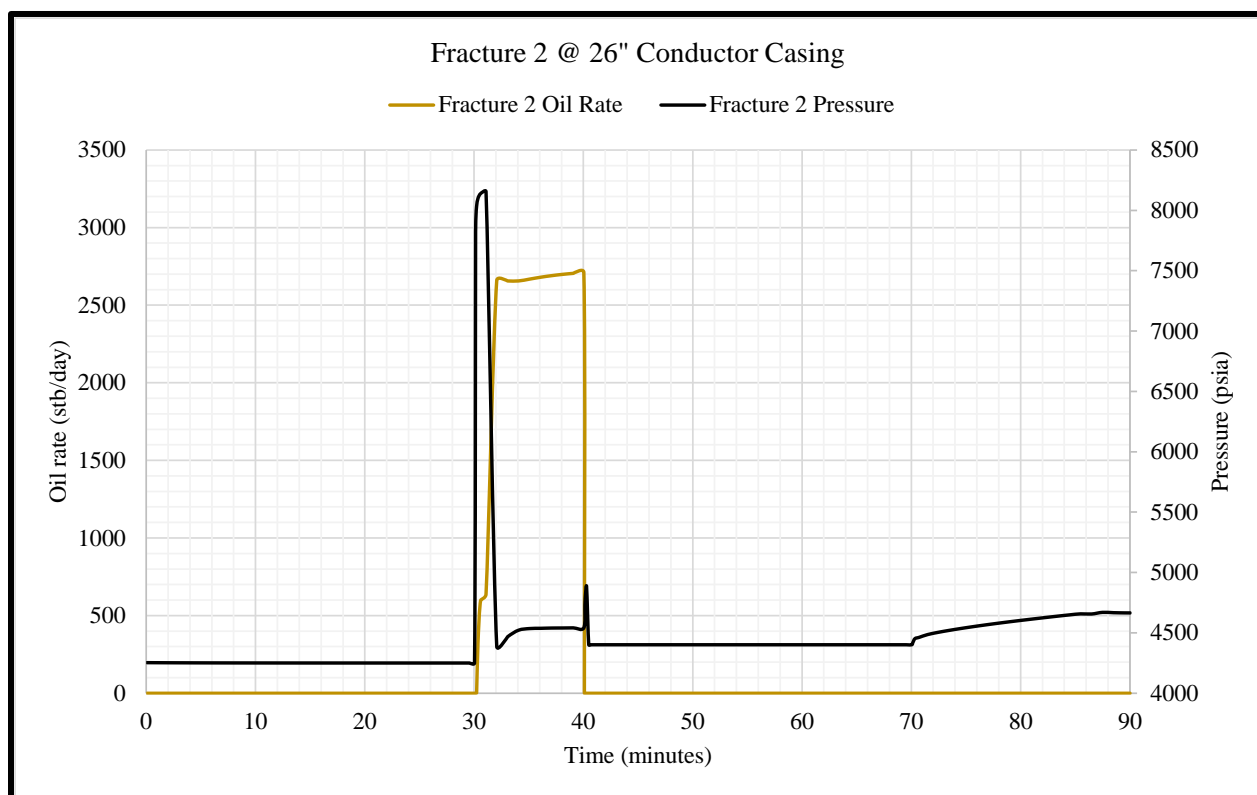


Figure 4. 12. Pressure at wellbore where the fracture has initiated and oil rate flowing into the fracture. Oil rate in the fracture displays an increase with time owed to the fracture breaching to the seafloor.

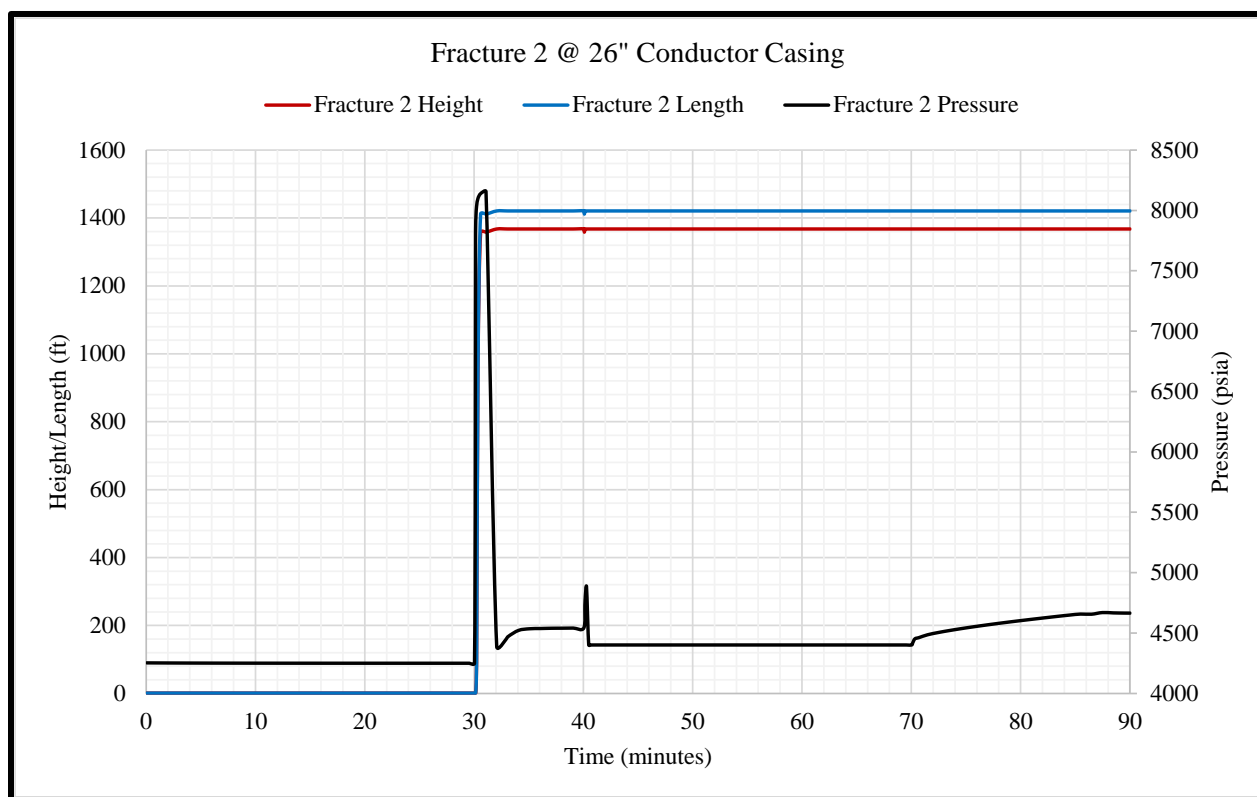


Figure 4. 13. Fracture pressure at wellbore with height and length shown as a function of time.

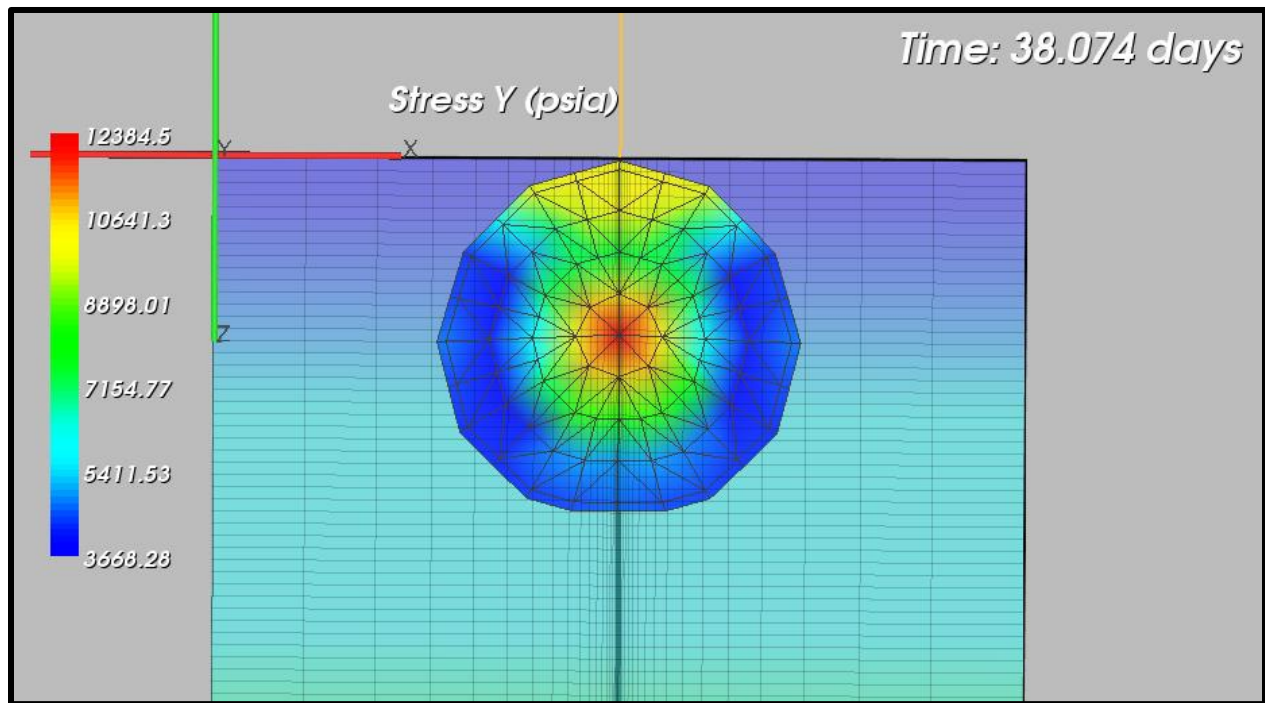


Figure 4. 14. Graphical illustration of the propagating fracture 2 at the 26" surface casing broaching into the seafloor close to the well head. Fracture shading shows the fluid velocity inside the fracture.

Table 4. 3. Model Results (Fracture 2 @ 26" Conductor Casing).

| Property   | Value   |
|--|---------|
| Period of fracture initiation post capping, days | 0.17    |
| Fracture depth, ft below seafloor                | 1,497.5 |
| Maximum fracture length, ft                      | 1,492.5 |
| Maximum fracture height, ft                      | 1,627   |
| Cumulative oil rate flowing into fracture, STB   | 25,689  |
| Broach into seafloor?                            | Yes     |

#### 4.3. Surface Casing Leak

In this model, hydrocarbon leakage through the confined annulus (microannulus) is only allowed between the open-hole section, up the 11.625", 13.625", 16" and the 20" surface casing. The location of the casing shoe is approximately 3000 ft below seafloor at the 20" surface casing. For this model, the fracture initiates 6 hours after capping shut-in is performed. The fracture

initiates after the wellbore block (where the fracture 3 is set) pressure exceeds the layer's  $p_i$  due to the void being filled with accumulated hydrocarbons. The fracture, provided by a substantial amount of oil, propagates through the layers and eventually broaches to the seafloor 48 hours after initiation. The fracture continues to deliver oil into the seafloor through the broached fracture at a steady rate of approximately 2,500 STB/day.

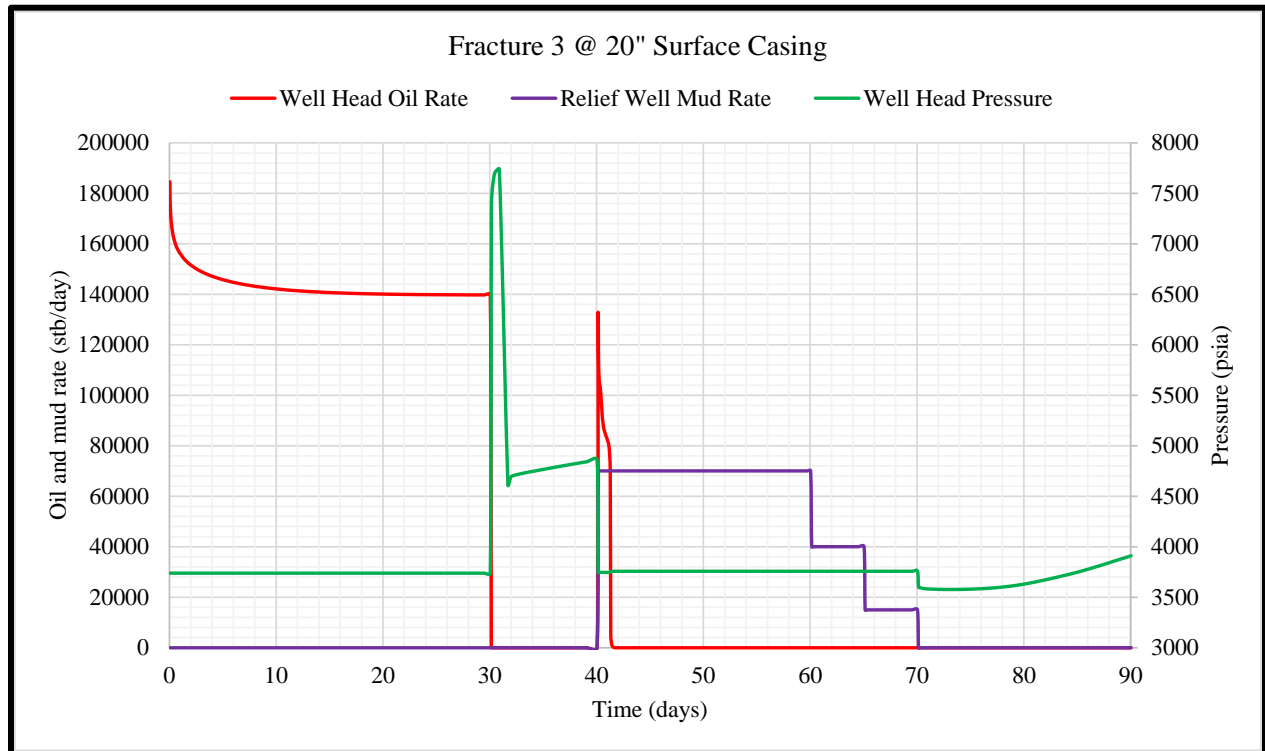


Figure 4. 15. Well head oil rate, capping pressure, and relief well injection rates as a function of time for fracture 3 at 20" surface casing shoe location. Significant drop in wellhead pressure is due to fracture initiation 3,000 ft below wellhead.

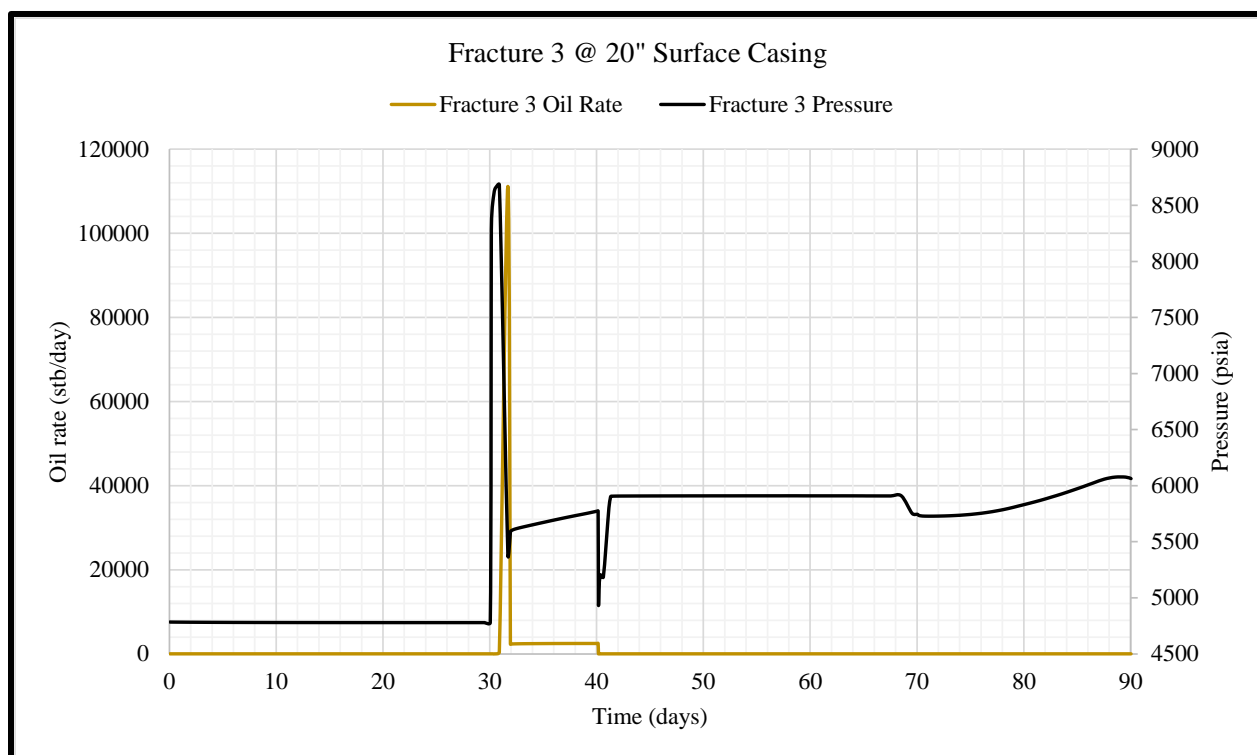


Figure 4. 16. Fracture 3 pressure at wellbore and oil rate shown with time. Significant oil is supplied into the fracture resulting in a drop in wellbore pressure.

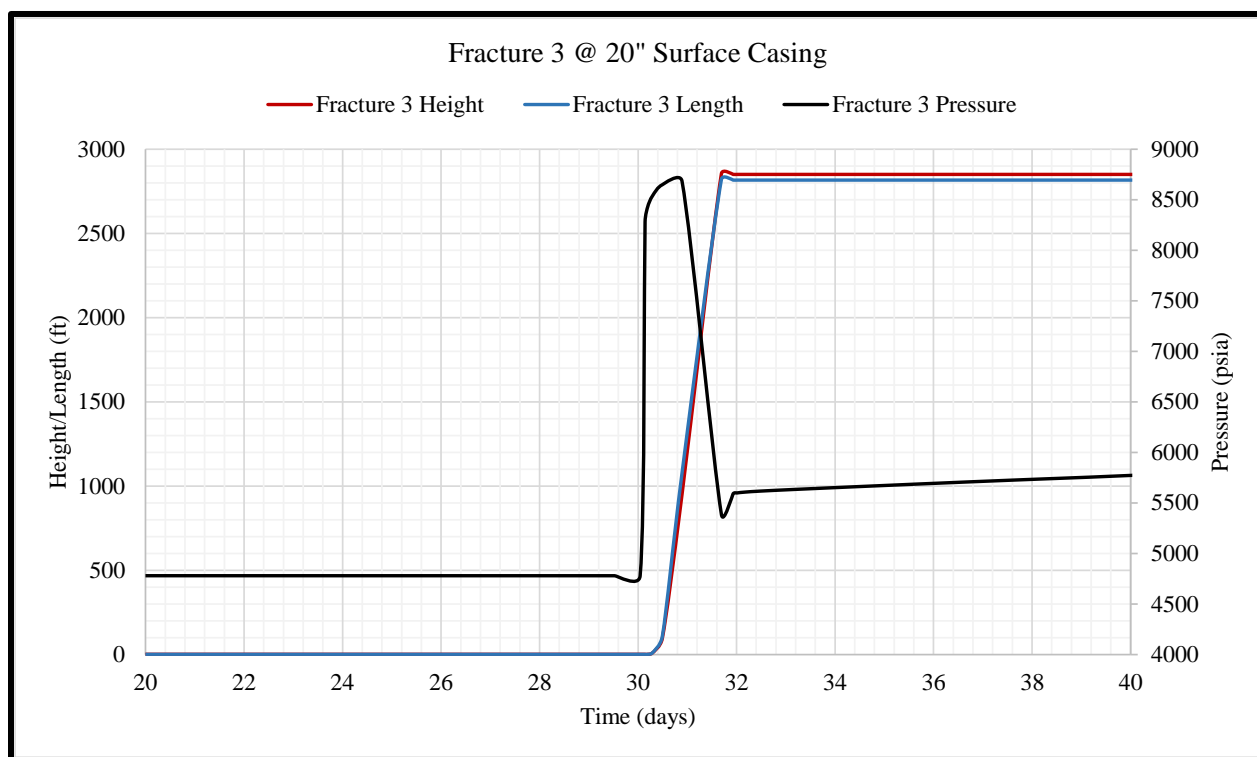


Figure 4. 17. Fracture 3 height and length. The rise in oil rate shown in figure 4.16 is due to the rapid fracture growth occurring upon initiation, evident here.

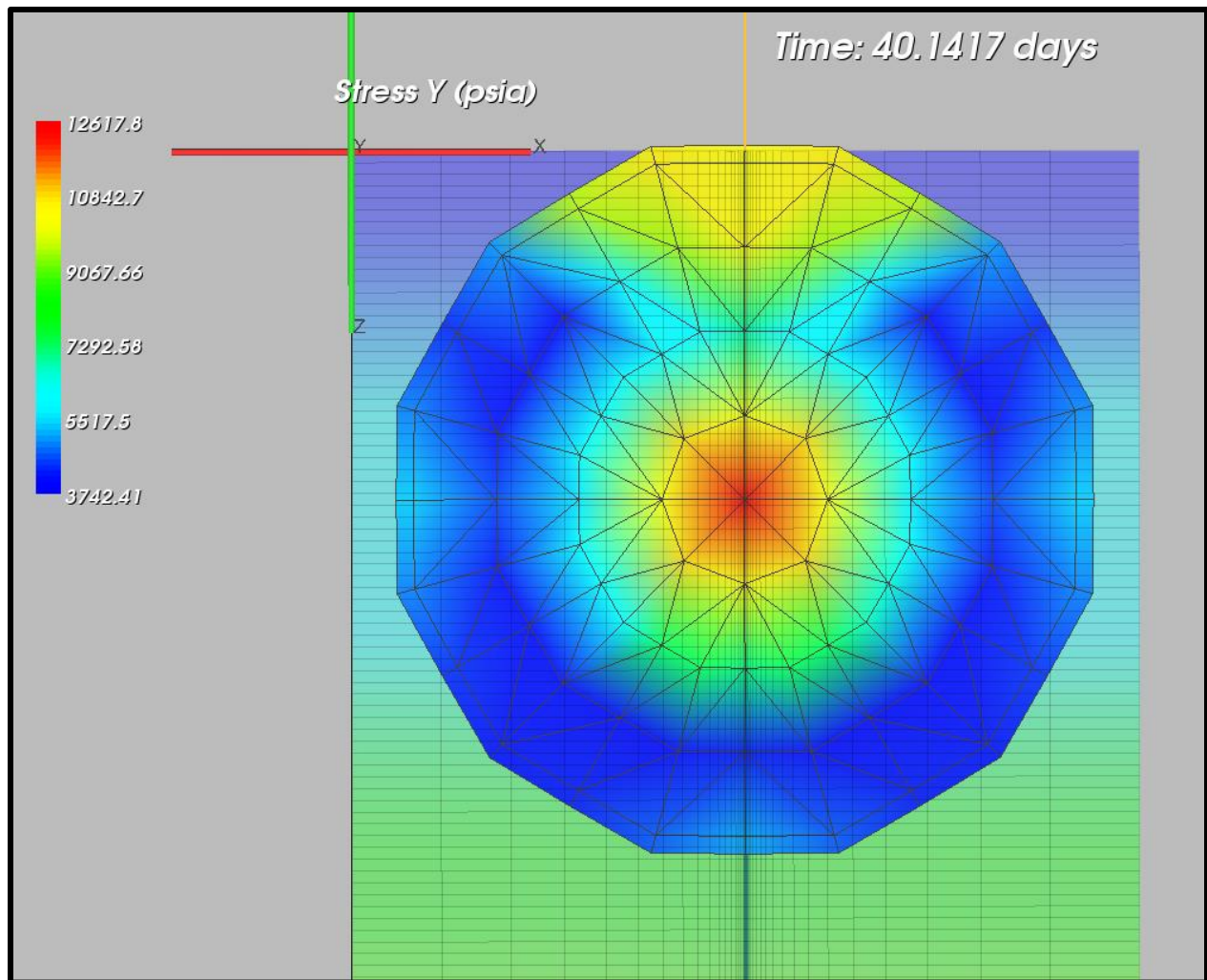


Figure 4. 18. Graphical representation of fracture 3 initiating at 20" surface casing shoe location upon breaching into the seafloor.

Table 4. 4. Model Results (Fracture 3 @ 20" Conductor Casing).

| Property   | Value   |
|--|---------|
| Period of fracture initiation post capping, days | 0.29    |
| Fracture depth, ft below seafloor                | 2,997.5 |
| Maximum fracture length, ft                      | 2,816   |
| Maximum fracture height, ft                      | 2,997.5 |
| Cumulative oil rate flowing into fracture, bbl   | 142,987 |
| Broach into seafloor?                            | Yes     |



#### **4.4. Drilling Liner Casing Collapse**

The following model assess the integrity of the 16” drilling liner and the possibility of a fracture initiating at the casing shoe location located 5,000 ft below seafloor. This model assumes that the casing collapse has occurred in the preceding blowout period pre-capping shut-in. Substantial drop in wellbore pressure takes place as the fluids are released to the seafloor through the BOP, open-pipe, LMRP. The large differential pressure between the internal side of the casing where the fluids flow and the external side where the formation is present is the main cause of casing collapse. In this study, casing collapse is modeled as a 5-foot long casing break where the fluids are allowed to escape the wellbore and enter the annulus region between the cement and the formation. Fracture 4 is placed in the center of the casing break. The fracture initiates 0.15 days after capping shut-in, this is shown by a slight drop in wellhead and fracture pressure as the fracture starts propagating in the geological media. Fracture 4 propagates for a period of time until eventually reaching the seafloor causing a significant amount (spike) of oil to be spilled into the ocean which is then followed by a steady rate of broaching oil around 2,500 STB/day. This is evident by the sharp fall in wellhead and fracture pressure at the wellbore block (shown in Figure 4.19 and 4.20). Enough energy is supplied to the fracture tip through the escaped hydrocarbons causing the fracture to propagate and ultimately broach to the seafloor.

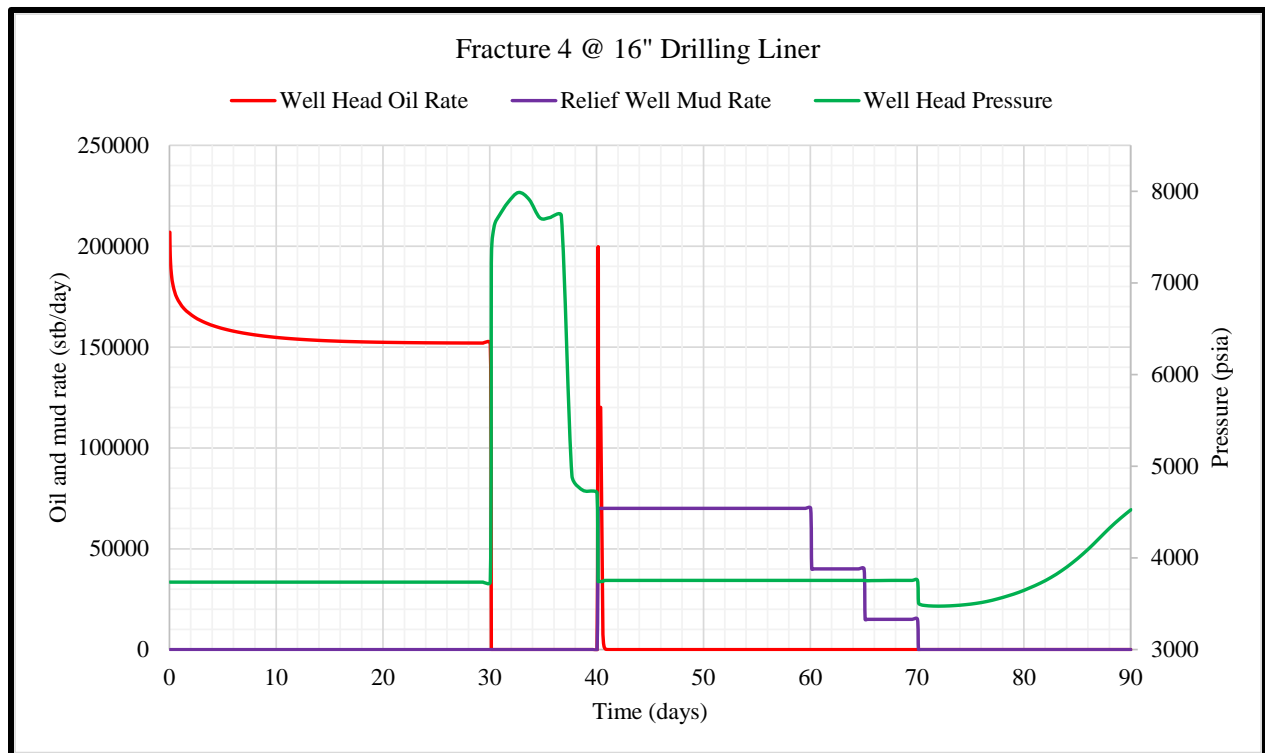


Figure 4. 19. Well head oil rate, capping (WH) pressure, and relief well injection rates as a function of time for fracture 4 at 16" drilling liner shoe location.

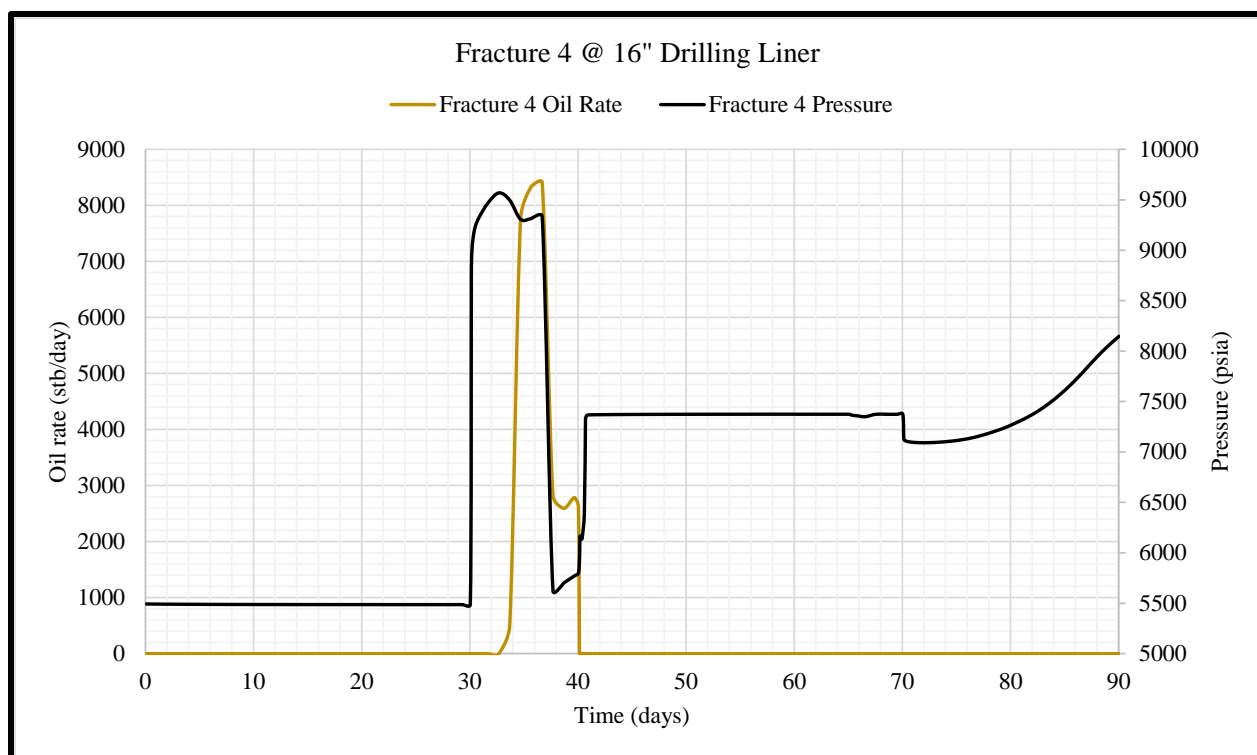


Figure 4. 20. Fracture 4 pressure at wellbore and oil rate into the fracture shown with time. Significant oil is supplied into the fracture resulting in a drop in wellbore pressure.

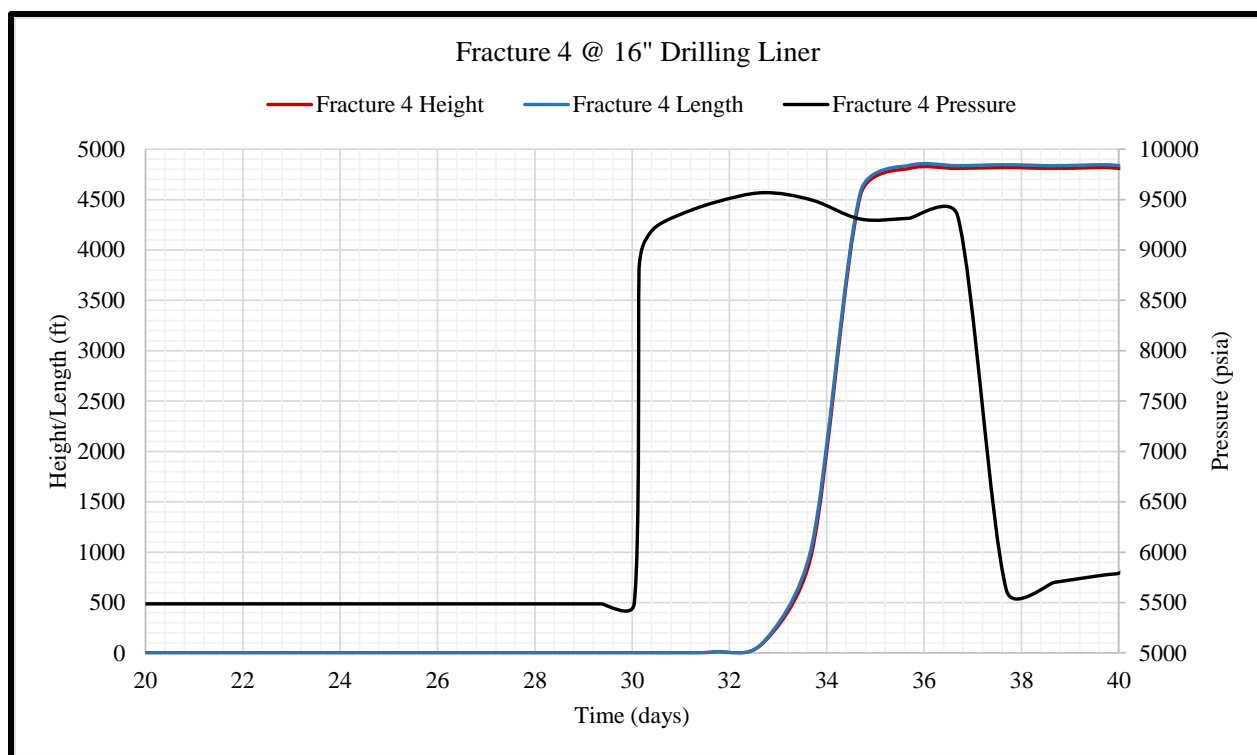


Figure 4. 21. Fracture 4 height and length. The rise in oil rate shown in figure 4.20 is due to the rapid fracture growth occurring upon initiation.

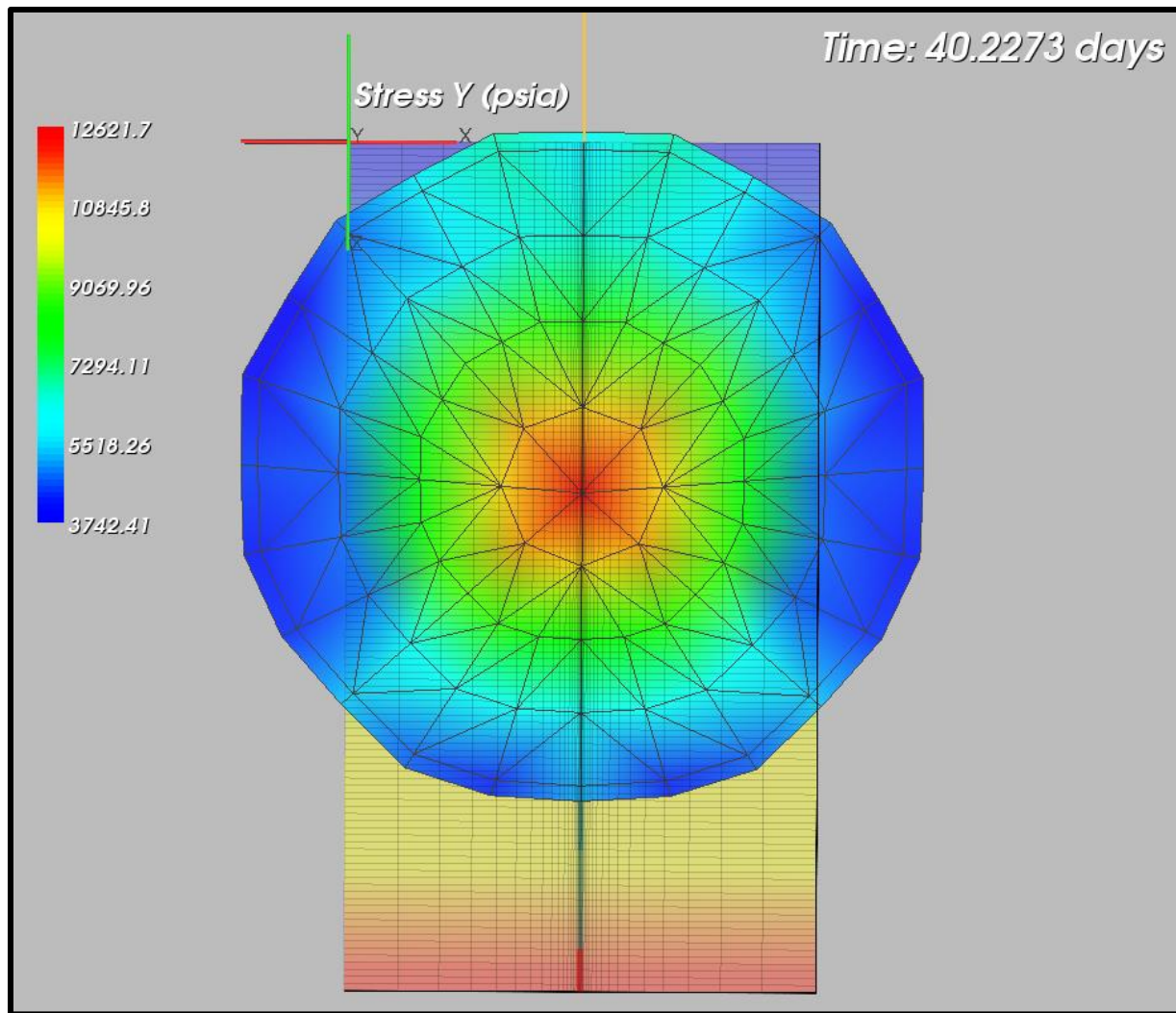


Figure 4. 22. Fracture 4 shown broaching into the seafloor 1.5 days after initiating. The fracture length exceeds the dimensions of the model resulting in fracture growing in the external grid blocks.

Table 4. 5. Model Results (Fracture 4 @ 16" Drilling Liner).

| Property   | Value   |
|--|---------|
| Period of fracture initiation post capping, days | 0.89    |
| Fracture Depth, ft below seafloor                | 4,497.5 |
| Maximum fracture length, ft                      | 4,837   |
| Maximum fracture height, ft                      | 4,497.5 |
| Cumulative oil rate flowing into fracture, bbl   | 35,826  |
| Broach into seafloor?                            | Yes     |

#### 4.5. Perfect Cement in Casings

In this case study, we assume perfect casing cement integrity with no voids in the cement-rock interface and no casing collapse has occurred. The aim is to investigate if a fracture will initiate and propagate after the last casing shoe location. The 11.875" intermediate liner is set at a depth of 11,400 ft, approximately 200 ft above the oil water contact. The fracture is modeled as an initially closed fracture, 2.5 ft below the casing (11,402.5 ft below the seafloor). Results indicate that at this depth, the pressure build-up is not high enough to exceed FIP, therefore no fracture initiation and subsequent propagation is observed. This is evident by a straight line in the fracture length and height in figure 4.24. The wellhead pressure continues to build-up as the reservoir is stabilizing.

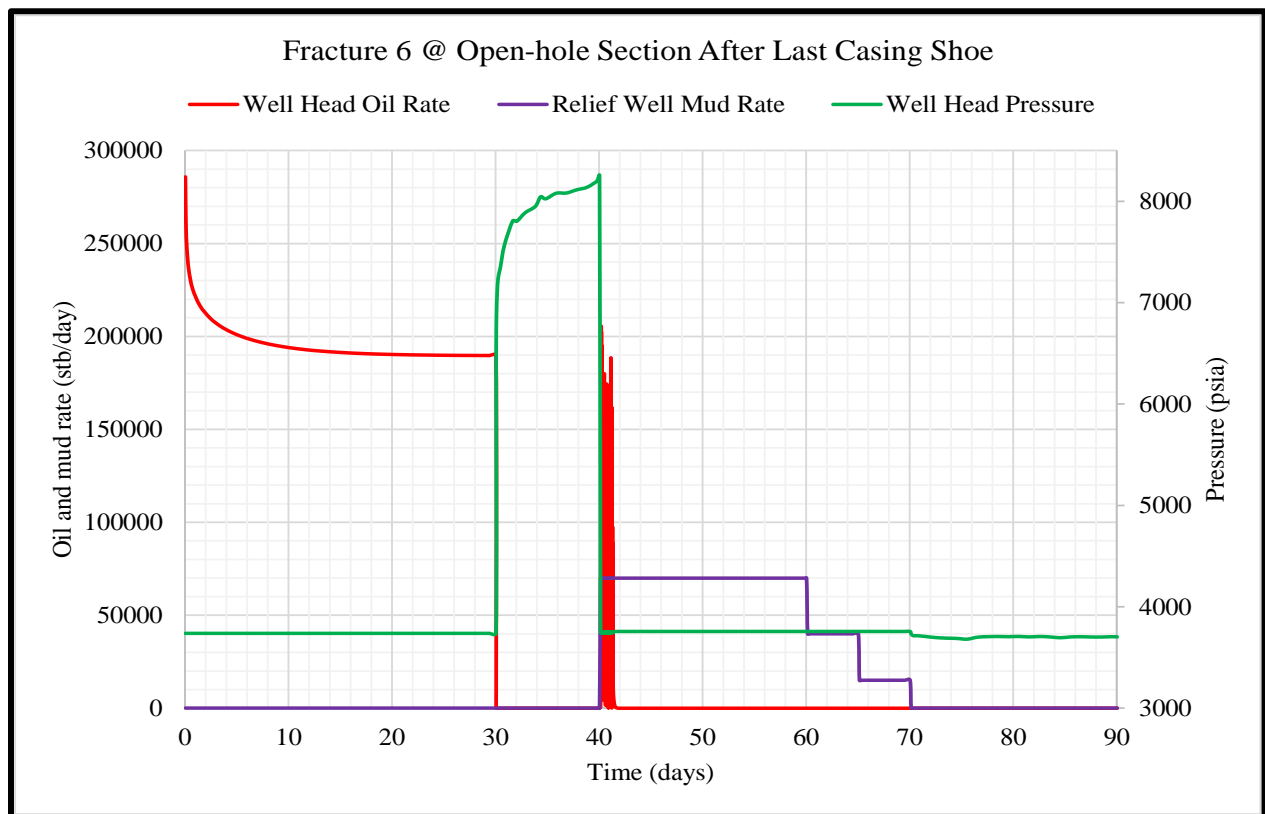


Figure 4. 23. Well head oil rate, mud rate injection, and well head pressure for the perfect casing integrity case study.

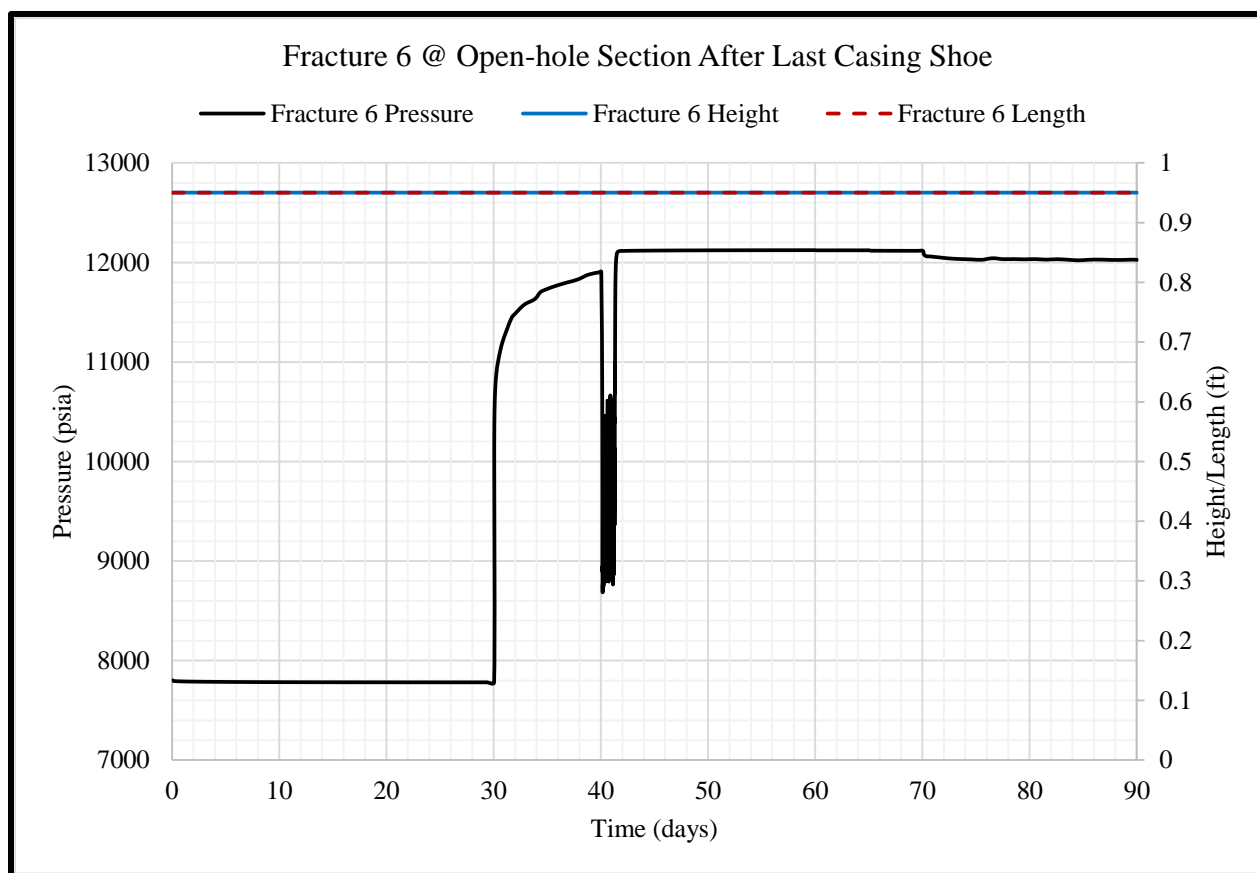


Figure 4. 24. Fracture pressure at wellbore block shown with height and length. No fracture initiated; hence straight line is shown.

#### 4.6. Young's Modulus Contrast

The objective of this study is to determine the effects of extreme discharge rates ( $>200,000$  STB/day) on crack propagation behavior at the reference fracture initiation depth below casing shoe. A shale layer, upon which the initially closed fracture is set, will be examined under various young's modulus,  $E$  contrast. Multiple runs with different contrast in sandstone and shale, Young's Moduli,  $E_{ss}$  and  $E_{sh}$  respectively, are performed.  $E_{sh}$  values ranging from  $2 \times 10^5$  to  $7 \times 10^6$  psi are populated distinctively throughout each shale layer while  $E_{ss}$  is kept constant at  $2 \times 10^6$  psi. Figures 4.25 and 4.26 summarize the results of the performed simulations. Results show that high shale/sandstone Young's modulus ratios ( $E_{sh}/E_{ss}$ ) are found to suppress fracture height and length. Fractures will tend to initiate faster as low Young's Modulus is encountered in the geological media. High Young's modulus will result in fracture propagation occurring in a slower rate than in a low Young's modulus layers. A fracture initiating in shale layers having  $E_{sh}$  of  $7 \times 10^5$  psi will occur 6 hours later as opposed to the shale layer having a  $E_{sh}$  of  $2 \times 10^5$  psi. On the other hand a shale layer having  $E_{sh}$  a magnitude higher at  $2 \times 10^6$  psi similar to the sandstone layers in this case, would occur almost 42 hours as opposed to the layer having  $2 \times 10^5$  psi.



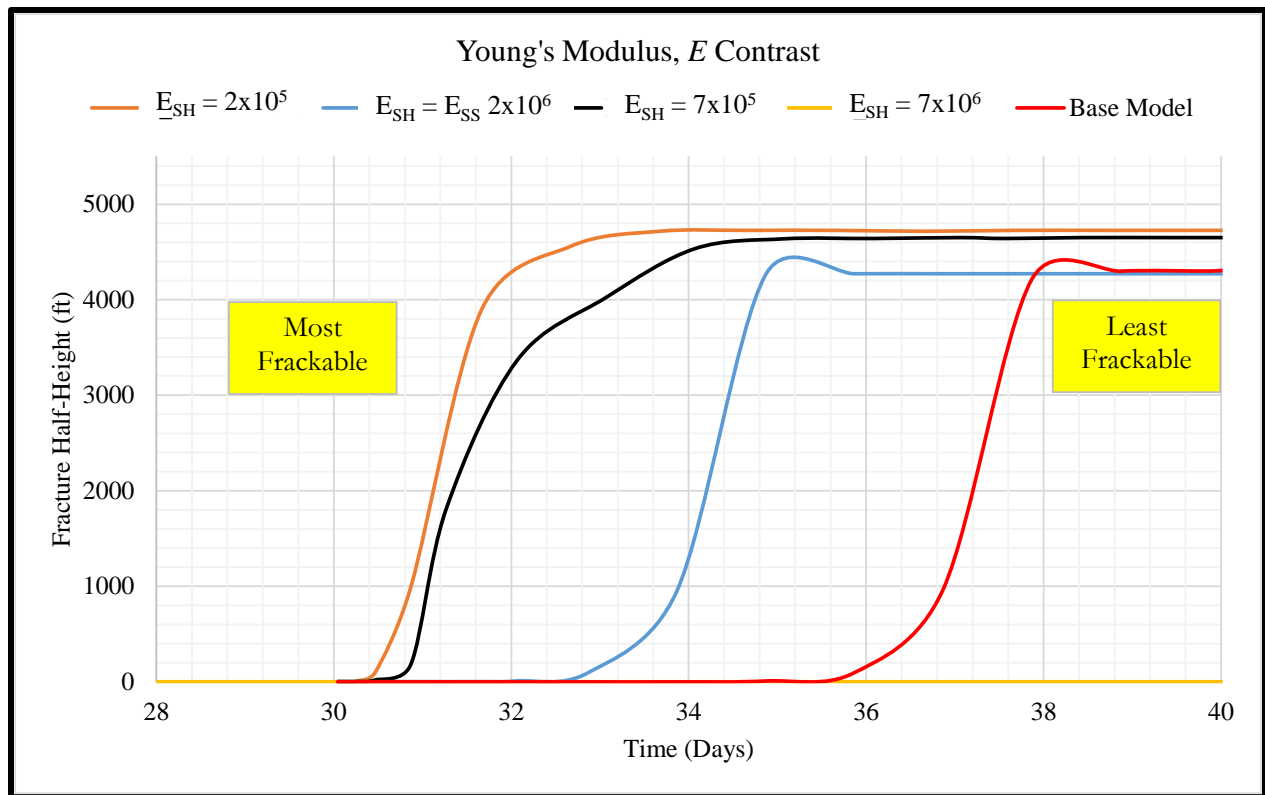


Figure 4. 25. Fracture height variation against time for four different  $E_{sh}$  values.

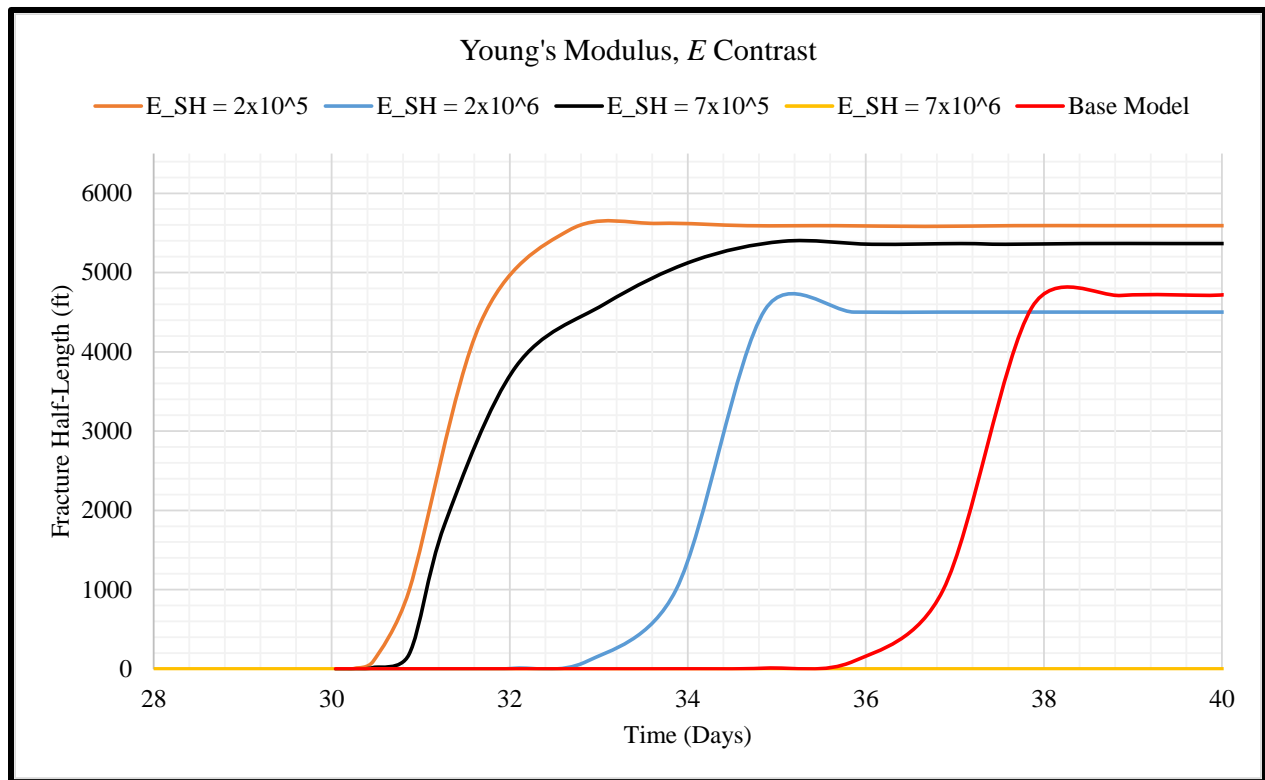


Figure 4. 26. Fracture length variation against time for four different  $E_{sh}$  values.

#### **4.7. Reservoir Overpressure Variation**

Geopressured basins can occur naturally and they are found mostly in sedimentary formations. They are typically encountered in the GoM region (Wys, 1992). Geologic overpressurization in stratigraphic layers is caused by the inability of connate pore fluids to escape as the surrounding mineral matrix due to, for example, an impermeable (such as shale) sealing layer that have compacted in a very high rate over the porous sandstone (Speight, 2019). In addition, overpressurization may also be a result of enhanced or improved recovery activities like water or gas injection (Zaki et al., 2015). While pressures approach hydrostatic gradients in some systems (0.465 psi/ft in this study), overpressured systems will exceed the hydrostatic gradient and even approach overburden pressure (shown in base case model figure 3.10), resulting in an abnormally over-pressured reservoir for their depth (Speight, 2019). To assess the impact of reservoir overpressurization on fracture initiation due to capping shut-in, three runs were made with 1,000 psi increments from normal pressure under lithostatic gradient at the depth of the reservoir. Pore-pressure under normal lithostatic gradient is around 9,115 psi. Results indicated that overpressurization of 2,000 psi or less is not adequate for fracture initiation, only at 3,000 psi overpressurization is fracture initiation observed. The 3,000 psi over-pressured model is the base case model described in section 3.2 with results in section 4.2.

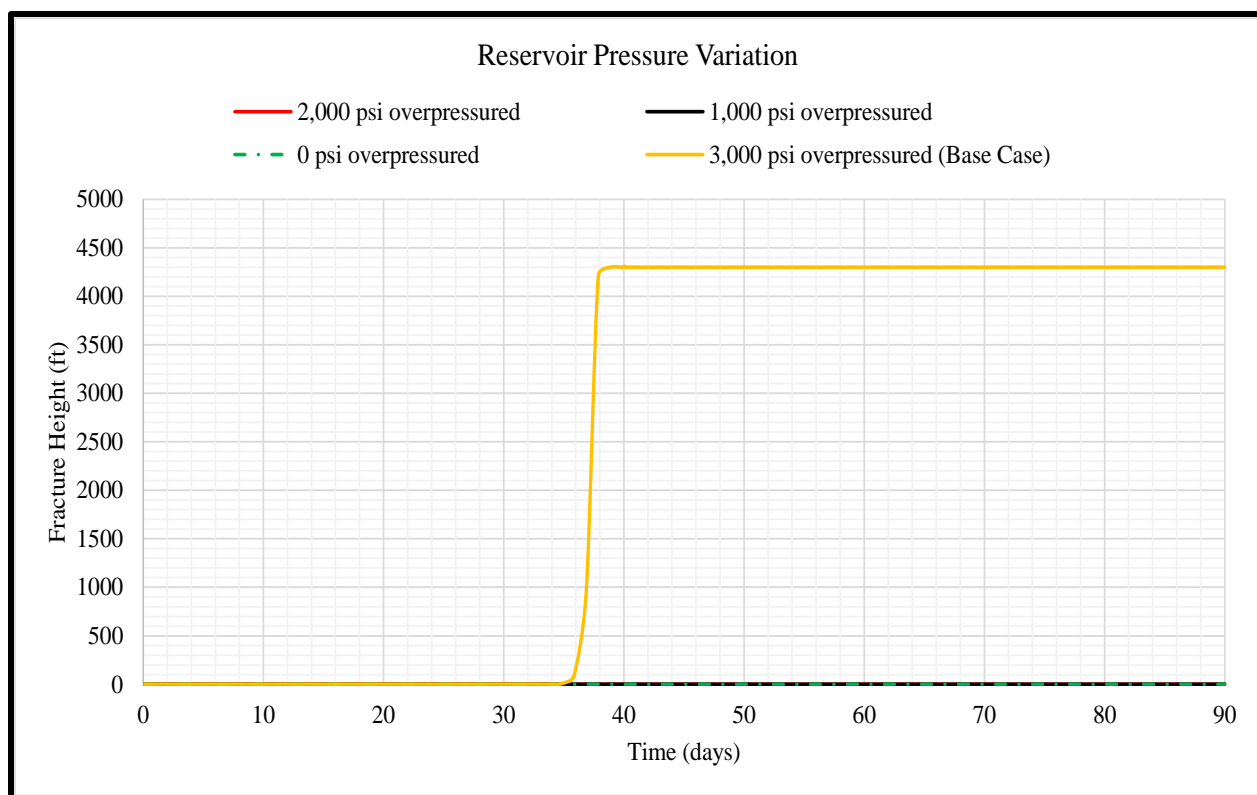


Figure 4. 27. Reservoir over-pressure variation with fracture height as the dependent variable.

#### 4.8. Total Discharge Duration

The aim of this model is to identify the effects of the preceding WCD period on the possibility of fracture initiation and propagation when the well is capped. A longer period of discharge means more produced fluids are discharged into the environment and less hydrocarbon reserves. Less hydrocarbons due to the declined pressure in the reservoir would be supplied to the wellbore, resulting in a lower build-up pressure. In some cases, the build-up pressure resulting from pro-longed WCD periods may not be enough to initiate a fracture and broach to seafloor. Furthermore, optimal and suboptimal source control timeframe will be modeled. According to BSEE, an optimal source control time frame is identified as the shortest time taken to mobilize and apply the containment equipment on the discharging well given minor delays such as adverse weather conditions, government approval, and near-wellhead subsurface debris removal. On the other hand, a sub-optimal source control timeframe may arise due to severe weather conditions such as hurricanes and storms, equipment delays due to maintenance or other reasons, excessive debris to be removed near wellhead, excessive delay in government approvals, failed attempts in containment, containment mechanical failures, and excessive volatile organic compounds (VOCs) near and above the wellhead till surface. Results indicate that the mid-point (40 days) and the sub-optimal (60 days) timeframe until well capping do not have any impact on fracture height or length growth, while the optimal period (20 days) only shortened the maximum fracture height by 100 feet before further growth. Figures 4.28 and 4.29 show the results of the case study.

Table 4. 6. Proposed periods for assessing impact of well capping timeframes.

| Model                          | Well Capping “A” as optimal | Well Capping “B” as mid-point | Well Capping “C” as sub-optimal |
|--------------------------------|-----------------------------|-------------------------------|---------------------------------|
| Well Capping Time Frame (days) | 20                          | 40                            | 60                              |

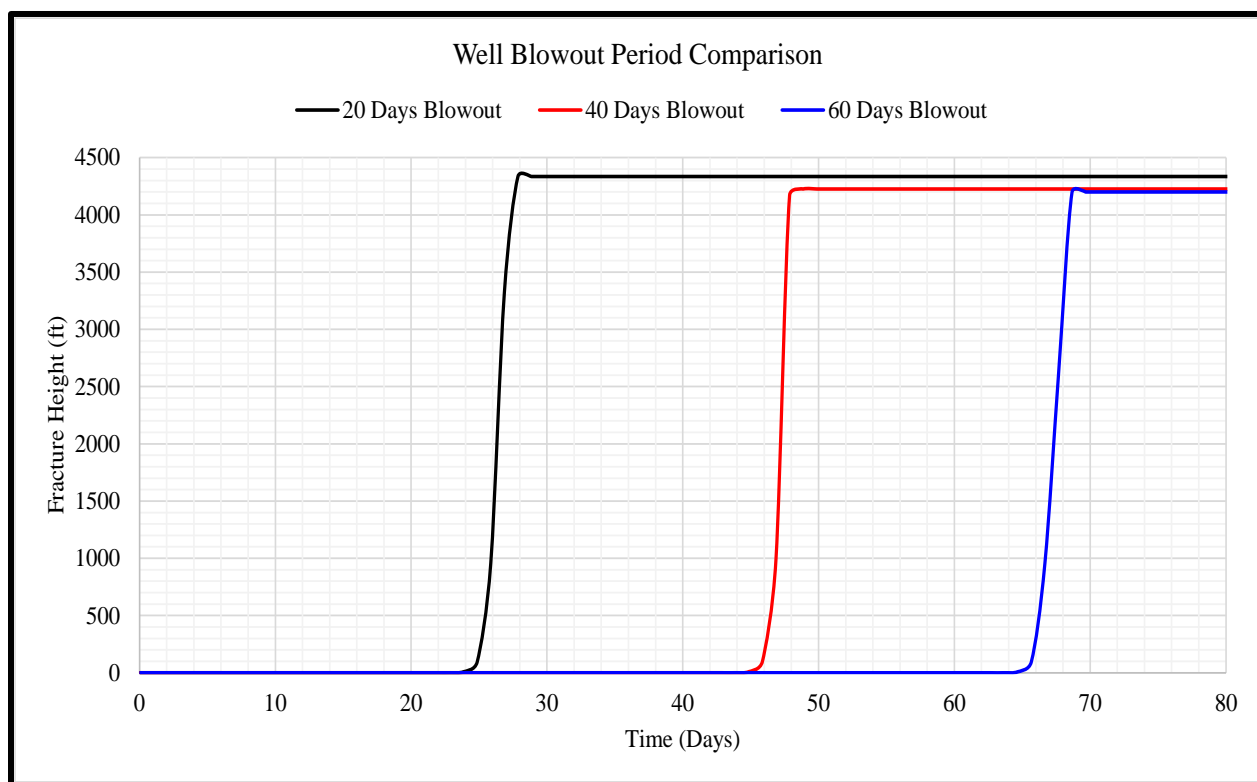


Figure 4. 28. Fracture height with time for different well blowout periods.

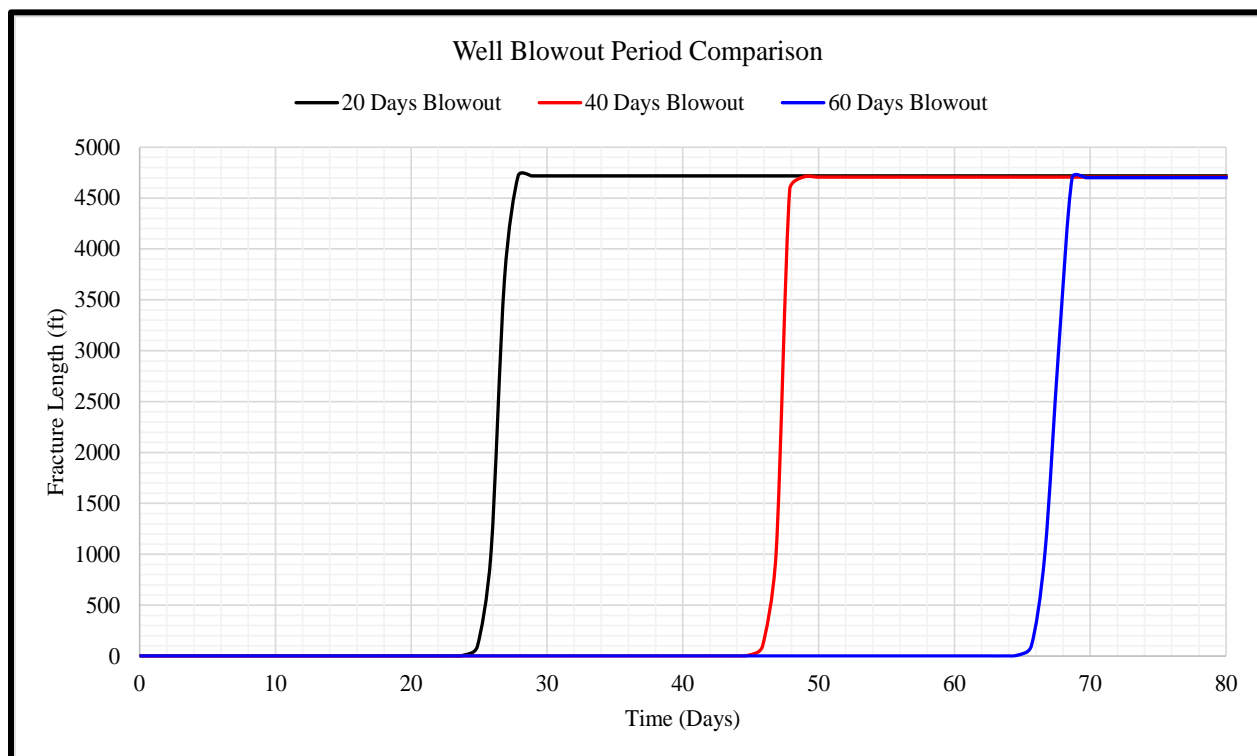


Figure 4. 29. Fracture length with time for different well blowout periods.

#### 4.9. Intervention Time

The objective of this case study is to research the influence of intervention time on fracture growth and potential broaching. Intervention time discussed here is referred to the time of relief well intersection to the incident wellbore. Intervention time for a relief well is dependent on various factors. Common circumstances that may hinder the relief well intervention time process may include but are not limited to the following: extended government regulations, severe weather conditions (hurricane and/or storms), insufficient rigs, and narrow drilling margin. For this model, 20 days capping period will be utilized before high density kill mud is injected through a relief well. Results illustrates that no impact of the extended relief well intervention period exists on fracture height and length growth. This is due to the fracture reaching its maximum growth prior to the additional 10 days period. Most of the fractures presented in the study reach their maximum dimensions in the first 5 days after abrupt shut-in capping.

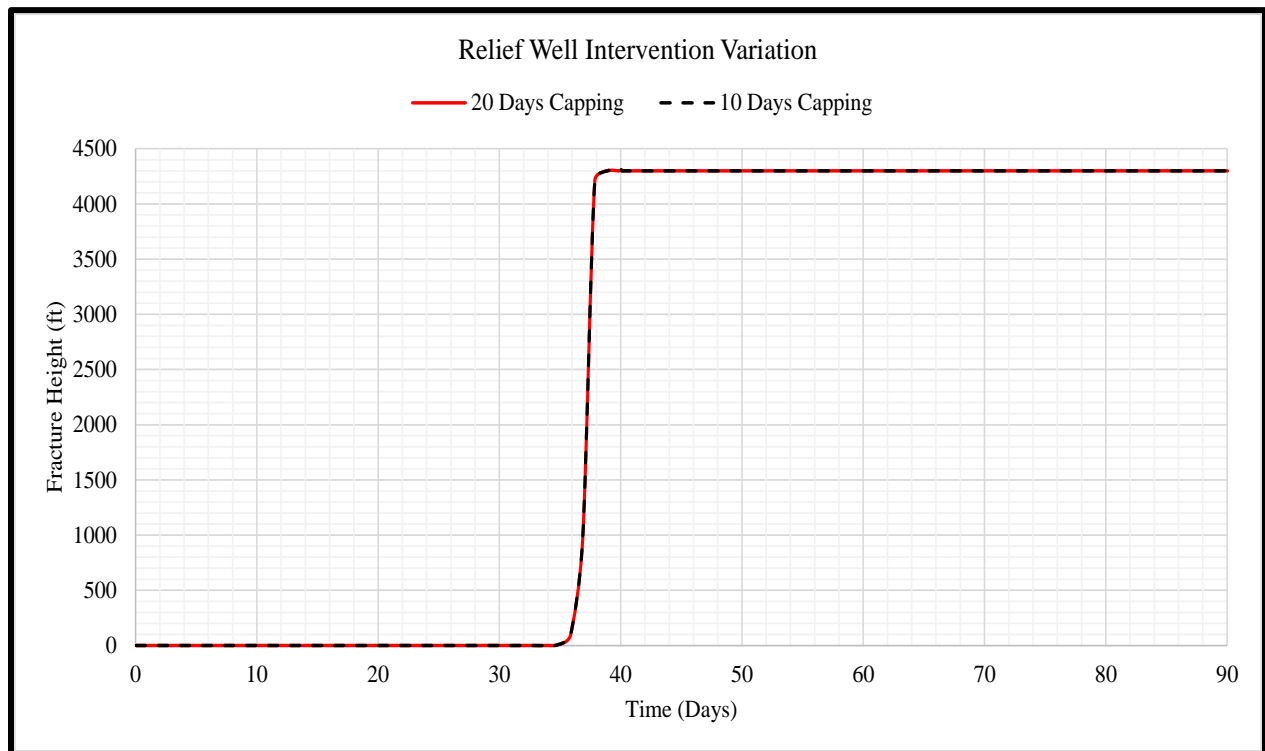


Figure 4. 30. Fracture height with time for different relief well intervention periods.

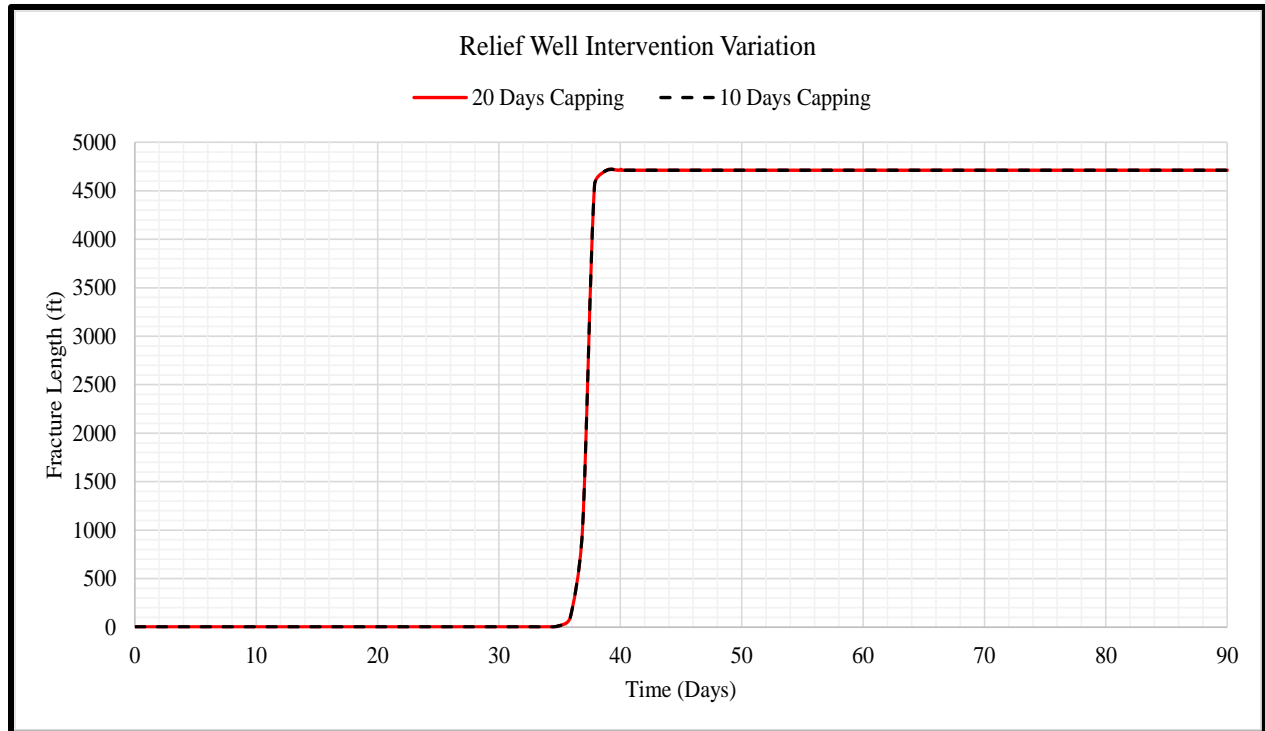


Figure 4. 31. Fracture length with time for different relief well intervention periods.

In summary, a workflow is developed for oil and gas practitioners to evaluate conditions under which fracture initiation may take place, and fracture propagation may occur. Several broaching scenarios are evaluated to assess the impact of casing shoe locations, contrast in Young's Modulus between layers, variation in reservoir over pressurization, and duration of spill and capping shut-in. The uniqueness of this study goes beyond computing WCD, total discharge volume, profile for flow rate decline, and duration of blowout period. The study further evaluates widely known techniques and practices, such as subsea capping stack "abrupt" shut-in and dynamic relief well drilling engineers would execute for bringing a well under control after a blowout has occurred. A great advantage of the workflow is it will provide oil and gas practitioners with a method to evaluate capping shut-in and relief well design ahead of time for safer drilling design such as the timeline for drilling a relief well to be determined to avoid fracture initiation and growth following capping. The designed workflow can be easily implemented in widely



available commercial software's. We hope that this workflow helps oil and gas engineers avoid the catastrophic consequences of WCD and broaching scenarios.

#### **4.10. Steady-State and Transient Wellbore Models**

The pressure behavior along the wellbore during multiphase flow in a vertical wellbore will differ depending on the terms included in the transient model. In this study, we observe the impact of using different wellbore models on fracture initiation, fracture travel-time, and final propagating height and length. The steady-state (developed) approach is presented and compared against various unsteady-state flow models in the wellbore. The accumulation, compressibility, and inertial terms are accounted for individually and as all in the comparison. For a steady-state condition, the pressure, velocity, and temperature at a certain location along the wellbore are constant over time (Al-Safran and Brill, 2017). The transient flow wellbore model is essential if sudden changes in fluid rate and pressure exceed the system capacity (Al-Safran and Brill, 2017). Known as time-dependent flow, the transient flow is defined as short-term, time-averaged flow variables such as pressure, velocity, and mass, vary with time at a specific location in the system (Al-Safran and Brill, 2017). A transient condition ends with a new steady-state condition. For our base case model and sensitivity studies, the transient flow condition is used without the accumulation, compressibility, and inertial terms. The accumulation term captures changing flow regime such as pipeline slugging, riser instability at low rates with changing tubular area or angle (*REVEAL* user guide, 2020). The inertial term is needed for rapid changes in momentum (e.g., water hammer at very short time scales) and is not relevant in most cases (*REVEAL* user guide, 2020). The compressibility term is important when changes in fluid compressibility occurs such as in the case of energy storage and release (e.g., surge volumes, closing valves etc. in compressible fluids) (*REVEAL* user guide, 2020). Inertia and compressibility work together to create

compression waves, surge volumes when e.g., chokes are changed. Closure relations are used such that the same result in transient and steady-state wellbore models is evaluated. This is important as this allows Reveal to use the same flow correlations for steady state and transient wellbore calculations. The closure relations give the same holdup calculated for steady state and transient models when conditions are stable (Houston PETEX, personal communication, March 15, 2021). The acceleration term is included however as noted this is generally small when calculated the pressure drop along the wellbore. Figures 4.32 and 4.33 show the result of this case study. The steady-state approach delays fracture initiation compared to the transient wellbore models by approximately 3.14 days (8.4% difference) and alters the fracture travel-time. As shown in the figures, the steady-state approach predicts a final fracture height and length within 2.75% and 5.75% difference, respectively, compared to the transient wellbore models once the transient wellbore have themselves stabilized. The “Transient Only”, “Transient with Accumulation”, and “Transient with Inertia” terms conclude similar initiation pressure, fracture travel-time and final fracture height and length. When the “Transient with Compressibility” term is added, the final fracture height increases by 360 ft and length decreases by 90 ft. The results indicate that if we were to drill a relief well on the 38<sup>th</sup> day for the problem at hand, the prediction of fracture height and length from the steady-state model would be significantly different from those of the transient models, thus underscoring the impact of transient wellbore models over steady-state models for prediction of fracture properties during propagation.

Results for the multiphase flow run (figure 3.34 and 3.35) are slightly different than for a single-phase oil. While almost all five transient wellbore models predict final fracture height and length within 1.1% and 2% respectively, fracture travel time are significantly different. For example, if drilling engineers were to drill a relief well on the 35<sup>th</sup> day after blowout, fracture

height and length prediction from the transient with inertia wellbore model would be 988 ft, and 995 ft respectively, while prediction from the transient with accumulation wellbore model would predict a 100 ft and a 90 ft fracture height and length. The five transient wellbore models predict fracture initiation on average 2.8 days after capping (1% difference between the models), however fracture travel time differs as shown by the different propagation time taking place.

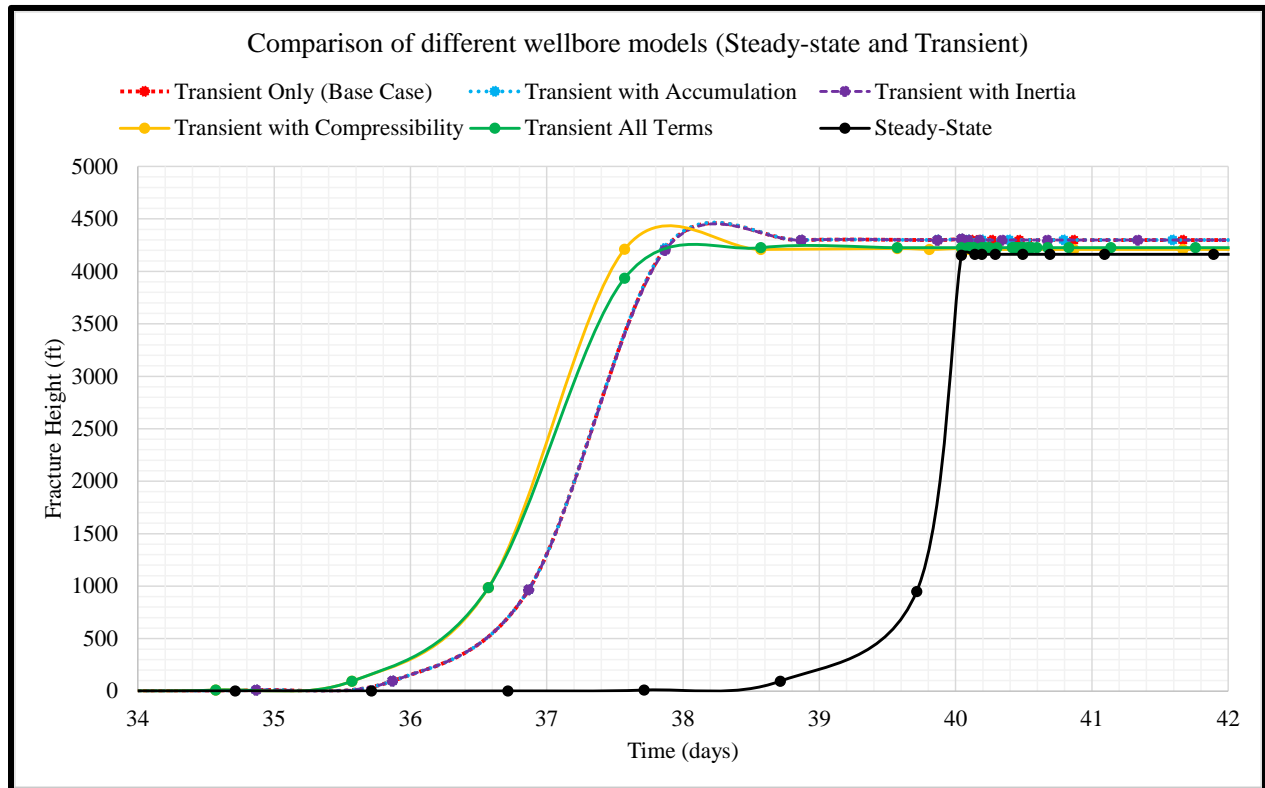


Figure 4. 32. Fracture height comparison using different wellbore models for transient and steady-state conditions. Capping shut-in appeared 30 days after blowout.

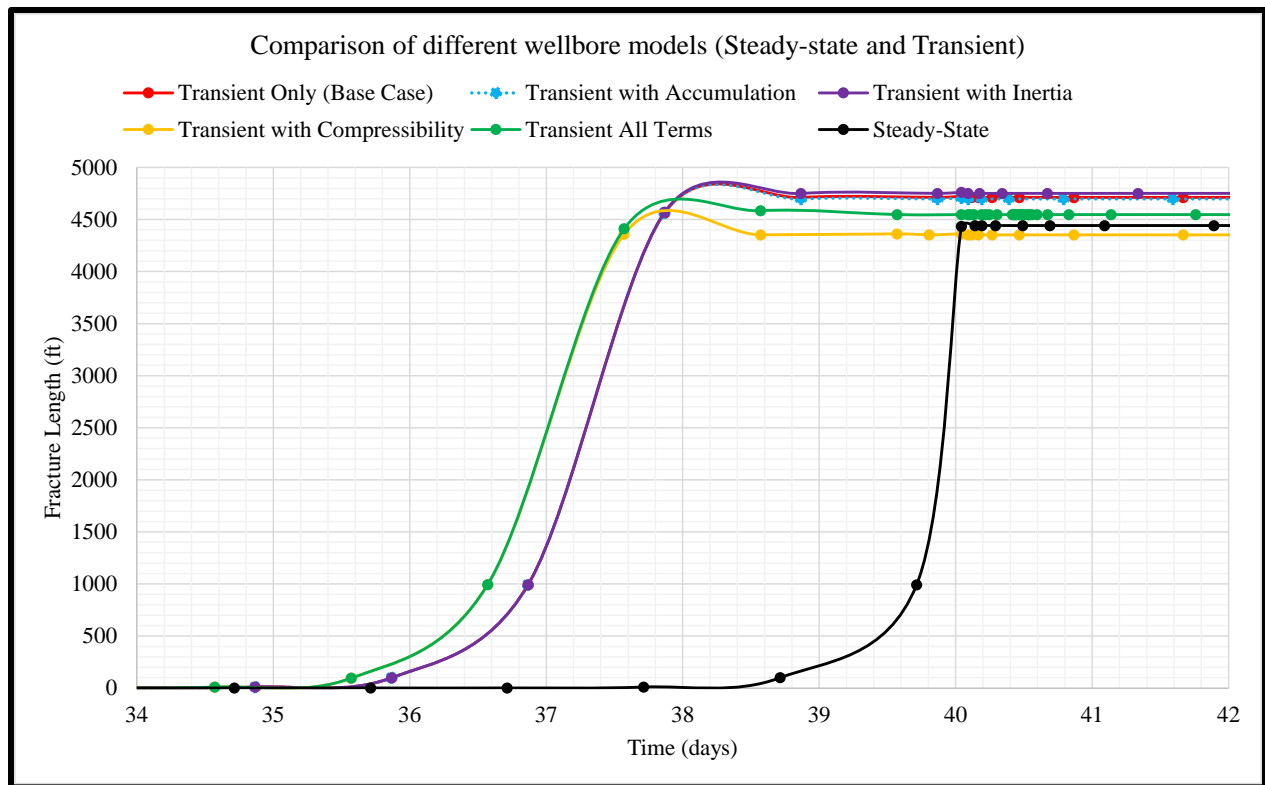


Figure 4. 33. Fracture length comparison using different wellbore models for transient and steady-state conditions.

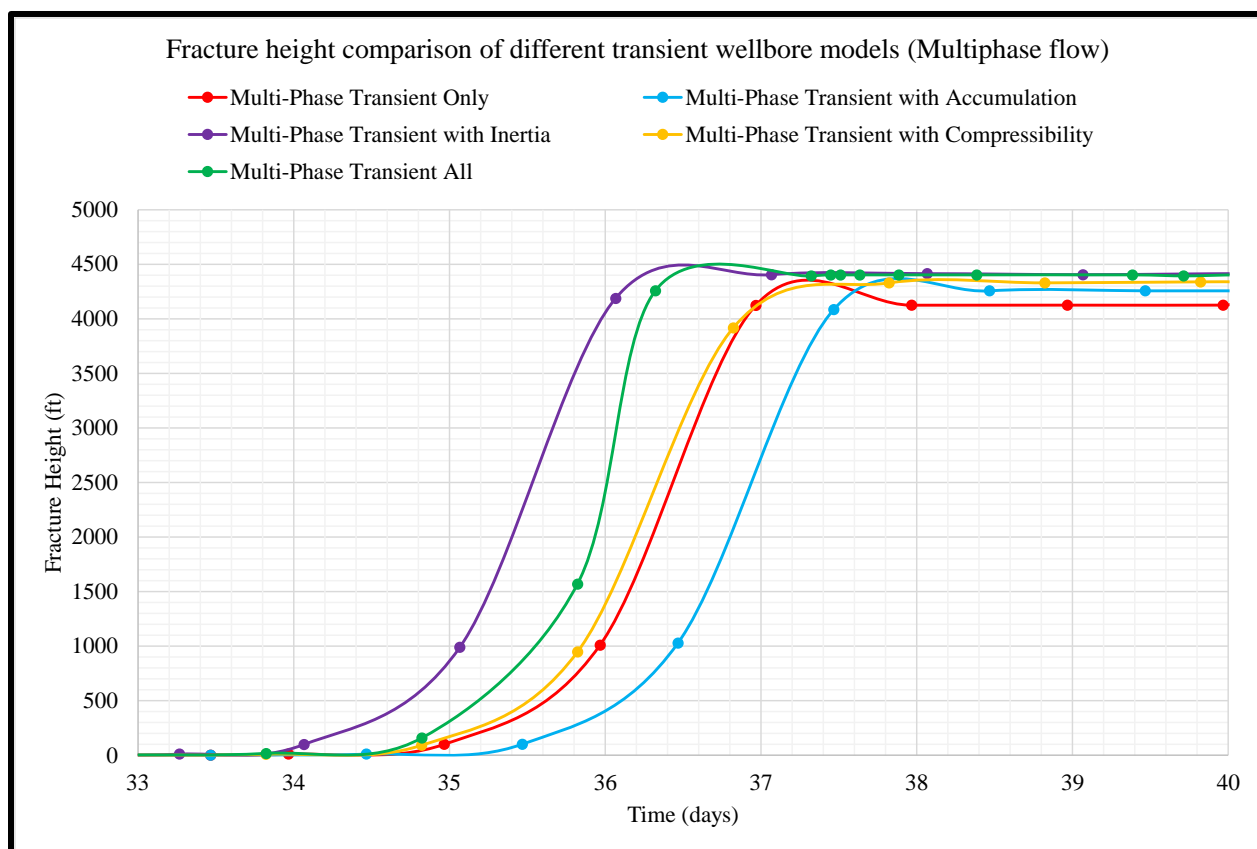


Figure 4. 34. Fracture height comparison for the multiphase flow model.

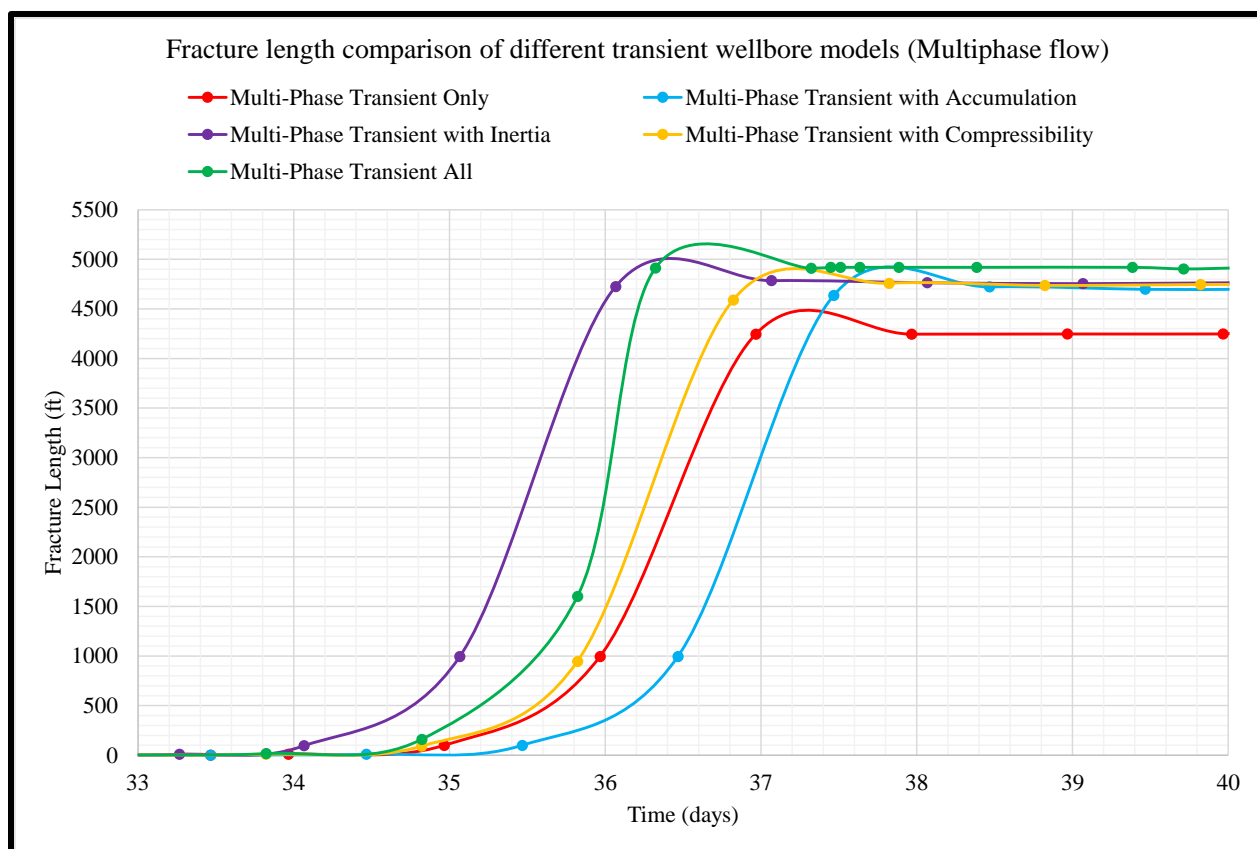


Figure 4. 35. Fracture length comparison for the multiphase flow model.

## 5. Conclusions, Recommendations, and Future Work

The objective of this study is to assess the propagation of fractures initiated during post-blowout capping, evaluating potential broaching scenarios for offshore well through fracture height growth. Based on numerical modeling performed on a deepwater case study, the following conclusions are drawn:

- Fracture initiation and propagation is possible after wellbore abrupt capping shut-in.
- Fracture broaching into seafloor is mainly dependent on casing shoe depth.
- Assuming perfect casing integrity, fracture growth and hence broaching time are sensitive to reservoir properties and dimensions with pressure depletion during post-blowout discharge playing a major role in fracture propagation after capping.
- Presence of a microannulus between the cement and surrounding rock formation interface increases the chances of seafloor broaching and leads to fracture initiation.
- Fractures initiating deeper than or equal to 8,000 feet below seafloor will not exhibit broaching into the seafloor in the timeframe investigated in this study and the 6-months regulatory period.
- The deeper the fracture, the less likely it is to broach. Fractures occurring at or below 4,500 feet are more likely to initiate, propagate and eventually broach.
- Young's modulus contrast between layer's affect fracture initiation time post shut-in, maximum fracture height and length, as well as travel time of the fracture to broach. High shale/sandstone Young's modulus ratios ( $E_{sh}/E_{ss}$ ) are found to suppress fracture growth. Low Young's modulus will result in a fracture initiating at a lower formation breakdown pressure and vice versa.

- Fractures occurring near the seafloor may have an adverse effect on oil rate broaching into the fracture, as well as relief well mud injection rates and density.
- Relief well intervention period may or may not have an impact on fracture growth. In our case, no influence is shown.

Broaching analysis is necessary for effective containment of fracture fluid flow. An appropriate wellbore model, used in this study as the transient wellbore is essential to capture the time-dependent properties for accurate fracture initiation and propagation prediction. The workflow used in this study can be employed for assessing any loss of well control situation leading to a blowout scenario, evaluation of fracture initiation and growth with time following capping shut-in and investigate successful well control through kill mud injection by a relief well. Detailed analysis of wellbore shut-in post blowout is essential prior to capping installation and is suggested to be included in BSEE and BOEM well design permit with the WCD scenario to be conducted by facilities' operator. The designed workflow will help operators determine the timing of drilling a relief well prior to fracture initiating from the sides of the wellbore.

In this regard, future broaching analyses studies post-blowout should focus on the impact of multi-step “soft” aka incremental shut-in on fracture initiation and propagation. Fluid flow inside the fracture and spill volume resulting from broached fractures into seafloors should be researched. Different stratigraphy of the geological media needs to also be addressed such as existing salt domes, nearby faults, naturally fractured porous media, rock and fluid compressibility, and variation in *in-situ* stress state.



## Appendix A. Schedule for WCD, Well Capping, and Relief Well Injection

section schedule

#WCD Initialization (60 minutes)

timestep initial 0.1 ! days

timestep max\_dt 1 ! days

restart\_file off

inject well WCD type gen\_liquid 0 713 ! fraction scf/STB

inject well WCD pressure 3720 temperature 100 ! psia deg F

inject well WCD component Mud concentration 0 ! ppm

inject well WCD rperm standard

well WCD transient\_flow on inertia\_flow off accumulation\_flow off compressible\_flow off

fracture WCDFrac5 update timesteps 1

for time 60 ! minutes

then

#WCD Duration (30 days)

timestep max\_dt 1 ! days

restart\_file off

inject well WCD type gen\_liquid 0 713 ! fraction scf/STB

inject well WCD pressure 3720 temperature 100 ! psia deg F

inject well WCD component Mud concentration 0 ! ppm

inject well WCD rperm standard

well WCD transient\_flow on inertia\_flow off accumulation\_flow off compressible\_flow off

fracture WCDFrac5 update timesteps 1

for time 43200 ! minutes

then

#Well Capping Period (10 days)

timestep initial 0.1 ! days

timestep max\_dt 1 ! days

restart\_file off

```

inject well WCD type gen_liquid 0 713 ! fraction scf/STB
inject well WCD rate 1 temperature 100 ! STB/day deg F
inject well WCD component Mud concentration 0 ! ppm
inject well WCD rperm standard
well WCD transient_flow on inertia_flow off accumulation_flow off compressible_flow off
fracture WCDFrac5 update timesteps 1

```

```

for time 14400 ! minutes

```

then

#Kill Mud Injection through Relief Well at 30,000 stb/day (20 days)

```

timestep initial 0.1 ! days
timestep max_dt 1 ! days

```

```

restart_file off

```

```

inject well WCD type water
inject well WCD pressure 3720 temperature 60 ! psia deg F
inject well WCD component Mud concentration 0 ! ppm
inject well WCD rperm standard
well WCD source tubing liq_rate 70000 temperature 60 wc 1 gor 0 md 20100 lateral 2 ! STB/day
deg F fraction scf/STB feet
well WCD source composition 300000 ! ppm
well WCD transient_flow on inertia_flow off accumulation_flow off compressible_flow off
fracture WCDFrac5 update timesteps 1

```

```

for time 28800 ! minutes

```

then

#Kill Mud Injection through Relief Well at 20,000 stb/day (10 days)

```

timestep initial 0.1 ! days
timestep max_dt 1 ! days

```

```

restart_file off

```

```

inject well WCD type water
inject well WCD pressure 3720 temperature 60 ! psia deg F
inject well WCD component Mud concentration 0 ! ppm
inject well WCD rperm standard
well WCD source tubing liq_rate 40000 temperature 60 wc 1 gor 0 md 20100 lateral 2 ! STB/day
deg F fraction scf/STB feet
well WCD source composition 300000 ! ppm

```

```
well WCD transient_flow on inertia_flow off accumulation_flow off compressible_flow off
fracture WCDFrac5 update timesteps 1
```

```
for time 7200 ! minutes
```

```
then
```

```
#Kill Mud Injection through Relief Well at 10,000 stb/day (10 days)
```

```
timestep initial 0.1 ! days
```

```
timestep max_dt 1 ! days
```

```
restart_file off
```

```
inject well WCD type water
```

```
inject well WCD pressure 3720 temperature 60 ! psia deg F
```

```
inject well WCD component Mud concentration 0 ! ppm
```

```
inject well WCD rperm standard
```

```
well WCD source tubing liq_rate 20000 temperature 60 wc 1 gor 0 md 20100 lateral 2 ! STB/day
deg F fraction scf/STB feet
```

```
well WCD source composition 300000 ! ppm
```

```
well WCD transient_flow on inertia_flow off accumulation_flow off compressible_flow off
```

```
fracture WCDFrac5 update timesteps 1
```

```
for time 7200 ! minutes
```

```
then
```

```
#Shut-in period, capped well and no mud injection (20 days)
```

```
timestep initial 0.1 ! days
```

```
timestep max_dt 1 ! days
```

```
restart_file off
```

```
inject well WCD type water
```

```
inject well WCD rate 0 temperature 60 ! STB/day deg F
```

```
inject well WCD component Mud concentration 0 ! ppm
```

```
inject well WCD rperm standard
```

```
well WCD source tubing liq_rate 0 temperature 60 wc 1 gor 0 md 20100 lateral 2 ! STB/day
deg F fraction scf/STB feet
```

```
well WCD source composition 300000 ! ppm
```

```
well WCD transient_flow on inertia_flow off accumulation_flow off compressible_flow off
```

```
fracture WCDFrac5 update timesteps 1
```

```
for time 28800 ! minutes
```

```
end
```

## Appendix B. Permissions for Published Work

Published permissions for various figures used throughout the chapters (1, 2, 3, and 4) are provided in this appendix. Permission for Figure 1.1 Diagram showing examples of qualitative ranking BOEM geoscientists have conducted on favorable and unfavorable pathways leading to broaching of hydrocarbons, below is the evidence.

### **Youssuf A Elnoamany**

---

**From:** Paula Sillman <psillman@aapg.org>  
**Sent:** Friday, February 12, 2021 3:26 PM  
**To:** Youssuf A Elnoamany; Valerie Lindsey  
**Subject:** Re: Copyrights to use figures  
**Attachments:** Pages from bltn18097.pdf

Dear Youssuf,

The data for figure 1 is proprietary, you will need permission from TGS to use. However, the permission for Figure 2 is granted per the following:

Figure 2 from: Bjerstedt, T. W., W. W. Shedd, M. G. Natter, P. B. Abadie, G. J. Moridis, and M. T. Reagan, 2020, Evaluation of hydrocarbon broaching after subsurface containment failure, Gulf of Mexico: AAPG Bulletin, v. 104, no. 4, p. 845-862.

Permission is granted for the above figures per the following conditions:

#### Condition of Grant of Permission

As a condition of the grant of permission contained under the single use only or multiple item usage, AAPG requires:

- (a) a full citation in your bibliography for each AAPG publication from which a table or figure of text is taken;
- (b) in figure and title captions a statement or citation including the author, identification of the AAPG publication from which the figure or table was taken; and
- (c) you must use the identical copyright notice as it appears in our publication; i.e. "AAPG©[year], and the phrase *"reprinted by permission of the AAPG whose permission is required for further use."*

As a condition of grant of permission when citing an internet or web page AAPG source:

- (a) Full citation in bibliography as listed below:  
Author name(s), year of publication or last revisions (if known), title of document, title of complete work (if applicable), URL, in angle brackets (underlined if hypertext), date of access (accessed January 1, 1998).  
Example: Eaton, Susan, 2003, Canada Hydrates get close study:  
<[http://www.aapg.org/explorer/2003/01jan/gh\\_stability.cfm](http://www.aapg.org/explorer/2003/01jan/gh_stability.cfm)> (accessed August 7, 2003)
- (b) You must use the identical copyright notice as in (c) above.

Kind regards,  
Paula Sillman  
AAPG Technical Publications

Permission for Figure 1.3 BP 001 Macondo Well design and lithologic section were provided by PNAS the publisher, below is the evidence.

---

**Youssuf A Elnoamany**

---

**From:** PNAS Permissions <PNASPermissions@nas.edu>  
**Sent:** Friday, February 5, 2021 9:20 AM  
**To:** Youssuf A Elnoamany  
**Subject:** RE: Copyright to use figure

Thank you for your message. Permission is granted for your use of the material as described in your request. Please include a complete citation for the original PNAS article when reusing its material. Because this material published after 2008, a copyright note is not needed. There is no charge for this material, either. Let us know if you have any questions.

Sincerely,

Kay McLaughlin for  
Diane Sullenberger  
PNAS Executive Editor

Figure 1A-B from <https://www.pnas.org/content/109/50/20288>

---

**From:** Youssuf A Elnoamany <yelnoa1@lsu.edu>  
**Sent:** Thursday, February 4, 2021 10:21 PM  
**To:** PNAS Permissions <PNASPermissions@nas.edu>  
**Subject:** Copyright to use figure

Dear Sir/Madame,

Hope this email finds you well! My name is Youssuf Elnoamany and I am a graduate student at Louisiana State University Craft and Hawkins Department of Petroleum Engineering. I would like to use the following figure (attached) from your paper "Scientific basis for safely shutting in the Macondo Well after the April 20, 2010 Deepwater Horizon blowout" (<https://doi.org/10.1073/pnas.1115847109>) for my thesis. Can you please advise on the appropriate action I should take to obtain the copyrights/official permission to use this figure? I have contacted Dr. Stephen Hickman (primary author) last year to use this figure in one of my conferences in which he agreed and I provided the full citation under the figure. Appropriate citation will be provided. Thank you in advance!

Best regards,

Youssuf Elnoamany



**Youssuf A. Elnoamany**  
Graduate Assistant at LSU CAS  
Dual Degree MS Candidate in Petroleum Engineering and Data Analytics  
Louisiana State University  
2240 Patrick F. Taylor Hall, Baton Rouge, LA 70803  
phone (929) 225-5753 | <https://lsu.zoom.us/j/4728618318>  
[yelnoa1@lsu.edu](mailto:yelnoa1@lsu.edu) | [lsu.edu](https://lsu.edu)

## References

- Almarri, Misfer. (2020). Efficient History Matching of Thermally Induced Fractures Using Coupled Geomechanics and Reservoir Simulation. *Energies*. 13. 3001. 10.3390/en13113001.
- Andreussi, H.P., and G. De Ghetto. "CUBE - A New Technology for the Containment of Subsea Blowouts." *J Pet Technol* 65 (2013): 32–35. doi: <https://doi.org/10.2118/0113-0032-JPT>
- Anderson, E. M. (1951) *The Dynamics of Faulting*. 2nd ed., Edinburgh: Oliver & Boyd.
- API RP 16ST, *Coiled Tubing Well Control Equipment Systems*, first edition. 2009. Washington, DC: API
- Al-Safran, E., & Brill, J. (2017). *Applied Multiphase Flow in Pipes and Flow Assurance: Oil and Gas Production*.
- Bartlit, F. H., Grimsley, S. C. and Sambhav, S. N. (2011). *Macondo: The Gulf Oil Disaster*. Chief Counsel's Report, National Commission on the BP Deepwater Horizon Oil Spill and Offshore Drilling.
- Bendiksen, K. H., Maines, D., Moe, R. et al. .1991. *The Dynamic Two-Fluid Model OLGA: Theory and Application*. *SPE Prod Eng* 6 (2): 171–180. SPE-19451-PA. <https://doi.org/10.2118/19451-PA>.
- Berkowitz, B. (2002). Characterizing flow and transport in fractured geological media: a review. *Adv. Water Res.* 25, 861–884. doi: 10.1016/S0309-1708(02)00042-8
- Bhardwaj, P., Hwang, J., Manchanda, R., & Sharma, M. M. (2016). *Injection Induced Fracture Propagation and Stress Reorientation in Waterflooded Reservoirs*. Paper presented at the SPE Annual Technical Conference and Exhibition, Dubai, UAE.
- Bird, R & Stewart, W & Lightfoot, E.. (2002). *Transport Phenomena*.
- BP. (2010). Deepwater horizon accident investigation report.
- Bjerstedt, Thomas & Shedd, William & Natter, Michael Abadie, Pierre & Moridis, George & Reagan, Matthew. (2020). *Evaluation of hydrocarbon broaching after subsurface containment failure, Gulf of Mexico*. *AAPG Bulletin*. 104. 10.1306/08161918097
- Bolton RS, Hunt TM, King TR, Thompson GEK (2009) *Dramatic incidents during drilling at Wairakei Geothermal field*, New Zealand. *Geothermics* 38:40–47.
- Bratslavsky and SolstenXP, *Suitability of Source Control and Containment Equipment versus Same Season Relief Well in the Alaska Outer Continental Shelf Region*, October 2018

- Bruist, E.H.. "A New Approach in Relief Well Drilling." *J Pet Technol* 24 (1972): 713–722. doi: <https://doi.org/10.2118/3511-PA>
- Buchholz, K., Krieger, A., Rowe, J., Etkin, D. S., McCay, D. F., Schroder Gearon, M., Grennan, M., & Turner, J. (2016). Worst Case Discharge Analysis (Volume I): Oil Spill Response Plan (OSRP) Equipment Capabilities Review, BPA No. E14PB00072. US Department of the Interior Bureau of Safety and Environmental Enforcement (BSEE).
- Choi, J., Pereyra, E., Sarica, C. et al. 2013. Development of a Fast Transient Simulator for Gas-Liquid Two-Phase Flow in Pipes. *J Pet Sci & Eng* 102 (February): 27-35.
- Chuprakov, D. A., Izimov, R. M., & Spesivtsev, P. E. (2017). *Contained Hydraulic Fracture Growth after Well Shutin*. Paper presented at the 51st US Rock Mechanics / Geomechanics Symposium, San Francisco, California, USA.
- Cordoba, F. A. V. (2018). *Integrated Reservoir – Wellbore Nodal Analysis Workflow For Worst-Case Discharge Modeling*. (MS), Louisiana State University, Baton Rouge.
- Cormack, D. E., Fung, R. L., & Vijayakumar, S. (1983). *Vertical Fracture Containment During Massive Hydraulic Fracturing*. Paper presented at the 34th Annual Technical Meeting of The Petroleum Society of CIM, Banff.
- Davies R, Manga M, Tingay M, Lusiana S, Swarbrick R (2010) Discussion—Sawalo et al. (2009) *the LUSI mud volcano controversy: Was it caused by drilling?* *Mar Pet Geol* 27:1651–1657
- Easton RO (1972) *Black Tide: The Santa Barbara Oil Spill and Its Consequences* (Delacorte Press, New York).
- Eidvin T, Øverland JA (2009) *Faulty Geology Halts Project, Norwegian Continental Shelf* No.2 2009. Available at [http://www.npd.no/Global/Engelsk/3%20-%20Publications/Norwegian %20Continental%20Shelf/PDF/10%20faulty%20geology.pdf](http://www.npd.no/Global/Engelsk/3%20-%20Publications/Norwegian%20Continental%20Shelf/PDF/10%20faulty%20geology.pdf). Accessed January 2, 2021.
- Elnoamany, Y. A., Michael, A., and I. Gupta. "Numerical Modeling of Fracture Propagation During Post-Blowout Capping in Offshore Wells." Paper presented at the 54th U.S. Rock Mechanics/Geomechanics Symposium, physical event cancelled, June 2020
- Elnoamany, Y. A., Michael, A., and I. Gupta. *Broaching Analysis During Post-Blowout Capping Following Worst Case Discharge: A Gulf of Mexico Case Study*. Poster presented at: AGU Annual Fall Meeting; December 1-17, 2020; Online.
- Energy Resources Conservation Board (2010) Staff Review and Analysis: Total E&P Canada Ltd., Surface Steam Release of May 18, 2006, Joslyn Creek SAGD Thermal Operation, 11 February 2010. Available at [http://www.ercb.ca/reports/ERCB\\_StaffReport\\_JoslynSteamRelease\\_2010-02.pdf](http://www.ercb.ca/reports/ERCB_StaffReport_JoslynSteamRelease_2010-02.pdf). Accessed August 26, 2012.

- Faybishenko, B., Witherspoon, P. A., and Benson, S. M. (2000). *Dynamics of Fluids in Fractured Rocks*. New York, NY: Wiley. doi: 10.1029/GM122
- Fisher, K., & Warpinski, N. (2012). Hydraulic-Fracture-Height Growth: Real Data. *SPE Production & Operations*.
- Fu, Y., 2014, Leak-Off Test (LOT) Models, Master's Thesis at the University of Texas at Austin.
- GeoMark Research, Ltd, PVT GoM Database
- Gidley, J., Holditch, S., Nierode, D., Veach, R., 1989. *Recent Advances in Hydraulic Fracturing*, Monograph Volume 12. Society of Petroleum Engineers 1989
- Haimson, B., and Fairhurst, C. (1967). Initiation and Extension of Hydraulic Fractures in Rocks. Society of Petroleum Engineers. September 1. doi:10.2118/1710-PA
- Herbst, L. 2014. *Effective Well Control - Prevention & Response*. Bureau of Safety and Environmental Enforcement, Gulf of Mexico Region. Presentation. 28 May 2014. 26 p
- Hickman, S. H. et al. *Scientific basis for safely shutting in the Macondo Well after the April 20, 2010 Deepwater Horizon blowout*. Proceedings of the National Academy of Sciences 109, 20268-20273, <https://doi.org/10.1073/pnas.1115847109> (2012)
- Holt, R. M., Flornes, O., Li, L., & Fjaer, E. (2004). Consequences Of Depletion-Induced Stress Changes On Reservoir Compaction And Recovery. *American Rock Mechanics Association*(04-589).
- Horner, D. R. (1951). Pressure Build-up in Wells. *World Petroleum Congress*.
- Hsieh, Paul A. (2011) "Application of MODFLOW for Oil Reservoir Simulation During the Deepwater Horizon Crisis." *Ground Water*, vol. 49, no. 3, pp. 319–323., doi:10.1111/j.1745-6584.2011.00813.x.
- IADC. (2013, 10 January 2020). *Definition of Loss of Well Control*. 10 December 2013.
- IOGP. 1st ed., vol. 1, ser. 1, IOGP Publications, 2020, *Subsea Capping Stack Design and Operability Assessment*.
- Ispas, I., Eve, R., Hickman, R. J., Keck, R. G., Willson, S. M., & Olson, K. E. (2012). Laboratory Testing and Numerical Modelling of Fracture Propagation from Deviated Wells in Poorly Consolidated Formations. *SPE Journal*. doi:10.2118/159262-MS
- Kholy, S. M., Ma, J., Mohamed, I. M., Abou-Sayed, O., & Abou-Sayed, A. (2019). Prediction of the Fracture Closure Pressure from the Instantaneous Shut-In Pressure ISIP for



Unconventional Formations: Case Studies. *Society of Petroleum Engineers*.  
doi:10.2118/197108-MS

Liu, F., Valiveti, D. M., & Gordon, P. A. (2015). *Modeling Fluid-Driven Fractures using the Generalized Finite Element Method (GFEM)*. Paper presented at the 49th US Rock Mechanics / Geomechanics Symposium, San Francisco, CA, USA.

McNutt M, et al. (2012) *Applications of science and engineering to quantify and control the Deepwater Horizon oil spill*. Proc Natl Acad Sci USA 109:20222–20228.

Michael, A. (2016). *Hydraulic Fracturing Optimization: Experimental Investigation of Multiple Fracture Growth Homogeneity via Perforation Cluster Distribution*. (MS), The University of Texas at Austin, Austin.

Michael, A., & Gupta, I. (2019). *Analysis of Fracture Initiation and Broaching Resulting from Worst Case Discharge Events*. Paper presented at the 53rd US Rock Mechanics/Geomechanics Symposium, New York, USA.

Michael, A., & Gupta, I. (2020). Fracture Prevention Following Offshore Blowouts: Selecting the Appropriate Capping Stack Shut-In Strategy. Society of Petroleum Engineers. *SPE Drilling & Completion*, Sept 2020, doi:10.2118/199673-PA

National Commission, 2011, Deep water: The Gulf oil disaster and the future of offshore drilling: Washington, DC, Government Publishing Office Report to the President, 398 p., accessed September 23, 2019, <https://www.gpo.gov/fdsys/pkg/GPO-OILCOMMISSION/pdf/GPO-OILCOMMISSION.pdf>

Ouchi, H., Foster, J. T., & Sahrma, M. M. (2017). Effect of Reservoir Heterogeneity on the Vertical Migration of Hydraulic Fractures. *Journal of Petroleum Science and Engineering*, 151, 384-408.

Peirce, A. and Bungler, A. 2015. *Interference Fracturing: Nonuniform Dis-tributions of Perforation Clusters That Promote Simultaneous Growth of Multiple Hydraulic Fractures*. SPE J.20(2): 384–395. SPE-172500-PA. <http://dx.doi.org/10.2118/172500-PA>.

Petroleum Experts. Newsletter; July 2016.

Petroleum Experts. User Manual, REVEAL v 9.5, IPM v 12.5 - Build # 42; 2020.

Philipp, S. L., Afs ar, F., & Gudmundsson, A. (2013). *Effects of mechanical layering on hydrofracture emplacement and fluid transport in reservoirs*. Frontiers in Earth Science, 1(4). <https://doi.org/10.3389/feart.2013.00004>

Received by Houston PETEX, *Transient Wellbore Inquiry*, 15 Mar. 2021.

- Robinson, J.D., and J.P. Vogiatzis. "*Magnetostatic Methods for Estimating Distance and Direction from a Relief Well to a Cased Wellbore.*" J Pet Technol 24 (1972): 741–749. doi: <https://doi.org/10.2118/3496-PA>
- Sawolo N, Sutriyono E, Istadi B, Darmoyo A (2010) *Was LUSI caused by drilling?*—Authors reply to discussion. Mar Pet Geol 27:1658–1675.
- SPE Technical Report (2015). *Calculation of Worst-Case-Discharge (WCD)*. Society of Petroleum Engineers.
- James G. Speight, 3 - Unconventional gas, Editor(s): James G. Speight, Natural Gas (Second Edition), Gulf Professional Publishing, 2019, Pages 59-98, ISBN 9780128095706, <https://doi.org/10.1016/B978-0-12-809570-6.00003-5>.
- Skalle, P., Jinjun, H., Podio, A.L.: "*Killing Methods and Consequences of 1120 Gulf Coast Blowouts during 1960-1996*", SPE 53974 presented at the 1999 SPE Latin America and Caribbean Petroleum Engineering Conference held in Caracas, Venezuela, 23-23 April 1999.
- Simonson, E. R., Abou-Sayed, A. S., & Clifton, R. J. (1978). Containment of Massive Hydraulic Fractures. *SPE Journal*, 1, 27-32.
- Taitel, Y., Shoham, O., and Brill, J.p. 1989. Simplified transient solution and simulation of two-phase flow in pipelines. *ChemEng Sci* 44 (6): 1353-1359.
- Teufel, L. M., & Clark, J. A. (1984). Hydraulic Fracture Propagation in Layered Rock: Experimental Studies of Fracture Containment. *SPE Journal*, 24(1), 19-32.
- The New York Times, "*Methods That Have Been Tried to Stop the Leaking Oil.*" 25 May 2010, [archive.nytimes.com/www.nytimes.com/interactive/2010/05/25/us/20100525-topkill-diagram.html?\\_r=0](http://archive.nytimes.com/www.nytimes.com/interactive/2010/05/25/us/20100525-topkill-diagram.html?_r=0).
- Tingay M, Hillis R, Morley C, Swarbrick R, Drake S (2005) *Present-day stress orientation in Brunei: A snapshot of prograding tectonics in a Tertiary delta*. J Geol Soc London 162:39–49.
- Usman, A. (1988). Fracture Height Prediction. *Society of Petroleum Engineering*. doi:10.2118/18338-PA.
- Vakó, Peter, and Michael J. Economides, (1995). *Hydraulic Fracture Mechanics*. Chichester: Wiley. Print.
- Van Eekelen, H. A. (1982). Hydraulic Fracture Geometry: Fracture Containment in Layered Formation. *SPE Journal*, 22(3), 341-349.

- Waltrich, P. J., Capovilla, M. S., Lee, W., de Sousa, P. C., Zulqarnain, M., Hughes, R., ... & Singh, J. (2019). Experimental Evaluation of Wellbore Flow Models Applied to Worst-Case Discharge Calculations for Oil Wells. *SPE Drilling & Completion*. doi:10.2118/184444-PA
- Warpinski, N. (1982). Laboratory Investigation on the Effect of In-Situ Stresses on Hydraulic Fracture Containment. *Society of Petroleum Engineers Journal*, 22(3), 333-340.
- Willson, S. M. (2012). *A Wellbore Stability Approach For Self-Killing Blowout Assessment*. Paper presented at the SPE Deepwater Drilling and Completions Conference, Galveston, Texas.
- Willson, S. M., Nagoo, A. S., & Sharma, M. M. (2013). *Analysis of Potential Bridging Scenarios During Blowout Events*. Paper presented at the SPE/IADC Drilling Conference and Exhibition Amsterdam, The Netherlands.
- Wood Group Kenny. 2016. *Subsea Capping Stack Technology Requirements Final Report*. Bureau for Safety and Environmental Enforcement, February 2016, <https://www.bsee.gov/sites/bsee.gov/files/tap-technical-assessment-program/756aa.pdf>.
- Wu, H., Golovin, E., Shulkin, Y., Chudnovsky, A., Dudley, J. W., & Wong, G. K. (2008). *Observations of Hydraulic Fracture Initiation and Propagation in a Brittle Polymer*. Paper presented at the 42nd US Rock Mechanics Symposium and 2nd U.S.-Canada Rock Mechanics Symposium, San Francisco.
- Yue, K. (2017). *Height Containment of Hydraulic Fractures In Layered Reservoirs*. (PhD), The University of Texas at Austin, Austin.
- Zaki, K. S., Dirkzwager, J. B., Hilarides, W. K., Connolly, P. T., Niemann, J., & Hawkins, J. G. (2015). Assessment of Fracture Containment and Broaching Resulting From Worst-Case-Discharge Events. *Society of Petroleum Engineers*. doi:10.2118/174079-PA
- Zhang, X., Jeffery, R. G., & Thiercelin, M. (2007). Deflection and Propagation of Fluid-Driven Fractures at Frictional Bedding Interfaces: a Numerical Investigation. *Journal of Structural Geology*, 29(3), 396-410.
- Zoback, M. D. (2007). *Reservoir Geomechanics*. Cambridge: Cambridge UP. Print.
- Zulqarnain, Muhammad, "Deepwater Gulf of Mexico Oil Spill Scenarios Development and Their Associated Risk Assessment" (2015). LSU Doctoral Dissertations. 3452.

## **Vita**

Youssuf Ahmed Elnoamany was born in Giza, Egypt. He received his bachelor's degree in Petroleum Engineering from Louisiana State University (LSU) with a minor in Geology in 2018. In August 2018, he joined the Craft and Hawkins Petroleum Engineering department and the Data Analytics (MSA) program at LSU where he anticipates graduating with his dual Master's degrees in May and August of 2021. Upon graduation, he will be joining Chevron as a Data Analyst.